

SIZE, CHARGE AND DOSE DEPENDENT INVITRO KINETICS OF
POLYSTYRENE NANOPARTICLES

by

YASMINE ABDELKAREM ABDELLATIF

Premaster Sc. Biotechnology, Cairo University, 2012

B.Sc. Biotechnology, Cairo University, 2011

A thesis submitted in partial fulfilment of the requirements
for the degree of Master of Science in Nanotechnology
in the NanoScience Technology Center
in the College of Graduate Studies
at the University of Central Florida
Orlando, Florida

Spring Term
2018

©2018 Yasmine A. AbdEllatif

ABSTRACT

The aim of the study described herein is to quantify the in-vitro kinetics of internalization of polystyrene nanoparticles (PS NPs) by cells. We used different charges, sizes and doses of fluorescently labelled PS NPs. Nanoparticles were characterized with UV-Vis, Fluorescence emission Dynamic Light Scattering (DLS) and Zeta potential for knowing their absorption, fluorescence spectra, size, charge, respectively. Additionally, cell viability was tested to know the toxicity of PS NPs. The quantitative uptake, the kinetics profile and rate of uptake were studied by using a new in-vitro fluorescence assay. This was achieved quantitatively and qualitatively by fluorescent plate reader and confocal imaging, respectively. It was found that the amine PS NPs are higher in cytotoxicity than the carboxy PS NPs due to the proton sponge phenomenon. It was observed that the fraction uptake of PS NPs changes by changing the physiochemical properties as charge, size & dose. The fraction uptake of neutral and amine PS NPs was higher than that of carboxy PS NPs. For the neutral PS NPs, the uptake depends on the macropinocytosis. For the amine PS NPs, the uptake depends on the electrostatic interaction and the rapid regeneration of new binding sites. Regarding the dose of PS NPs, for the amine PS NPs, it was found that the concentrations lower and higher than 5nM had lower fraction uptake, because the 5nM achieved the balance between the available number of binding sites and the rapid regeneration of new binding sites. For the kinetics profile of the amine and carboxy PS NPs, by comparing both of them, it was observed that the rate of uptake of applied doses lower than 5nM was different, but higher than 5nM was similar. However, for the neutral Ps NPs, they exhibit a steady state of rate of uptake in between the amine and carboxy PS NPs. Also, it was confirmed by the confocal images that as the concentration of amine PS NPs increase, the stress on the cells increase, leading to the cell death. These results were aligned with the results obtained from the cytotoxicity test.

Keywords: Polystyrene nanoparticles, uptake, rate of uptake, carboxy polystyrene nanoparticles, amine polystyrene nanoparticles, fraction of uptake, concentration uptake, confocal, proton sponge, polystyrene cytotoxicity.

This work is dedicated to my father & soulmate

AbdElkarem AbdEllatif Elkashef

ACKNOWLEDGMENT

There are no words that can describe my feelings right now, but I'll try to do my best for expressing these unique & mixed feelings. It has been a long time since I began my research not only here in the USA but back home in Egypt as well. My way wasn't easy and smooth, it was full of many obstacles and hard times. Fortunately, I was surrounded by good people that gave me the enthusiasm and the push to reach my desired destination.

First of all, I want to thank Allah that helped me and was by my side in all the situations, the bad before the good ones. I'd like to thank my father "AbdElkarem Elkashef" and my mother "Feryal Elkashef" for everything that they have done for me and for their prayers. Also, I should thank my support and partner in all the funny crimes, my brother "Mohamed", his wife "Faten" and my cutie nephew "AbdElkarem" that brought all the happiness to our family.

Secondly, I'd like to express my deepest appreciation to the rest of my family: Uncle AbdElrady, Ahmed, Mohamed, Ahmed Elkashef, Ahmed Mansour and Khalaf. Aunt Marwa, Aya, Heba, Magda, Eman. Cousins Hossam, Mohamed, Mahmoud, Ahmed, Hesham, Sherif, Orked, Bassant, Tagreed, Basmala, Ahmed, Hana and Schirin.

Thirdly, I'd like to acknowledge with gratitude my friends: Marwan Yasser, Omar Zedan, Amr Shetta, Ahmed Emad, Ahmed Barakat, Walaa Adly, Osama Sebaai, Edward Price, Torus Washington and Claudine Clay.

Also, I don't want to forget my Fulbright colleagues Mohamed Galal, Abdullah Altameemi, Abeer Hafez, Ahmed Shaarrawi, Ahmed Magdy, Andre Nono, Andrew Boules, Aya Tarek, Batka

Batbayar, Claudline Saint Vil, Darcy, Haidy Giratallah, Husam Mostafa, Ilka Sanchez, Jamal Hayat Khan, Julio Diarte, Kamal Rashad, Khalidou Ba, Phat, Thida Lin, Mai Abdelaziz, Mauricio Vela, Miguel, Mohamed Adel, Mohamed Halim, Mirna, Nesma, Omnia Reda, Omnia Usama, Ovidio Torres, Sarah Hisham, Shawqi Wadhah, Rhagda, Loay, Nora, Salma, Sara Saed, Ossama Mahmoud. We had shared a lot of tough stories and hard moments. I hope the best for all of you as well.

Fourthly, this master degree would not have been possible without the guidance of my doctors, professors and teachers at Cairo University (CU), The American University in Cairo (AUC), Portland State University (PSU) and University of Central Florida (UCF): Dr. Andre Gesquiere, Dr. Qun Huo, Dr. Hyeran Kang, Dr. Swaminathan Rajaraman, Dr. Lauren, Dr. Santra, Dr. Ahmed Osman, Dr. Mohamed Aly, Dr. Kohar Varjabedian, Dr. Maha Alkhazindar, Dr. Rashika Elridi, Dr. Hatem Elmahdy, Dr. Mahmoud Sakr, Dr. Tarek Moussa, Dr. Adel Khalil, Dr. Alaa Elseoufy, Dr. Ahmed Galal, Dr. Hamdy Hassanen, Dr. Salwa Sabet, Dr. Sherif Elnagdy, Dr. Tarek Kabil, Dr. Tarek Hussein, Dr. Walid Aduelsoud, Dr. Amr Adel, Dr. Hanna Elbadawy, Dr. Doaa Samir, Dr. Jehan Ibrahim, Dr. Ehab Ahmed, Dr. Basma Zakaria, Dr. Mohamed Nour, Dr. Magda Fikry, Dr. Mahmoud ElHefnawi, Dr. Mai Farid, Dr. Radwa Youssef, Dr. Ramy Yehia, Dr. Taiba Gamal Eldin, Dr. Adham Ramadan, Dr. Wael Mamdouh, Dr. Hanadi Salem, Dr. Nageh Allam, Dr. Mayada Elsayed, Dr. Mohab Anis, Mr. Mohamed Choucri, Mr. Mahdy El-Tahtawy, Mr. Ahmed Rashad, Mr. Mohamed Rashad, Mr. Mohamed Abdelaziz, Mr. Amir Fekry Mr. Gamal Shams, Mr. Mohamed Salah, Mr. Aly Salah, Mr. Lashen, Mr. Hossam El gedawy, Mrs. Nadia Jack, Mrs. Fatma Rasmy, Mrs. Eveline, Mrs. Magda Khafaga, Mrs. Karema, Mrs. Phoebe Daurio,

Mrs. Ella Barrett, Mrs. Julia Youst, Mrs. Gwen, Mrs. Rebekah Disbrow, Mrs. Kristi Kang and Mr. Greg Steward. They taught me how to be a good student and researcher as well.

A special thanks to Mrs. Mariam Abdelfatah, Mrs. Malaka Ali, Dr. Farkhonda Hassan, Dr. Maha Swelem, Mrs. Wafa Eltokhy, Mrs. Nervin Abdelghany, Mrs. Asmaa Ehakim, Ms. Marwa Shahin, Ms. Mona Shahin and Ms. Shimaa Shahin

Finally, I'd like to thank the Fulbright sponsored by the U.S. Department of State, Bureau of Educational and Cultural Affairs, the Binational Fulbright Commission in Egypt, the Amideast and in person Ms. Dianne Price, Ms. Shannon Conheady, Mr. Brian Dillehay, Dr. Maggie Nassif, Ms. Reem Elhassan, Ms. Iman Jamal, Ms. Dina Gaafar, Ms. Ranya Rashed for giving me the opportunity to pursue my studies in the USA. I want to thank Portland State University faculty members. I want also to thank each and every person who helped me for reaching my goal. I couldn't do this without your help and support.

TABLE OF CONTENTS

LIST OF FIGURES	xi
LIST OF TABLES	xvi
LIST OF ABBREVIATIONS	xviii
CHAPTER 1: INTRODUCTION	1
CHAPTER 2: LITERATURE REVIEW	5
CHAPTER 3: METHODOLOGY.....	11
3.1 Materials	11
3.2 Basic Polystyrene Nanoparticles Characterization	12
3.2.1 UV-Visible Spectrophotometer.....	12
3.2.2 Fluorescence Emission.....	12
3.2.3 Dynamic Light Scattering	12
3.2.4 Zeta Potential	13
3.3 In-vitro Polystyrene Nanoparticles characterization.....	13
3.3.1 Polystyrene Nanoparticles Toxicity	13
3.3.2 Polystyrene Nanoparticles Degradation.....	14
3.4 Uptake and Kinetics of Polystyrene Nanoparticles.....	14
3.4.1 Quantitative Measurement: Fluorescent Plate Reader	15
3.4.2 Qualitative Measurement: Confocal Imaging	16
CHAPTER 4: CHARACTERIZATION OF POLYSTYRENE NANOPARTICLES	17

4.1	Polystyrene Nanoparticles Characterization	17
4.1.1	UV-Visible Spectroscopy	17
4.1.2	Fluorescence emission	18
4.1.3	Dynamic Light Scattering	18
4.1.4	Zeta Potential	19
CHAPTER 5: CYTOTOXICITY & DEGRADATION OF POLYSTYRENE NANOPARTICLES.....		21
5.1	Polystyrene Nanoparticles Toxicity	21
5.2	Polystyrene nanoparticles degradation.....	23
5.2.1	Study of NP degradation for varying PS NPs surface charge	23
5.2.2	Study of NP degradation for varying PS NPs size	24
5.2.3	Study of NP degradation for varying PS NPs concentration	25
CHAPTER 6: UPTAKE & KINETICS OF POLYSTYRENE NANOPARTICLES		28
6.1	Quantitative Measurement: Fluorescent Plate Reader	28
6.1.1	Charge dependent uptake study	28
6.1.2	Size dependent uptake study	33
6.1.3	Concentration dependent uptake study	36
6.2	Analysis of the rate of polystyrene nanoparticles uptake.....	45
CHAPTER 7: QUALITATIVE MEASUREMENTS BY CONFOCAL IMAGING		53
7.1.1	Charge dependent uptake study	53
7.1.2	Size dependent uptake study	55

7.1.3	Concentration dependent uptake study	56
CHAPTER 8: CONCLUSION AND FUTURE WORK.....		60
APPENDIX: CONFOCAL IMAGES		62
LIST OF REFERENCES		104

LIST OF FIGURES

Figure 3-1: Experimental design of the 96 well plate for one nanoparticle.....	16
Figure 4-1: Absorption spectrum for the 10nM neutral, amine and carboxy-functionalized polystyrene nanoparticles diluted in PBS.	17
Figure 4-2: Emission spectrum for the 10nM neutral, amine and carboxy-functionalized polystyrene nanoparticles.....	18
Figure 4-3: DLS data for the polystyrene nanoparticles (A) 50nm Neutral/ Amine & Carboxy-functionalized polystyrene nanoparticles; (B) 100nm Carboxy-functionalized polystyrene nanoparticles; (B) 500nm Carboxy-functionalized polystyrene nanoparticles.....	19
Figure 4-4: Zeta potential for the 50nm neutral, amine and carboxy-functionalized PS NPs in PBS.	20
Figure 5-1: Percentage of cell viability and the toxicity of 50nm neutral, amine and carboxy-functionalized polystyrene nanoparticles with 1, 10, 50, 75 & 100nM concentrations.....	22
Figure 5-2: Total fluorescence count of nanoparticles with cell exposure (CT) and nanoparticles without cell exposure (NP) for 50nm neutral, amine and carboxy-functionalized polystyrene nanoparticles of 5nM in concentration at 0, 1, 4, 12 & 24h time intervals. Standard errors are represented by error bars attached to each column (n=3).	23
Figure 5-3: Total fluorescence count of nanoparticles with cell exposure (CT) and nanoparticles without cell exposure (NP) for 50, 100 and 500nm carboxy-functionalized polystyrene nanoparticles at 0, 1, 4, 12 & 24h time intervals. Standard errors are represented by error bars attached to each column (n=3).	25

Figure 5-4: Total unwashed fluorescence count of nanoparticles with cell exposure (CT) and nanoparticles without cell exposure (NP) for A) 50nm neutral-functionalized PS NPs, B) 50nm amine-functionalized PS NPs and C) 50nm carboxy-functionalized PS NPs with different concentrations at 0, 1, 4, 12 & 24h time intervals. Standard errors are represented by error bars attached to each column (n=3)..... 27

Figure 6-1: Uptake profile of 50nm neutral, amine and carboxy-functionalized polystyrene nanoparticles of 5nM in concentration over 24h period obtained from the raw fluorescent data. Standard errors are represented by error bars attached to each point (n=3). 29

Figure 6-2: The two main steps of the uptake mechanism of nanoparticles: the nanoparticle’s adsorption and internalization..... 31

Figure 6-3: Fractional uptake of dose of 5nM neutral, amine and carboxy-functionalized polystyrene nanoparticles obtained from the ratio between the washed fluorescence at time =x (CK) and the unwashed nanoparticles with cell exposure (CT) at time=0. Standard errors are represented by error bars attached to each point (n=3)..... 31

Figure 6-4: Concentration of uptake fraction of 5nM neutral, amine and carboxy-functionalized polystyrene nanoparticles. The concentration is the F_{cell} (fraction of dose) multiplied by concentration of the nanoparticle. Standard errors are represented by error bars attached to each point (n=3). 32

Figure 6-5: Uptake profile of 50, 100 and 500nm carboxy-functionalized polystyrene nanoparticles over 24h period. Standard errors are represented by error bars attached to each point (n=3)..... 33

Figure 6-6: Fractional uptake of 50, 100 and 500nm carboxy-functionalized polystyrene nanoparticles from the ratio between the washed fluorescence at time =x (CK) and the unwashed nanoparticles with cell exposure (CT) at time=0. Standard errors are represented by error bars attached to each point (n=3)..... 34

Figure 6-7: This graph shows the concentration of the uptake fraction 50, 100 and 500nm carboxy-functionalized polystyrene nanoparticles. The concentration is the F_{cell} (fraction of dose) multiplied by concentration of the nanoparticle. Standard errors are represented by error bars attached to each point (n=3). 35

Figure 6-8: This graph shows the uptake profile of 50nm neutral polystyrene nanoparticles with 5 and 10nM concentrations over 24h period. Standard errors are represented by error bars attached to each point (n=3)..... 37

Figure 6-9: This graph shows the uptake profile of 50nm amine-functionalized polystyrene nanoparticles with different concentrations (0.3, 0.5 & 0.7, 5 and 10nM) over 24h period. Standard errors are represented by error bars attached to each point (n=3)..... 37

Figure 6-10: This graph shows the uptake profile of 50nm carboxy-functionalized polystyrene nanoparticles with different concentrations (0.25, 3, 5 and 10nM) over 24h period. Standard errors are represented by error bars attached to each point (n=3)..... 38

Figure 6-11: Fractional uptake 50nm neutral-functionalized polystyrene nanoparticles of 5 and 10nM concentrations from the ratio between the washed fluorescence at time =x (CK) and the unwashed nanoparticles with cell exposure (CT) at time=0. Standard errors are represented by error bars attached to each point (n=3). 40

Figure 6-12: Fractional uptake 50nm amine-functionalized polystyrene nanoparticles of 0.3, 0.5, 0.7, 5 and 10nM concentrations from the ratio between the washed fluorescence at time =x (CK) and the unwashed nanoparticles with cell exposure (CT) at time=0. Standard errors are represented by error bars attached to each point (n=3). 40

Figure 6-13: Fractional uptake 50nm carboxy-functionalized polystyrene nanoparticles of 0.25, 3, 5 and 10nM concentration from the ratio between the washed fluorescence at time =x (CK) and the unwashed nanoparticles with cell exposure (CT) at time=0. Standard errors are represented by error bars attached to each point (n=3). 41

Figure 6-14: Concentration of the uptake fraction of 5 and 10nM neutral polystyrene nanoparticles. The concentration is the F_{cell} (fraction of dose) multiplied by concentration of the nanoparticle. Standard errors are represented by error bars attached to each point (n=3)..... 43

Figure 6-15: Concentration of the uptake fraction of 0.3, 0.5, 0.7, 5 and 10nM amine-functionalized polystyrene nanoparticles. The concentration is the F_{cell} (fraction of dose) multiplied by concentration of the nanoparticle. Standard errors are represented by error bars attached to each point (n=3). 43

Figure 6-16: Concentration of the uptake fraction of 0.25, 3, 5 and 10nM carboxy-functionalized polystyrene nanoparticles. The concentration is the F_{cell} (fraction of dose) multiplied by concentration of the nanoparticle. Standard errors are represented by error bars attached to each point (n=3). 44

Figure 6-17: This figure shows the rate of neutral- functionalized nanoparticles uptake, A) Log cell uptake versus log time for each concentration 0.25, 0.7, 3, 5 & 10nM. B) the rate of uptake nM/hr of nanoparticles different concentrations..... 49

Figure 6-18: This figure shows the rate of amine- functionalized nanoparticles uptake, A) Log cell uptake versus log time for each concentration 0.3, 0.5, 0.7, 5 & 10nM. B) the rate of uptake nM/hr of nanoparticles different concentrations..... 50

Figure 6-19: This figure shows the rate of carboxy- functionalized nanoparticles uptake, A) Log cell uptake versus log time for each concentration 0.25, 3, 5 & 10nM. B) the rate of uptake nM/hr of nanoparticles different concentrations..... 51

Figure 6-20: Rates of uptake (nM/hr) of neutral, amine and carboxy PS NPs. 52

Figure 7-1: Confocal images for the uptake of 50nm neutral, amine and carboxy-functionalized polystyrene nanoparticles 5nM in concentration at 0, 1, 4, 12 & 24h time interval. The blue color indicates the nucleus and the red color indicates the PS NPs. 54

Figure 7-2: Confocal images for the uptake of 50, 100 & 500nm carboxy-functionalized polystyrene nanoparticles at 0, 1, 4, 12 & 24h time interval. The blue color indicates the nucleus and the red color indicates the PS NPs. 55

Figure 7-3: Confocal images for the uptake of 5 and 10nM neutral polystyrene nanoparticles at 0, 1, 4, 12 & 24h time interval. The blue color indicates the nucleus and the red color indicates the PS NPs. 56

Figure 7-4: Confocal images for the uptake of 0.3, 0.5, 0.7, 5 and 10nM amine-functionalized polystyrene nanoparticles at 0, 1, 4, 12 & 24h time interval. The blue color indicates the nucleus and the red color indicates the PS NPs. 57

Figure 7-5: Confocal images for the uptake of 0.25, 3, 5 and 10nM carboxy-functionalized polystyrene nanoparticles at 0, 1, 4, 12 & 24h time interval. The blue color indicates the nucleus and the red color indicates the PS NPs. 58

LIST OF TABLES

Table 4-1: Dynamic light scattering results of various polystyrene nanoparticles in Nano-pure water.....	19
Table 4-2: Zeta potential results of 10nM neutral, amine and carboxy-functionalized PS NPs 50nm in PBS.	20
Table 6-1: The concentration uptake of 5nM neutral, amine and carboxy PS NPs at 0, 1, 4, 12 & 24hrs.....	32
Table 6-2: The concentration uptake of 50, 100 & 500nm carboxy-functionalized PS NPs at 0, 1, 4, 12 & 24hrs.....	35
Table 6-3: The concentration uptake of 5 and 10nM neutral PS NPs at 0, 1, 4, 12 & 24hrs.....	42
Table 6-4: The concentration uptake of 0.3, 0.5, 0.7, 5 & 10nM amine PS NPs at 0, 1, 4, 12 & 24hrs.....	42
Table 6-5: The concentration uptake of 0.25, 3, 5 & 10nM amine PS NPs at 0, 1, 4, 12 & 24hrs.	42
Table 6-6: This table shows the concentration of internalized neutral PS NPs with 0.25, 0.7, 3, 5 & 10nM at 0, 1, 4, 12 & 24h time intervals.....	45
Table 6-7: This table shows the log values for both time and the concentration of internalized neutral PS NPs with 0.25, 0.7, 3, 5 & 10nM.....	46
Table 6-8: This table shows the concentration of internalized amine PS NPs with 0.3, 0.5, 0.7, 5 & 10nM at 0, 1, 4, 12 & 24h time intervals.....	46
Table 6-9: This table shows the log values for both time and the concentration of internalized amine PS NPs with 0.3, 0.5, 0.7, 5 & 10nM.....	46

Table 6-10: This table shows the concentration of internalized carboxy PS NPs with 0.25, 3, 5 & 10nM at 0, 1, 4, 12 & 24h time intervals. 47

Table 6-11: This table shows the log values for both time and the concentration of internalized carboxy PS NPs with 0.25, 3, 5 & 10nM..... 47

Table 6-12: The concentration versus the slope of each concentration for the neutral PS NPs with 0.25, 0.7, 3, 5 & 10nM..... 48

Table 6-13: The concentration versus the slope of each concentration for the amine PS NPs with 0.3, 0.5, 0.7, 5 & 10nM..... 48

Table 6-14: The concentration versus the slope of each concentration for the carboxy PS NPs with 0.25, 3, 5 & 10nM..... 48

LIST OF ABBREVIATIONS

PS NPs: Polystyrene nanoparticles.

DLS: Dynamic Light Scattering.

nm: nanometers.

nM: nanomolar.

PBS: Phosphate Buffered Saline.

PDI: Polydispersity Index.

CHAPTER 1:

INTRODUCTION

The aim of the study described herein is to quantify the in vitro kinetics of internalization of polystyrene nanoparticles (PS NPs) by cells. Neutral, amine and carboxy-functionalized PS NPs with different sizes (50, 100 and 500nm) and different concentrations were applied in this study. Characterization of PS NPs was achieved by UV-Vis spectrophotometer, fluorescence emission, dynamic light scattering (DLS) and Zeta potential for obtaining their absorption, fluorescence spectra, size and charge, respectively. Moreover, cytotoxicity of polystyrene nanoparticle was measured with *Mus musculus* liver cells (AML12). Then, charge, size and concentration dependent uptake studies were performed. Quantitative and qualitative measurements were completed by fluorescent plate reader and confocal microscopy. Furthermore, the rate of internalization of nanoparticles was determined studied.

The focus of our study is the uptake of PS NPs and the influence of changing PS NPs physiochemical properties (charge, size and dose) on the uptake. The uptake changes the pathway and the mechanism that the PS NPs exhibit for internalization. The rate of the internalization with Time/ Dose, fraction uptake of the PSNPs and concentration PS NPs internalized will be studied

Nanotechnology is one of the rapidly growing technologies within the past few years. There are many applications and uses of nanomaterials including polymer nanoparticles in clinical sector as drug delivery and cancer research and non-clinical fields.¹⁻² One of the main concerns regarding dealing with nanoparticles is their toxicity. That's why researchers must examine the cytotoxicity of nanoparticles with different cell types.³⁻⁵ Firstly, in order to know the cell types that we can work with when we deal with nanoparticles, we should know the main routes of nanoparticles

internalization through the body which are; inhalation through respiratory system, ingestion through digestive system, penetration through skin, injection through blood stream and ocular through eyes.⁶⁻⁷

Polystyrene nanoparticles are made up of polystyrene (PS) which is a polymer that contains an aromatic benzene ring attached with an ethylene group. The styrene molecule is then polymerized by polymerization reactions for producing the polystyrene. The size of the polystyrene can be tailored from macro to Nano-level. Polystyrene nanoparticles (PS NPs) range from 50-100nm. PS can be functionalized according to the application, it can be neutral, negatively or positively charged.⁸ Polystyrene is used in food, non-food, energy, packaging, communication technologies, in addition to lab and refrigeration equipment.^{9,10}

Polystyrene is a highly biocompatible and non-biodegradable polymer.^{8, 11} It was found that the polystyrene among different polymers has the lowest toxicity, which makes it a good candidate when it comes to human health, because it will not be degraded after certain period in the human body.¹² The United States Food and Drug Administration (FDA) according to the Federal regulation code, title 21, volume 3, Department of Health and Human Services, they stated that the use of polystyrene and the modified polystyrene in food is safe in certain circumstances, when it interacts with human body.¹²

Our work is mainly divided into basic characterization, in-vitro characterization, uptake studies (quantitative measurement), kinetics of internalization and confocal imaging (qualitative measurement). In the basic characterization, we obtained the absorption spectrum, size and the charge of polystyrene nanoparticles, this will be shown in Chapter 4. In the in-vitro characterization, we tested the cytotoxicity and the degradation of polystyrene nanoparticles, this will be shown in Chapter 5. In the uptake studies, we tested the effect of charge, size and dose on

the polystyrene nanoparticles uptake, the kinetics of internalization and rate of nanoparticles uptake, this will be shown in Chapter 6. Finally, the confocal images for various uptake studies will be shown in Chapter 7.

We found that the amine-functionalized PS NPs are more cytotoxic than carboxy-functionalized PS NPs due to the “proton sponge” phenomenon that occur with the amine-functionalized PS NPs, at which at low pH inside the cell the positive charge of the amine groups are protonated by accepting protons, leading to the entrance of H₂O and ions into the endosome, increasing its size and finally the rupture of the endosome and liberating the amine-functionalized PS NPs with the cell’s cytoplasm.¹³⁻¹⁴ After that the amine-functionalized PS NPs are free to interact with the cell’s organelles including the mitochondria by decreasing the mitochondrial metabolic activities that is crucial for the cells viability and increasing reactive oxygen species (ROS). Then the ROS can interrupt enzymatic reactions, damaging the genetic material which is the deoxyribonucleic acid (DNA) and finally leading to the cell death.

It was also observed that the fraction uptake of PS NPs changes by changing the physiochemical properties as charge, size & dose. The fraction uptake of neutral and amine PS NPs was higher than that of carboxy PS NPs. For the neutral PS NPs, the uptake depends on the macropinocytosis at which the cell membrane is elongated outwards enclosing the PS NPs into a macropinosome. For the amine PS NPs, the uptake depends on the electrostatic interaction and the rapid regeneration of new binding sites. Regarding the dose of PS NPs, for the amine PS NPs, it was found that the concentrations lower and higher than 5nM had lower fraction uptake, because the 5nM achieved the balance between the number of available binding sites and the rapid regeneration of new binding sites. For the kinetics profile of the amine and carboxy PS NPs, by comparing both of them, it was observed that the rate of uptake lower than 5nM was different, but

higher than 5nM was slightly similar, at which as the concentration of amine PS NPs increase, the rate of uptake decrease, but for the carboxy PS NPs as the concentration of increase, the rate of uptake increases until 5nM. However, for the neutral Ps NPs, they exhibit a steady state of rate of uptake in between the amine and carboxy PS NPs. Also, it was confirmed by the confocal images that as the concentration of amine PS NPs increases, the stress on the cells increase, leading to the cell death. These results were aligned with the results obtained from the cytotoxicity test.

CHAPTER 2: LITERATURE REVIEW

Polystyrene nanoparticles have received great attention from researchers due to their outstanding functions and capabilities for drug delivery and fighting cancer cells as well. A considerable amount of literature has been published on the uptake of polystyrene nanoparticles with various cell lines. In this literature review we will highlight previously reported research.

To understand the entry of nanoparticles through cells, both functional and physical properties must be studied, in addition to the parameters affecting the response and the uptake of nanoparticles. There are different parameters affecting the nanoparticles uptake, including size, composition, shape, charge and concentration; in addition to cell properties (e.g. antigens expressed on cell membrane) and environmental factors such as pH, temperature and pressure.^{7, 15-17} The behavior of nanoparticles in their interaction with cells changes dramatically by changing one or more parameter at a time. Moreover, the protein corona can affect the uptake and the toxicity of nanoparticles as well.¹⁸⁻¹⁹ A protein corona that surrounds the nanoparticles is typically composed of two layers of proteins; hard and soft layers, they contain proteins and tiny molecules as amino acids.⁶

There are various entry mechanisms for the internalization of nanoparticles within cells called endocytosis mechanisms. They are divided into two main mechanisms, phagocytosis and pinocytosis.²⁰ *Phagocytosis* is the endocytosis for large molecules more than 500nm, this is for the removal of bacteria, dead cells, etc. Phagocytosis is mainly related to the immune system cells such as: macrophages and neutrophils. In this case the cell membrane surrounds the undesirable solid material forming a vesicle by the aid of actin that is degraded by the lysosome.²¹⁻²²

Pinocytosis is endocytosis for fluids or liquids which is called the “cell drinking”. Pinocytosis is further divided into three mechanisms which are: macropinocytosis, clathrin-mediated endocytosis (CME) and caveolin-mediated endocytosis.^{6, 22} *Macropinocytosis* is a mechanism for fluid uptake such as: glucose and amino acids, the size of the produced vesicle more than 1µm, one side of the membrane enclose the fluid by the aid of actin forming a macropinosome. *Clathrin-mediated endocytosis* is a mechanism at which the Clathrin peptide and the adaptor protein from the interior of the cell membrane bound forming a vesicle from outside and by the aid of dynamin (GTPase), surround itself around the vesicle for releasing it from the cell membrane to inside the cell.²¹⁻²² *Caveolin-mediated endocytosis*, unlike the CME the protein caveolin merge with the membrane cholesterol producing vesicle that is released by dynamin as well. Different nanoparticles exhibit different endocytosis mechanisms.^{6, 21-24}

On one hand, *Rejman et al.*, found that the polystyrene nanoparticles in mouse melanoma cells more than 200nm internalized via CME, 50-500nm via Caveolin-mediated endocytosis and nanoparticles more than 500nm exhibit no entry.²⁵ Researches have found that gold nanoparticles ranges from 3-8nm internalized by pinocytosis in mouse leukemic macrophage cells.²⁶ On the other hand, it was found that the nanoparticles can enter the cells via passive mechanism instead of the endocytosis such as; cadmium selenide nanoparticles with 8nm in red blood cells²⁷ and silicon oxide nanoparticles with 14nm in human colon cancer.²⁸ The results of previous studies indicate that the mechanism of nanoparticle internalization depend on many factors including cell and nanoparticle type and size.

Several studies tested the relationship between the charge of polystyrene nanoparticle and their uptake. The 50nm neutral, positively and negatively charged polystyrene nanoparticles were tested for their uptake with the intestinal Caco-2 (human colonic adenocarcinoma cell line) and HT29-

MTX (human colon adenocarcinoma mucus secreting cell line). Researchers found that the translocation of the positively charged polystyrene nanoparticles were the highest through the in-vitro intestinal barrier followed by the negatively charged polystyrene nanoparticles; and the neutral didn't exhibit any translocation.³ Positively and negatively charged PS NPs of 50nm in size were used with BeWo (human choriocarcinoma cell line). This cell line composed of cancer cells from the women's womb. It was found that the positively charged PS NPs internalized in the placenta model more than the negatively charged ones.²⁹ The human intestinal adenocarcinoma cancer cells was tested with positively and negatively charged PS NPs with 50 and 100nm. The positively charge PS NPs exhibit more uptake than the negatively charged ones.²⁰ The uptake of neutral and positively charged PS NPs of 100nm in size with MSCs (mesenchymal stem cells) was also tested. The uptake and the internalization of the positively charged PS NPs were higher than the neutral PS NPs.³⁰ The translocation of 51 and 110nm neutral polystyrene nanoparticles and 52nm positively charged polystyrene nanoparticles with Calu-3 (pulmonary epithelial cells), THP-1 (macrophages) and HPMEC-ST1.6R (pulmonary epithelial cells) was studied. This study mimics the effect of nanoparticles on the alveolo-capillary barrier in the lung. The 51 nm neutral polystyrene nanoparticles translocated and were found in the cell culture. But, both 110nm neutral and 52nm positively charged polystyrene nanoparticles did not pass the cell lines which resemble the pulmonary epithelial cells in the lung.⁴ The uptake, biocompatibility, compartmentalization and intracellular retention of 50nm amine-functionalized PS NPs and 30nm carboxy-functionalized PS NPs was also tested with NIHOVCAR3 (Human ovarian cancer cell line). It was discovered that the uptake of the 50nm amine-functionalized PS NPs was higher than that of 30nm carboxy-functionalized PS NPs.³¹ The uptake of carboxy and amine-functionalized polystyrene nanoparticles of 100nm size were tested with human macrophages, undifferentiated monocytic

THP-1 cells and differentiated human monocytic leukemia THP-1 cells. It was found that the macrophages internalized carboxy-functionalized polystyrene nanoparticles four times higher than THP-1 cells. THP-1 cells internalized amine-functionalized polystyrene nanoparticles more than macrophages. It was concluded that the uptake of nanoparticles differs according to the cell type and the mechanism of endocytosis.³²

To wrap up, we can interpret from the previous studies that the uptake of the amine PS NPs is higher than that of the carboxy PS NPs, because normally the cell membrane carries negative charge that interact electrostatically with the positive charge of the amine group, increasing its uptake, but there is a repulsion force between the membrane and the negative charge of the carboxylic group, decreasing its uptake.^{6, 23, 29, 33}

Numerous studies have attempted to explain the relationship between the size of polystyrene nanoparticles and their uptake. Researchers carried out experiments for knowing the kinetics interaction of the fluorescently labelled PS NPs 20, 100, 200 and 500nm with HUVEC (Primary human umbilical vein endothelial cells). They concluded that the number of binding sites per cell decreases with increasing the nanoparticle size; but, the attachment coefficient increases.³⁴ The uptake of 20, 40 and 100nm carboxy-functionalized PS NPs with 1321N1 (human astrocytoma) and A549 (Human lung carcinoma cells) was tested. It was observed that the internalization of the 40nm nanoparticles were more than 20 and 100nm. They suggested that this may be due to the difference in the internalization mechanisms. In the case of 20nm NPs Vander Waals forces are low between the nanoparticles and the cells and diffusion is high, leading to lower uptake.³⁵ Researchers investigated the uptake of polystyrene microspheres range: 20, 93, 220, 560 and 1010nm with six cell lines including human and mouse cell lines; HUVEC (Primary human umbilical vein endothelial cells), ECV304 (Human bladder Carcinoma), HNX14C (Human head

and neck squamous cell carcinoma), KLN205 (Mouse squamous cell carcinoma), Hepa 1-6 (Mouse hepatoma) and HepG2 (Human hepatocyte carcinoma). It was found that HUVEC, ECV304 and HNX14C up took all the polystyrene microspheres, but the uptake decreases as the size increases. KLN205 up took all sizes except 1010nm. Hepa 1-6 internalized 20nm with the highest percentage compared with very low uptake of 93 and 220nm, and with the least uptake of 560 and 1010nm. HepG2 internalized 20nm with the highest percentage compared to barely uptake of 93 and 220nm, and with no uptake of 560 and 1010nm. It was deduced that the uptake of the same size of PS NPs is different in both normal and cancer cell, this may be due to the expressed antigens and receptors on the cell membrane that changes the endocytosis mechanism.⁵ The uptake of carboxy PS NPs of 20 and 200nm with C3A (Primary rat hepatocytes hepatoblastoma) and HepG2 (Human hepatocyte carcinoma) was tested. It was inferred that the uptake of the 20nm nanoparticles were higher than 200nm, this is due to the increased binding sites and higher availability of the 20nm PS NPs than the 200nm PS NPs.⁷

Several studies have found that the cytotoxicity of amine PS NPs is higher than the carboxy PS NPs. For example, researchers have done an experimental investigation to know the cytotoxicity of different polymer nanoparticles with 2 cell lines: CACo-2 (human colonic adenocarcinoma) and NR8383 (rat alveolar macrophage). Positively and negatively charged PS NPs were made up of three different polymers.³⁶ They found that the positively charged PS NPs were toxic to the cells, however there was no toxicity for the negatively charged PS NPs. Amine PS NPs are proposed to be more toxic than the carboxy PS NPs, due to the higher interaction between the amine group and the cell membrane and the decrease in the energy barrier needed by the positively charged PS NPs to pass the cell membrane, so the amine uptaken by the cell more than the carboxy PS NPs, increasing the cytotoxicity of the cells in case of amine PS NPs.^{4, 11, 20, 31, 36-39} From the literature

review, we can deduce that there are many parameters affecting the uptake of the polystyrene nanoparticles. But there is a lack of the fraction uptake and internalization kinetics profiles for polystyrene nanoparticles as well.

CHAPTER 3:

METHODOLOGY

3.1 Materials

Polystyrene nanoparticles used in this research are: 50nm Red Fluorescent PS Latex (Cat No. PSFR050NM), 50nm Red Fluorescent Aminated PS Latex (Cat No. AMFR050NM), 50nm Red Fluorescent Carboxylated PS Latex (Cat No. CAFR050NM), 100nm Red Fluorescent Carboxylated PS Latex (Cat No. CAFR100NM) and 500nm Red Fluorescent Carboxylated PS Latex (Cat No. CAFR500NM) purchased from MAGSPHERE INC, CA, USA. AML12, Normal epithelial hepatocytes cells from *Mus musculus* cell line (ATCC[®] CRL2254[™]) purchased from American Type Culture Collection, VA, USA. Dulbecco's mod. Of Eagle's Medium (DMEM) F-12, 1X purchased from CORNING cellgro., NY, USA. Fetal Bovine Serum (FBS) purchased from CORNING, NY, USA. Penicillin Streptomycin L-Glutamine Antibiotic, 100X purchased from CORNING, NY, USA. Phosphate Buffered Saline (PBS) pH 7.4, 1X purchased from gibco[®] by life technologies[™], MA, USA. Dulbecco's Phosphate Buffered Saline (DPBS) purchased from BioWhittaker[®] by LONZA, Switzerland. 0.25% Trypsin, 1X purchased from CORNING, NY, USA. CellTiter 96[®] Aqueous Non-Radioactive Cell Proliferation Assay purchased from Promega, WI, USA. Paraformaldehyde, 16% Aqueous Solution purchased from Electron Microscopy Sciences, PA, USA. UltraPure Distilled Water purchased from invitrogen[™] by life technologies[™] MA, USA. Hanks' Balanced Salt Solution (HBSS + Ca⁺⁺) purchased from BioWhittaker[®] by LONZA, Switzerland. Hoechst 33342 dye purchased from Thermo SCIENTIFIC, MA, USA.

3.2 Basic Polystyrene Nanoparticles Characterization

Firstly, Polystyrene nanoparticles were characterized to know the absorption, fluorescence spectra and the excitation wavelength by using Agilent 8453 UV-Visible Spectrophotometer. Secondly, the size and the zeta potential of the nanoparticles were measured by using the Zetasizer Nano ZS90 that contain dynamic light scattering and zeta potential measurements.

3.2.1 UV-Visible Spectrophotometer

The neutral, amine and carboxy-functionalized polystyrene nanoparticles were characterized to identify the absorption spectrum from 400-700nm. Nanoparticles were diluted by Phosphate Buffered Saline (PBS) for preparing the 10nM concentration of the polystyrene nanoparticles. The PBS were used as a blank as well.

3.2.2 Fluorescence Emission

The neutral, amine and carboxy-functionalized polystyrene nanoparticles were characterized to identify the emission spectrum to know the fluorescence emission peak by using the excitation wavelength obtained from the UV-Vis Spectrophotometer.

3.2.3 Dynamic Light Scattering

To validate the size of the nanoparticles applied in the study, Dynamic light scattering (DLS) was used. The samples were prepared in different concentrations according to the size of the polystyrene nanoparticles. For the 50nm neutral, 50nm amine and 50, 100 & 500nm carboxy-functionalized polystyrene nanoparticles, 10, 10, 10, 3 & 0.005nM concentrations were prepared, respectively. The samples were diluted with UltraPure Distilled Water. Then, the size versus percentage number were plotted.

3.2.4 Zeta Potential

The zeta potentials for both the neutral, amine and carboxy-functionalized polystyrene nanoparticles were tested. Samples were diluted with PBS to reach 10nM concentration of polystyrene nanoparticles. Then, the zeta potential versus the total count intensity was plotted.

3.3 In-vitro Polystyrene Nanoparticles characterization

3.3.1 Polystyrene Nanoparticles Toxicity

A Cell Viability test was carried out to define the percentage of cell viability of the cells after exposure of the polystyrene nanoparticles. Normal epithelial hepatocytes cells from *Mus musculus* AML12 Cell line was used in this experiment. Cells were plated onto 96 well plate at 34,000 cell/well and left for attachment from 24-48h at 37°C and 5% CO₂. Different concentrations (1, 10, 50, 75 and 100nM) of the 50nm neutral, amine and carboxy-functionalized polystyrene nanoparticles were used in this assay. Nanoparticles were incubated with the cells for 24h. Then, a ratio of 1:6 of Cell viability test reagent to Media was used. Then, the plate was incubated for 1hr at 37°C. Media and UltraPure Distilled Water were used as positive and negative controls, respectively. Then the absorbance was measured at 490nm by BioTek ELx808 Absorbance Reader. Then, the results were implemented in *Equation (3.1)*, s is the mean value of the sample and x is the mean value of control cells. Finally, the percentage of cell viability Versus concentration was plotted.

$$\% \text{ Cell Viability} = \left(\frac{s}{x} \right) \times 100 \quad (3.1)$$

3.3.2 Polystyrene Nanoparticles Degradation

The degradation of the polystyrene nanoparticles was tested to know if the AML12 cells degrade the nanoparticles when incubated with them. In order to know the degradability of the PS NPs, the total fluorescence count of nanoparticles with cell exposure (CT) and nanoparticles without cell exposure (NP) were measured for the at 0, 1, 4, 12 & 24h time intervals.

Then the T-test were done to know if there is any significant difference between the two populations (CT and NP). If the P-value of the T-test is > 0.05 , this means that there is no difference between them, so no degradation, however if the P-Value is < 0.05 , this this means that there is difference between them, so degradation occurred. T-test was done by the data analysis with two tail distribution and unequal variances by using Microsoft Excel. The P-values for the 50nm neutral PS NPs were 0.17, 0.10, 0.08, 0.14 and 0.08, for 50nm amine PS NPs were 0.13, 0.11, 0.26, 0.61 and 0.7, for the 50nm carboxy PS NPs were 0.12, 0.13, 0.24, 0.35 and 0.8, for the 100nm carboxy PS NPs were 0.16, 0.38, 0.61, 0.06 and 0.15 and for the 500nm carboxy PS NPs were 1.7×10^{-6} , 1.4×10^{-6} , 7.2×10^{-7} , 1.2×10^{-4} and 9.8×10^{-4} .

3.4 Uptake and Kinetics of Polystyrene Nanoparticles

Three uptake studies were performed: the first with different charges of nanoparticles (Charge dependent uptake study), the second with different sizes of nanoparticles (Size dependent uptake study), and the third with different concentrations (Concentration dependent uptake study).

In the first uptake study, 50nm neutral, amine and carboxy-functionalized polystyrene nanoparticles of 5nM in concentrations were used. *In the second uptake study*, 50 and 100nm carboxy-functionalized polystyrene nanoparticles of 0.25nM in concentrations were used. *In the third uptake study*, 50nm neutral polystyrene nanoparticles with 5 and 10nM were tested for their

uptake. Also, 50nm amine-functionalized polystyrene nanoparticles with 0.3, 0.5, 0.7, 5 and 10nM were tested for their uptake. Similarly, 50nm carboxy-functionalized polystyrene nanoparticles with 0.25, 3, 5 and 10nM were tested for their uptake. Each uptake study was done in triplicate. The AML12 cells were plated in the 96 well plate at 37,400 cell/well and incubated for 48h at 37°C and 5% CO₂. Then, the nanoparticles were added for 0, 1, 4, 12 & 24h incubation. At each time point the cells were washed, trypsinized and the fluorescence was measured by TECAN Infinite 200 PRO fluorescent plate reader and then imaged under the confocal microscopy (Axioskop2).

3.4.1 Quantitative Measurement: Fluorescent Plate Reader

The experimental design of the 96 well plate was as follows: washed wells at time =x, x=0, 1, 4, 12 & 24hrs (CK), unwashed wells of cells and nanoparticles (CT), unwashed wells of nanoparticles (NP), media wells (CM) and trypsin wells (T). Each one of them was made in triplicate wells for each nanoparticle type. The whole experiment was made in triplicate (n=3) as shown in *Figure 3-1*. At time=x, the cells were washed and trypsinized, then they were measured by the fluorescent plate reader at excitation wavelength of 530nm and emission wavelength of 590nm. Washed polystyrene nanoparticles uptake (fluorescence versus time), unwashed fluorescence count of nanoparticles with cell exposure (CT) and nanoparticles without cell exposure (NP) versus time, fraction cell uptake (Fraction of dose versus time), and the concentration uptake (concentration versus time) were plotted. Moreover, the rate of polystyrene nanoparticles uptake was measured, calculated and plotted to know the rate of the internalized concentration per hour. This experiment was done on the neutral nanoparticles of concentrations 0.25, 0.7, 3, 5 & 10nM, amine nanoparticles of concentrations 0.3, 0.5, 0.7, 5 & 10nM and carboxy nanoparticles of concentrations 0.25, 3, 5 & 10nM.

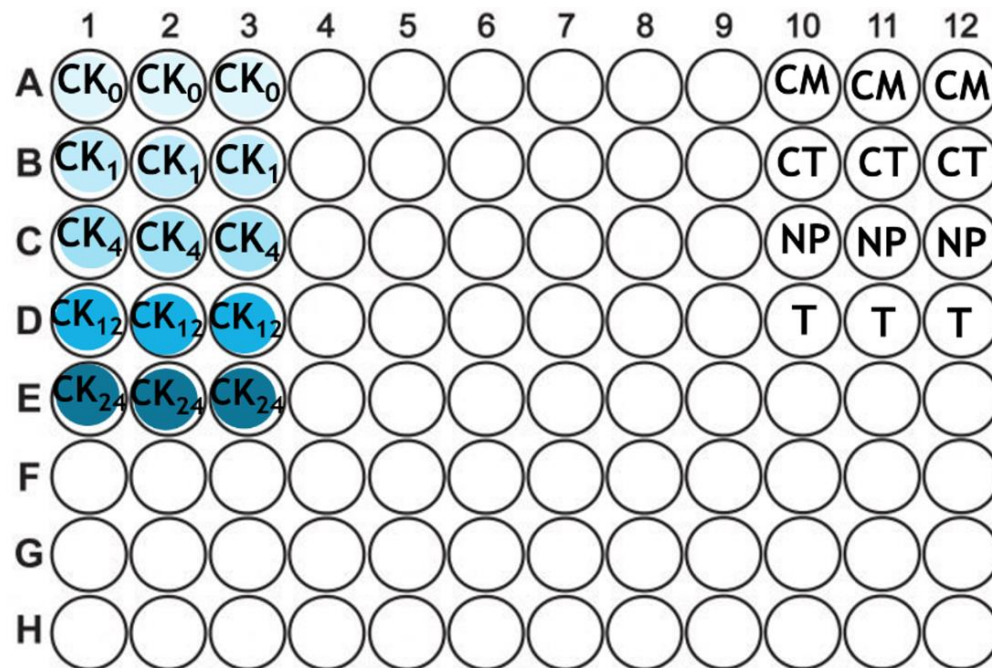


Figure 3-1: Experimental design of the 96 well plate for one nanoparticle.

3.4.2 Qualitative Measurement: Confocal Imaging

Cell samples were collected after the fluorescent plate reader, fixed by paraformaldehyde and stained by Hoechst 33342 dye for the nucleus staining. We used 607/45nm emission filter for the visualization of the nanoparticles. Images were processed by ImageJ 1.51j8. The confocal microscopy is used to obtain 3D images for the cell, to localize the nanoparticles inside the cell, and how far it is from the nucleus. In the next section the results obtained from the characterization, toxicity, uptake, rate of internalization and confocal images will be shown.

CHAPTER 4:

CHARACTERIZATION OF POLYSTYRENE NANOPARTICLES

4.1 Polystyrene Nanoparticles Characterization

The results obtained from the characterization of the different charges of polystyrene nanoparticles are shown in this section.

4.1.1 UV-Visible Spectroscopy

The UV-vis spectrum shows that there is an absorption peak at about 530nm for both amine and carboxy-functionalized polystyrene nanoparticles. It was also found that the absorption peak for the neutral polystyrene nanoparticles were a little bit shifted at 560nm, but still absorb at 530nm as in the amine and the carboxy nanoparticles as shown in *Figure 4-1*.

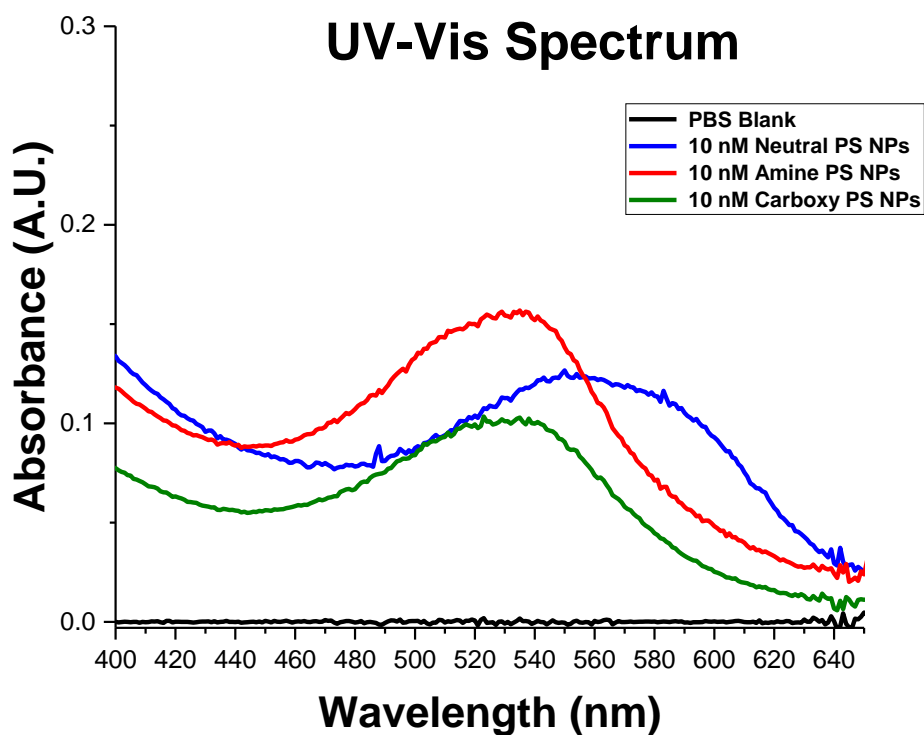


Figure 4-1: Absorption spectrum for the 10nM neutral, amine and carboxy-functionalized polystyrene nanoparticles diluted in PBS.

4.1.2 Fluorescence emission

It was found that the fluorescence emission peak for the neutral, amine and carboxy-functionalized polystyrene nanoparticles appeared at about 590nm as shown in *Figure 4-2*.

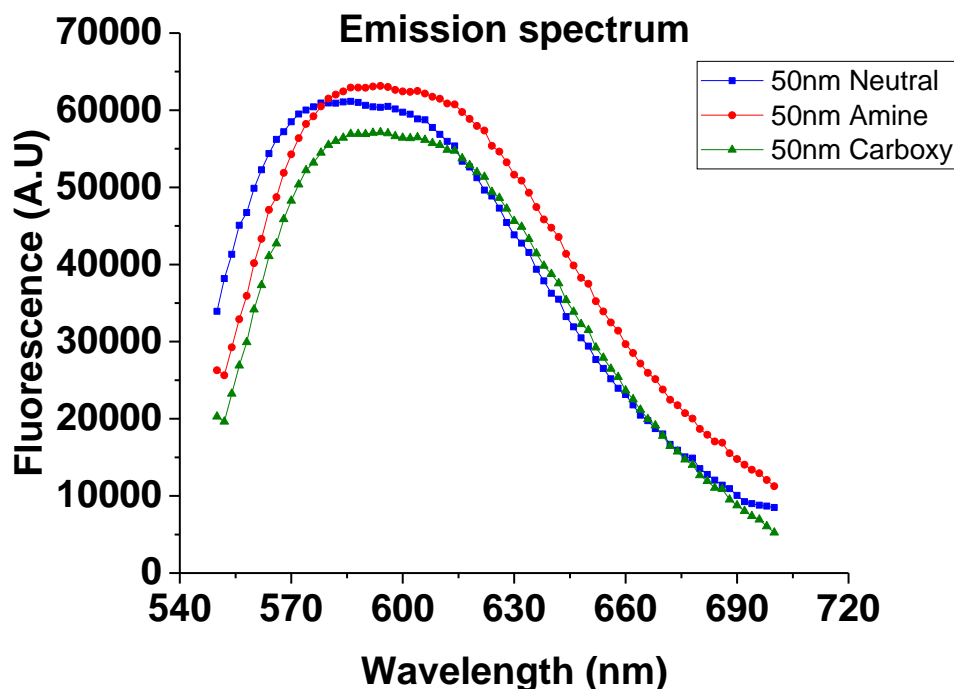


Figure 4-2: Emission spectrum for the 10nM neutral, amine and carboxy-functionalized polystyrene nanoparticles

4.1.3 Dynamic Light Scattering

We validated the sizes of the polystyrene nanoparticles used in this study by DLS. We found that the size of the 50nm neutral PS NPs reach $53.0 \pm 0.7\text{nm}$ with a value of 0.06 polydispersity index (PDI), 50nm amine PS NPs reach $51.2 \pm 0.6\text{nm}$ with a value of 0.11 PDI and 50nm carboxy PS NPs reach $46.7 \pm 0.5\text{nm}$ with a value of 0.04 PDI. The 100nm carboxy PS NPs reach $99.2 \pm 0.2\text{nm}$ with a value of 0.04 PDI, while the 500nm carboxy PS NPs reach $523.2 \pm 9.3\text{nm}$ in diameter with a value of 0.18 PDI. Their size was verified as purchased and there was no aggregation of the nanoparticles as shown in the data in *Table 4-1* and *Figure 4-3*.

Table 4-1: Dynamic light scattering results of various polystyrene nanoparticles in Nano-pure water

Nanoparticle	Medium	Size(nm)	Polydispersity index(PDI)
Neutral PS NPs 50nm	UltraPure Distilled Water	53.0 ± 0.7	0.06
Amine- PS NPs 50nm	UltraPure Distilled Water	51.2 ± 0.6	0.11
Carboxy- PS NPs 50nm	UltraPure Distilled Water	46.7 ± 0.5	0.04
Carboxy- PS NPs 100nm	UltraPure Distilled Water	99.2 ± 0.2	0.04
Carboxy- PS NPs 500nm	UltraPure Distilled Water	523.2 ± 9.3	0.18

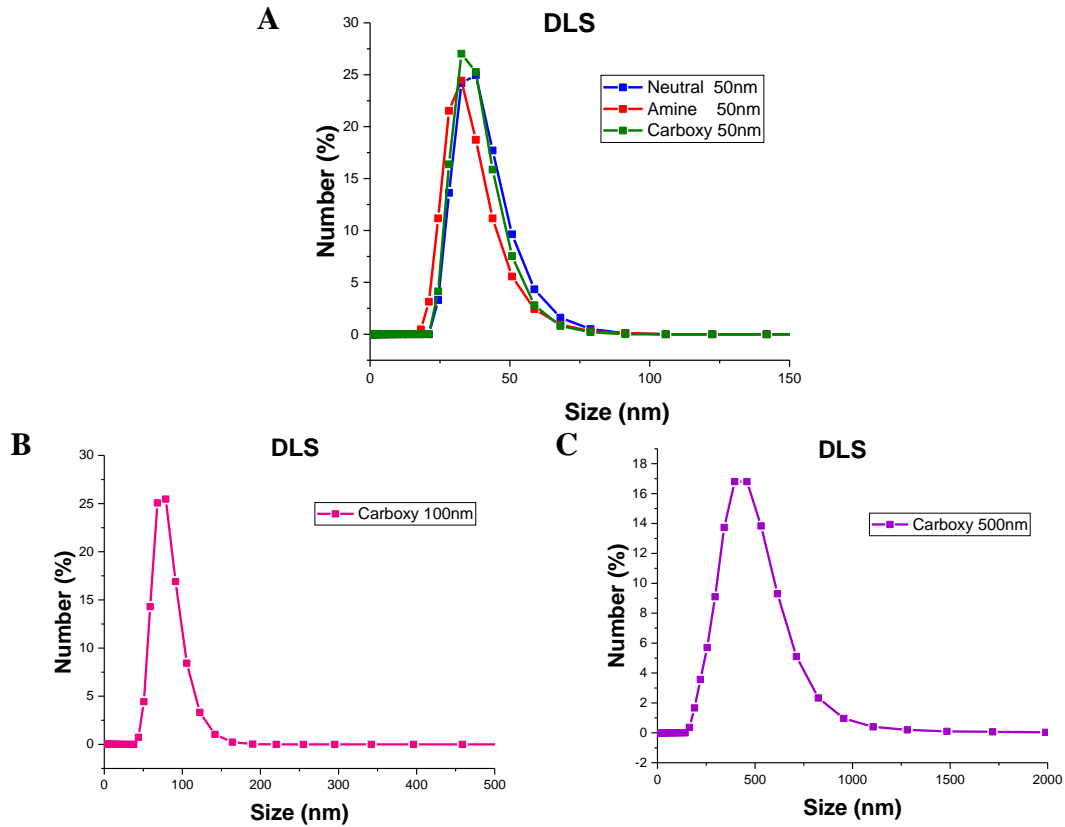


Figure 4-3: DLS data for the polystyrene nanoparticles (A) 50nm Neutral/ Amine & Carboxy-functionalized polystyrene nanoparticles; (B) 100nm Carboxy-functionalized polystyrene nanoparticles; (B) 500nm Carboxy-functionalized polystyrene nanoparticles.

4.1.4 Zeta Potential

The zeta potential was measured for the 50nm neutral, amine and carboxy-functionalized polystyrene nanoparticles in phosphate buffered saline. It was found that the zeta potential for the neutral, amine and carboxy functionalized PS NPs was $-25 \pm 4.1\text{mV}$, $44.2 \pm 1.9\text{mV}$ and $-44.8 \pm 3.3\text{mV}$, and, respectively. It was observed that the zeta potential of the neutral PSNPs is negative,

we argued this due to the presence of negatively charged surfactant. Several studies noticed that the zeta potential of the neutral PSNPs had a negative charge,^{3-4, 11, 14, 29, 40-41} and one of them from the same vendor.⁴² The results are shown in *Table 4-2* and *Figure 4-4*.

Table 4-2: Zeta potential results of 10nM neutral, amine and carboxy-functionalized PS NPs 50nm in PBS.

Nanoparticle	Medium	Zeta Potential (mV)
Neutral- polystyrene NPs 50nm	Phosphate-Buffer Saline (PBS)	-25.7 ± 4.1
Amine- polystyrene NPs 50nm	Phosphate-Buffer Saline (PBS)	44.2 ± 1.9
Carboxy- polystyrene NPs 50nm	Phosphate-Buffer Saline (PBS)	-44.8 ± 3.3
Phosphate-Buffer Saline (PBS)	-	-23 ± 3.4

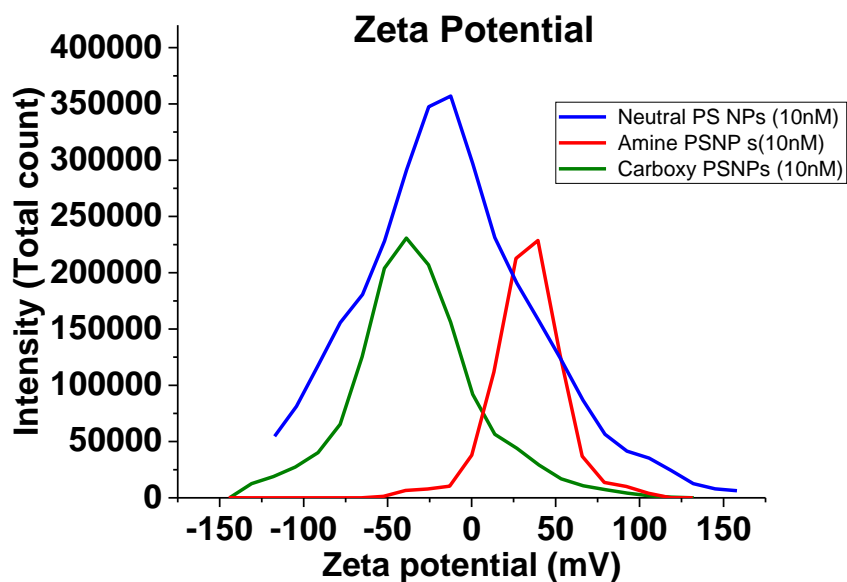


Figure 4-4: Zeta potential for the 50nm neutral, amine and carboxy-functionalized PS NPs in PBS.

CHAPTER 5:

CYTOTOXICITY & DEGRADATION OF POLYSTYRENE NANOPARTICLES

5.1 Polystyrene Nanoparticles Toxicity

The MTS toxicity assay was performed for knowing the percentage of cell viability of AML12 with 50nm neutral, amine and carboxy-functionalized polystyrene nanoparticles. Different concentrations were used: 1, 10, 50, 75 & 100nM. The main concept of the MTS assay is that the alive cells convert the MTS reagent in the presence of NADPH/ NADH to colored formazan and NADP⁺/ NAD⁺ by the aid of dehydrogenase enzymes. If the color of formazan becomes deeper, this means that there are more cells producing formazan, the amount of formazan produced is directly proportional to the number of living cells.⁴³⁻⁴⁵ It was found that amine PS NPs killed more than half of the population with 1nM after the 60min. incubation period for the MTS assay. The carboxy-functionalized PS NPs only become toxic at 50nM, where they killed about half of the population as shown in *Figure 5-1*. These findings agreed with the previous studies that used silica nanoparticles and polystyrene nanoparticles with positive and negative functionalization.^{6, 23, 29, 31, 46-47} It was observed that the amine-functionalized PS NPs had more toxicity than the neutral and the carboxy-functionalized PS NPs. This can be due to the “proton sponge” effect.^{13-14, 48} On one hand, the amine-functionalized PS NPs are adsorbed and bound to the cell membrane, then internalized through endosomes. Due to the low pH inside the cell, the positive charge of the amine groups is protonated by accepting more protons, leading to the entrance of H₂O and ions into the endosome, increasing its size. Finally the endosome ruptures and liberating the amine-functionalized PS NPs with the cell’s cytoplasm.¹³⁻¹⁴ After that the amine-functionalized PS NPs

are free to interact with the cell's organelles including the mitochondria. They decrease the mitochondrial metabolic activities that is crucial for the cells viability and increase reactive oxygen species (ROS). Then the reactive oxygen species can interrupt enzymatic reactions, damaging DNA and finally leading to cell death.^{42, 49-51} So that, the amine-functionalized PS NPs are more toxic to the AML12 cells than the neutral and the carboxy-functionalized PS NPs that don't exhibit the proton sponge phenomenon. On the other hand, the neutral polystyrene nanoparticles were non-toxic to the AML12 cells and reached more than 100% of cell viability, this may be due to the increased enzymatic and metabolic activity of the cells, thus increasing the amount of formazan produced from the MTS reagent reduction, finally increasing the absorbance.⁵² Because these findings, in particular for the amine-functionalized PS NPs, we adjusted the study by using concentrations lower than 1nM which are: 0.3, 0.5 and 0.7nM for the uptake studies.

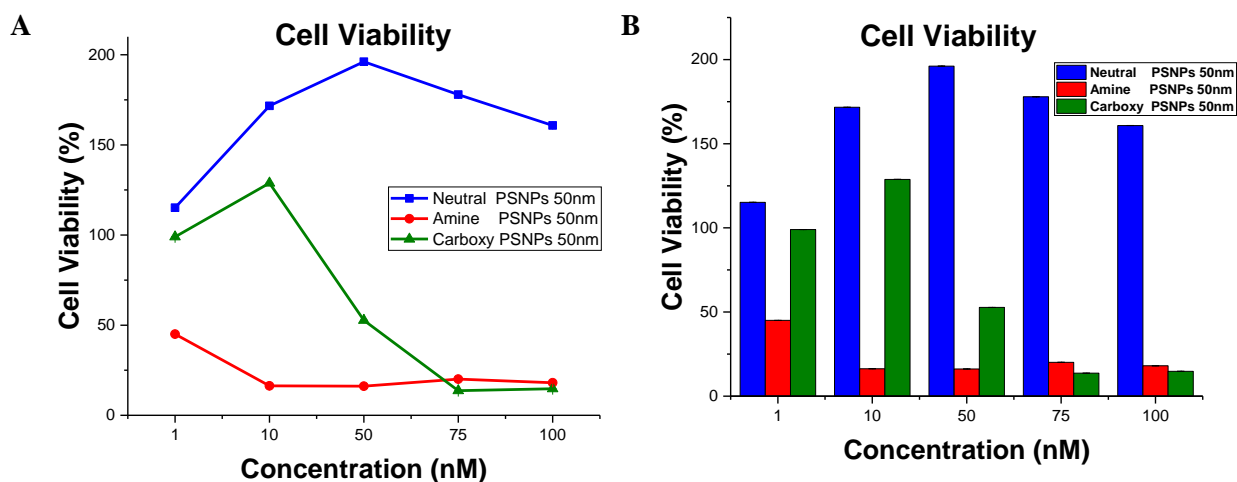


Figure 5-1: Percentage of cell viability and the toxicity of 50nm neutral, amine and carboxy-functionalized polystyrene nanoparticles with 1, 10, 50, 75 & 100nM concentrations.

5.2 Polystyrene nanoparticles degradation

5.2.1 Study of NP degradation for varying PS NPs surface charge

In this study we used 50nm neutral, amine and carboxy-functionalized PS NPs with 5nM in concentration. Degradation is one of the important aspects that must be tested to know if the AML12 cells degrade the nanoparticles or not. In order to achieve this, the total fluorescence count of nanoparticles with cell exposure (CT) and nanoparticles without cell exposure (NP) were measured for the at 0, 1, 4, 12 & 24h time intervals as shown in *Figure 5-2*. It was found that the P-value in the t-test between the two populations (CT and NP) was 0.17, 0.10, 0.08, 0.14 & 0.08 at which the $P > 0.05$, which means that there is no significant difference between the fluorescence of the nanoparticles alone and with the cells. Thus, there is no nanoparticle degradation induced by the AML12 cells or in-vitro environment. This observation supports the high stability and non-biodegradability of polystyrene nanoparticles.^{8, 11}

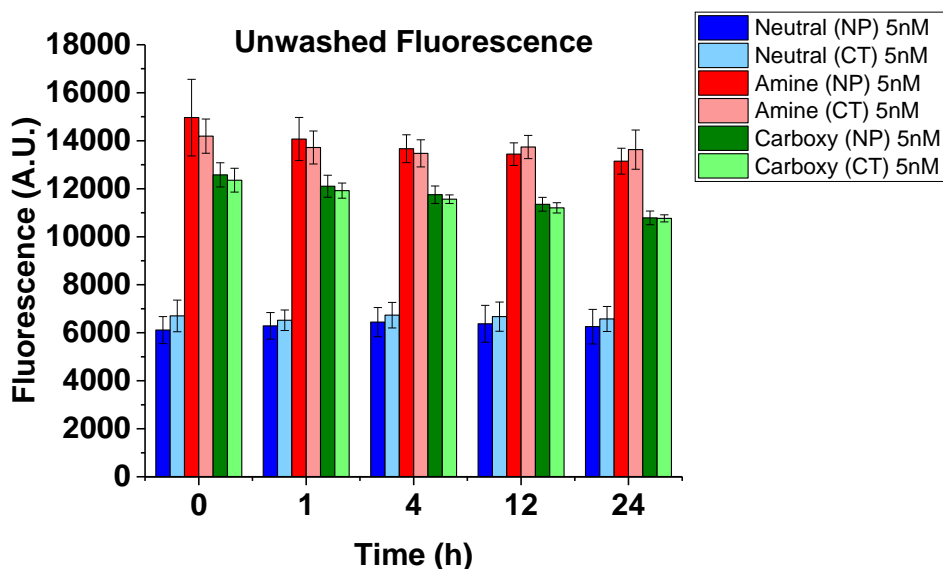


Figure 5-2: Total fluorescence count of nanoparticles with cell exposure (CT) and nanoparticles without cell exposure (NP) for 50nm neutral, amine and carboxy-functionalized polystyrene nanoparticles of 5nM in concentration at 0, 1, 4, 12 & 24h time intervals. Standard errors are represented by error bars attached to each column (n=3).

5.2.2 Study of NP degradation for varying PS NPs size

In this study we used 50, 100 and 500nm carboxy-functionalized polystyrene nanoparticles at 0, 1, 4, 12 & 24h time intervals to test if the nanoparticle degrades or not. We used the carboxy-functionalized polystyrene nanoparticles with different sizes as a model, due to their lower toxicity to the cells. It's important to note that the concentrations used for both the 50 and 100nm carboxy-functionalized PS NPs are different from the 500nm carboxy-functionalized PS NPs. We used 0.25nM for 50 and 100nm and 0.01nM for the 500nm PS NPs, because the commercially available carboxy-functionalized PS NPs are all 2.5% (w/w), but as the size of the nanoparticle increases the molar concentration decreases with constant 2.5% weight percent. In our case the concentration of the stock solution for the 50, 100 and 500nm carboxy-functionalized PS NPs is 640, 75.89 and 0.607nM, respectively. We found P-value between the CT and NP through t-test for the 50 and 100nm $P > 0.05$ and the values for the 50nm carboxy PS NPs were 0.12, 0.13, 0.24, 0.35 and 0.8, for the 100nm carboxy PS NPs were 0.16, 0.38, 0.61, 0.06 and 0.15, which means that there is no significant difference between CT and NP, thus no PS NPs degradation. While, the P-value for the 500nm carboxy PS NPs were 1.7×10^{-6} , 1.4×10^{-6} , 7.2×10^{-7} , 1.2×10^{-4} and 9.8×10^{-4} , so there was degradation for the 500nm carboxy PS NPs as shown in *Figure 5-3*.

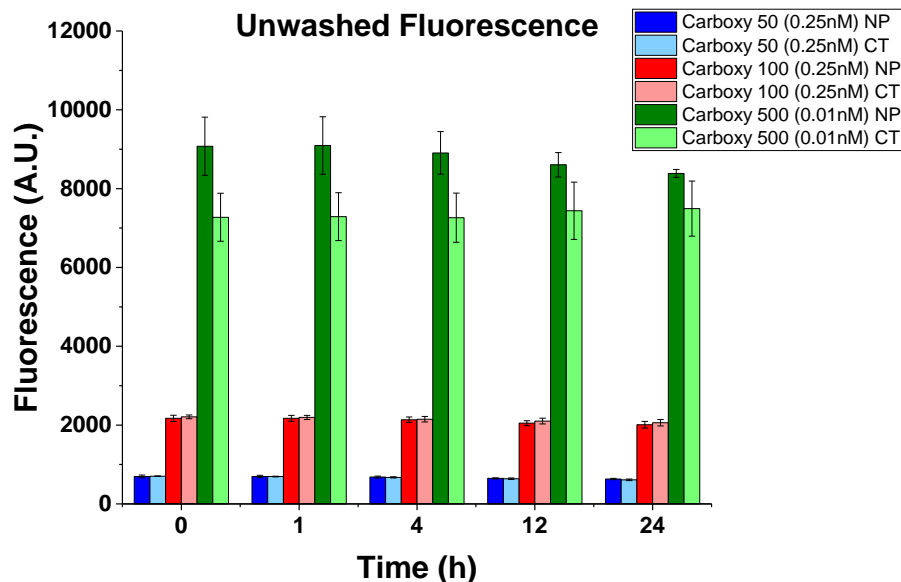
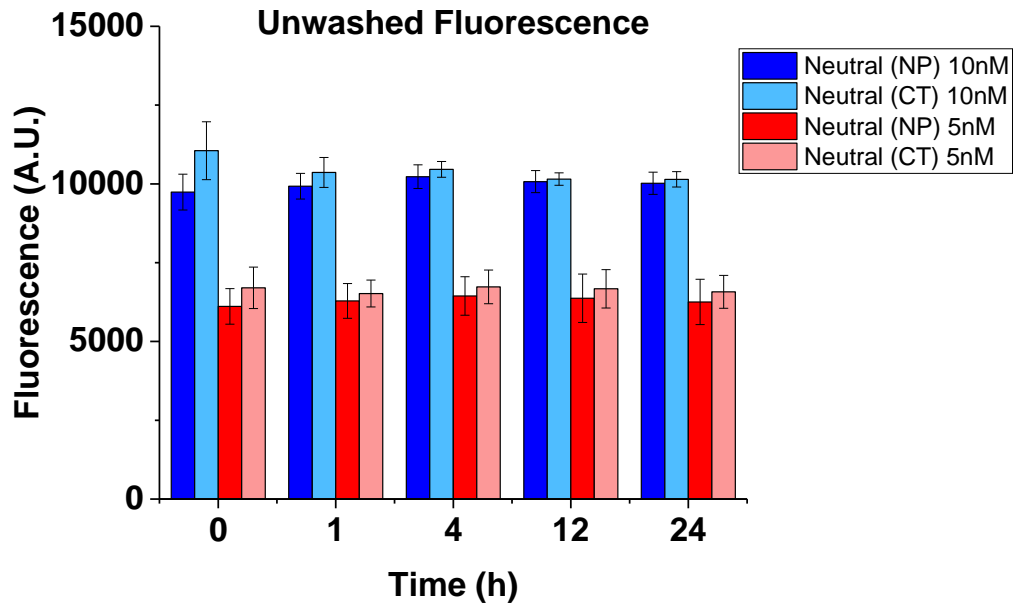


Figure 5-3: Total fluorescence count of nanoparticles with cell exposure (CT) and nanoparticles without cell exposure (NP) for 50, 100 and 500nm carboxy-functionalized polystyrene nanoparticles at 0, 1, 4, 12 & 24h time intervals. Standard errors are represented by error bars attached to each column (n=3).

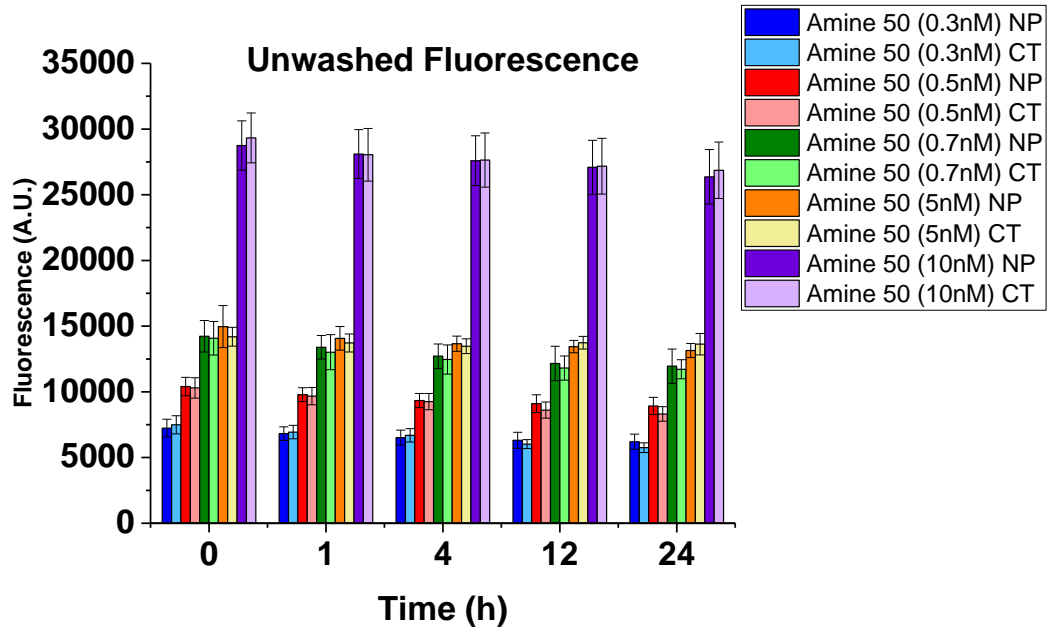
5.2.3 Study of NP degradation for varying PS NPs concentration

For the concentration dependent degradation study, we completed three sets of experiments including: 50nm neutral PS NPs of 5 and 10nM in concentration; 50nm amine-functionalized PS NPs of 0.3, 0.5, 0.7, 5 and 10nM in concentration; and 50nm carboxy-functionalized PS NPs of 0.25, 3, 5 and 10nM in concentration. Experiments were completed for 0, 1, 4, 12 and 24h time intervals. It was found that there is no nanoparticle degradation from the AML12 cells for all the polystyrene nanoparticles with different concentrations as shown in *Figure 5-4.*, and $P > 0.05$ of the CT and NP which means that there is no significant difference between CT and NP. The results obtained in the degradation test aligned with what stated in literature about the non-biodegradability of polystyrene nanoparticles.^{8,11}

A



B



C

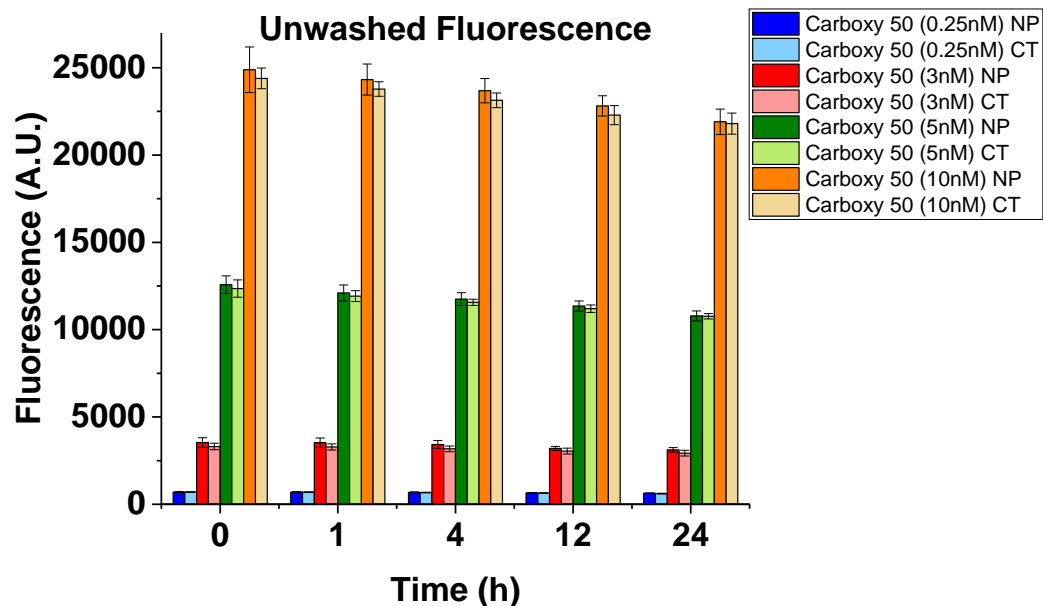


Figure 5-4: Total unwashed fluorescence count of nanoparticles with cell exposure (CT) and nanoparticles without cell exposure (NP) for A) 50nm neutral-functionalized PS NPs, B) 50nm amine-functionalized PS NPs and C) 50nm carboxy-functionalized PS NPs with different concentrations at 0, 1, 4, 12 & 24h time intervals. Standard errors are represented by error bars attached to each column (n=3).

CHAPTER 6:

UPTAKE & KINETICS OF POLYSTYRENE NANOPARTICLES

We carried out three uptake studies with different physiochemical properties including: charge dependent (50nm neutral, amine and carboxy-functionalized PS NPs), size dependent (50, 100 and 500nm carboxy-functionalized PS NPs) and concentration dependent (50nm neutral with 5 & 10nM in concentration) (50nm amine-functionalized 0.3, 0.5, 0.7, 5 & 10nM in concentration) (50nm carboxy 0.25, 3, 5 & 10nM in concentration). They will be shown in this chapter.

6.1 Quantitative Measurement: Fluorescent Plate Reader

The fluorescence plate reader used to know the uptake of the fluorescently labelled polystyrene nanoparticles quantitatively after washing the excess nanoparticles that weren't internalized by the cells.

6.1.1 Charge dependent uptake study

An uptake study was performed to know the effect of the surface charge of the PS NPs on quantitative nanoparticle uptake. In this study 50nm neutral, amine and carboxy-functionalized PS NPs with 5nM in concentration were used. From the results of the raw fluorescent data at time (0, 1, 4, 12 & 24h), we found that the amine-functionalized PS NPs had the highest fluorescence followed by neutral, and carboxy-functionalized PS NPs as shown in *Figure 6-1*. However, note that this reflects on both uptake and the fluorescent brightness of nanoparticles. It was observed that the amine-functionalized nanoparticles were brighter than neutral and the carboxy functionalized nanoparticles.^{6, 23, 29}

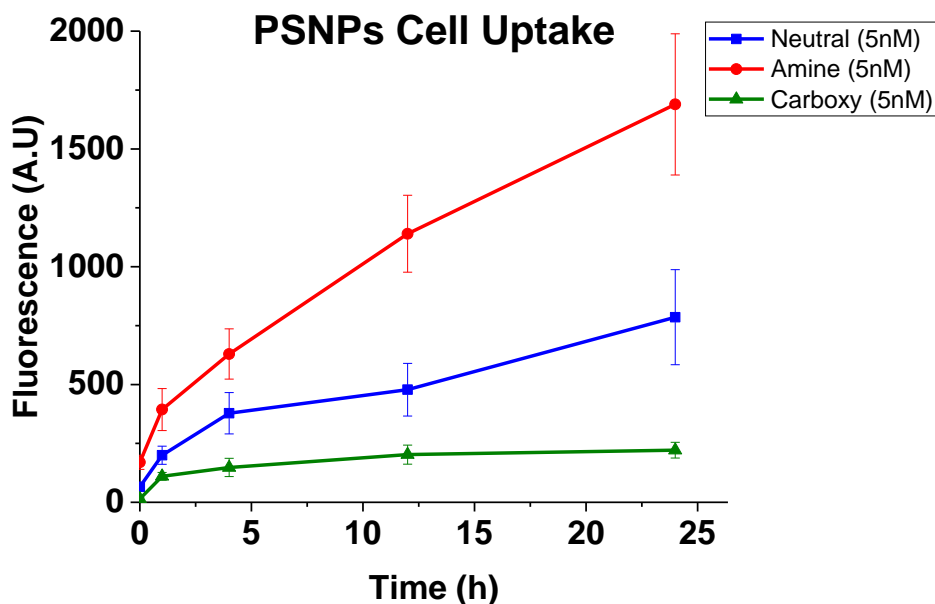


Figure 6-1: Uptake profile of 50nm neutral, amine and carboxy-functionalized polystyrene nanoparticles of 5nM in concentration over 24h period obtained from the raw fluorescent data. Standard errors are represented by error bars attached to each point (n=3).

When it comes to the fraction uptake of the nanoparticles dose, the PS NP fluorescence signal was measured and used in calculations. In our study, in order to know the exact fraction uptaken of the PS NPs by the cells, an internal calibration was used to account for the difference in fluorescent labelling of different PS NPs. The design of the 96 well plate was made as following: washed wells at time =x (CK), unwashed wells of cells and nanoparticles (CT), unwashed wells of nanoparticles (NP), media wells (CM) and trypsin wells (T). Each one of them was made in triplicate wells for each nanoparticle type. The whole experiment was made in triplicate (n=3). The F_{cell} (fraction of dose) is the washed fluorescence at time =x (CK) divided by the total fluorescence of the nanoparticles with cell exposure (CT) at time=0 as shown in *Equation (6.1)*.

$$F_{Cell} = \frac{I_{washed\ t=x}}{I_{CT\ t=0}} \quad (6.1)$$

By using this way, we can calculate the fraction of nanoparticles uptaken by cells from the original dose. Fraction of dose F_{Cell} was plotted versus time for the 50nm neutral, amine and

carboxy-functionalized PS NPs with 5nM in concentration. It was found that the uptake of the amine PS NPs was higher than the carboxy PS NPs. Also, the fraction uptake of the neutral PS NPs was similar to the amine ones. In order to understand the differences in uptake, the uptake mechanism of different polystyrene nanoparticles must be known. The uptake of any nanoparticle occurs in two main steps: the nanoparticle's adsorption and internalization as shown in *Figure 6-2*. The first adsorption step occurs spontaneously according to Langmuir adsorption.⁵³⁻⁵⁶ At which, the adsorbate (nanoparticles) adsorbs on the adsorbent surface (cell membrane) in the available binding sites via Van der Waals interactions until reaching equilibrium or steady state at which the number of binding sites equals to the occupied ones. Then the second step is the binding and then potential internalization via various endocytosis mechanisms can occur beside desorption. After reaching the equilibrium of binding, the endosome is formed and internalized forming new binding sites on the surface of the cell for the production of more endosomes.⁵³⁻⁵⁴

In the case of amine-functionalized PS NPs as shown in *Figure 6-3* the adsorption is enhanced due to the electrostatic interaction between the positive charge of the amine group and the negative charge of the lipids in the cell membrane.⁵³ This way of interaction occurs with different nanoparticles with positive charge functionalization.⁵⁷⁻⁶⁰ But for the carboxy-functionalized PS NPs there are repulsive forces with the cell membrane that limit the adsorption. In addition, when the nanoparticles with the DMEM media containing fetal bovine serum (FBS) are added to the cells, the proteins of the fetal bovine serum surround the carboxy-functionalized PS NPs decreasing their adsorption on the cell membrane and uptake as well. According to literature, the uptake of the carboxy-functionalized PS NPs without serum was higher than that with serum, because the proteins in the serum prevent the interaction between the nanoparticles and the cells.⁵⁴ For the neutral PS NPs, they exhibit a high uptake fraction as the amine PS NPs, they adopt a

different internalization mechanism which is the macropinocytosis at which part of the cell membrane protrudes outwards enclosing the nanoparticles within a macropinosome to be internalized according to literature.^{6, 14, 20, 23-24, 29, 36, 41, 54}

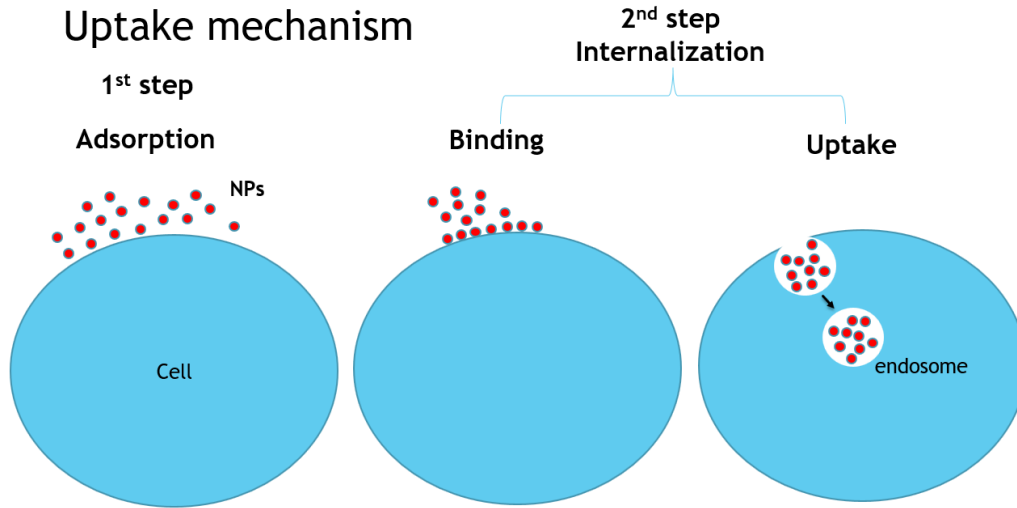


Figure 6-2: The two main steps of the uptake mechanism of nanoparticles: the nanoparticle’s adsorption and internalization.

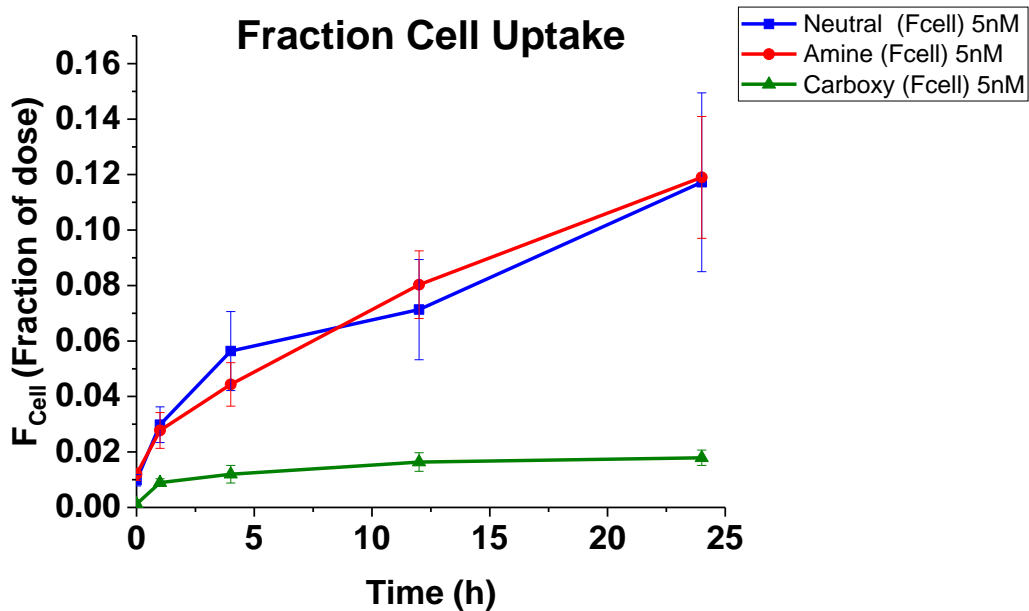


Figure 6-3: Fractional uptake of dose of 5nM neutral, amine and carboxy-functionalized polystyrene nanoparticles obtained from the ratio between the washed fluorescence at time =x (CK) and the unwashed nanoparticles with cell exposure (CT) at time=0. Standard errors are represented by error bars attached to each point (n=3).

Also, the concentration uptake was plotted versus time. The data were obtained by multiplying F_{cell} by the concentration of the nanoparticle applied to the assay. We found that the concentration of NPs internalized after 24hr of the amine PS NPs was about 1.2nM from the 5nM initial concentration, while for the carboxy PS NPs was about 0.1nM from the 5nM initial concentration as shown in *Table 6-1* and *Figure 6-4*. It was also observed that the carboxy PS NPs uptake saturates at 4hr. This may be due adsorption on the cell membrane or internalization being a rate limiting step.^{20, 29}

Table 6-1: The concentration uptake of 5nM neutral, amine and carboxy PS NPs at 0, 1, 4, 12 & 24hrs

	Initial concentration (nM)	0hr	1hr	4hr	12hr	24hr
Neutral PS NPs	5	0.09	0.29	0.56	0.71	1.17
Amine PS NPs	5	0.11	0.27	0.44	0.80	1.18
Carboxy PS NPs	5	0.012	0.08	0.11	0.16	0.17

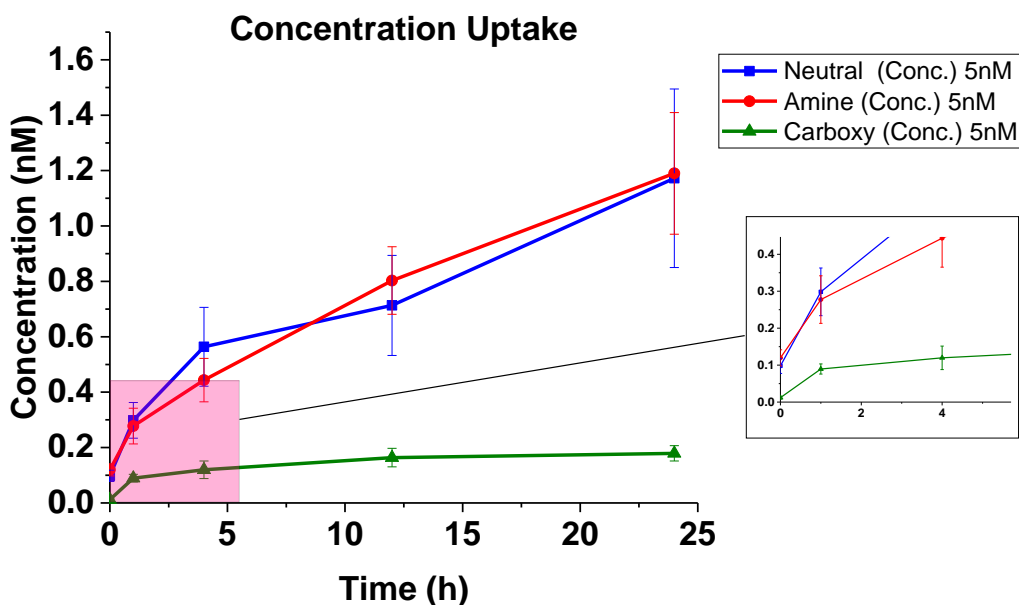


Figure 6-4: Concentration of uptake fraction of 5nM neutral, amine and carboxy-functionalized polystyrene nanoparticles. The concentration is the F_{cell} (fraction of dose) multiplied by concentration of the nanoparticle.

Standard errors are represented by error bars attached to each point (n=3).

6.1.2 Size dependent uptake study

In this study we used carboxy PS NPs as a model for different sizes, due to their lower toxicity than the amine PS NPs. We used 0.25nM for 50 and 100nm carboxy PS NPs and 0.01 for the 500nm carboxy PS NPs. As stated earlier in chapter 4, we used a different concentration for the 500nm carboxy-functionalized PS NPs because the commercially available carboxy-functionalized PS NPs are 2.5% (w/w) and as the size of the nanoparticle increases the molar concentration decreases with constant 2.5% weight percent. From the results of the raw fluorescence washed, we observed that the fluorescence signal of the 500nm carboxy PS NPs with 0.01 in concentration were higher than for the 100 and 50nm carboxy with 0.25nM in concentration as shown in *Figure 6-5*. Note that these results reflect on both uptake and fluorescent brightness of the PS NPs.^{7, 20, 35}

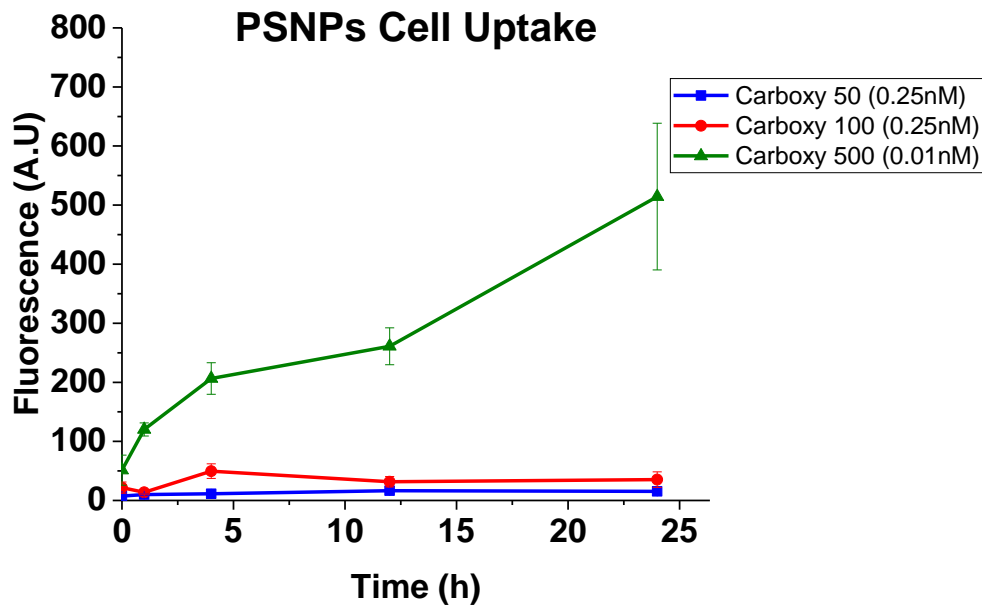


Figure 6-5: Uptake profile of 50, 100 and 500nm carboxy-functionalized polystyrene nanoparticles over 24h period. Standard errors are represented by error bars attached to each point (n=3).

Regarding the F_{cell} , it was found that the uptaken fraction of the 500nm were higher than 100 and 50nm carboxy nanoparticles. The fraction dose of the 500nm nanoparticles taken by the cell was about triple that of the 100 and 50nm carboxy-functionalized PS NPs. The fraction uptake of the 50nm was higher than that of the 100nm carboxy-functionalized PS NPs as shown in *Figure 6-6*. This can be clarified by the difference in internalization mechanism between 50, 100 and 500nm PS NPs. At which the 500nm carboxy-functionalized PS NPs used the macropinocytosis, however the 50 and 100nm used clathrin mediated endocytosis. We can deduce also that as the size of the carboxy PS NPs decreases, the reactivity between the PS NPs and the cell surface increase, the repulsive forces increase leading to lower adsorption and lower nanoparticles internalization as well.^{7, 25, 31, 35, 41, 61}

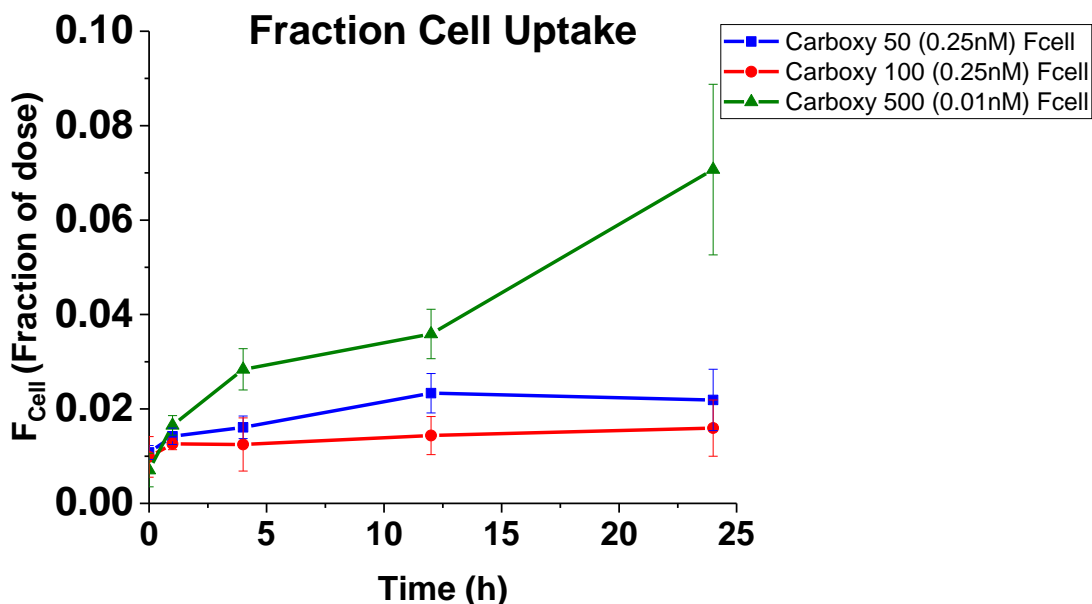


Figure 6-6: Fractional uptake of 50, 100 and 500nm carboxy-functionalized polystyrene nanoparticles from the ratio between the washed fluorescence at time =x (CK) and the unwashed nanoparticles with cell exposure (CT) at time=0. Standard errors are represented by error bars attached to each point (n=3).

Regarding the concentration of PS NPs uptaken, it was found that the concentration of the 50nm carboxy PS NPs internalized is higher than that of 100nm carboxy PS NPs and the 500nm

carboxy PS NPs had the lowest concentration of PS NPs internalized as shown in *Table 6-2* and *Figure 6-7*. This means that as the size of the nanoparticle decrease the binding sites on the cell membrane increases, so increasing the amount of internalized nanoparticles and hence increasing the concentration of PS NPs internalized, which means that the size of carboxy PS NPs is inversely proportional to the concentration uptake.^{7, 35}

Table 6-2: The concentration uptake of 50, 100 & 500nm carboxy-functionalized PS NPs at 0, 1, 4, 12 & 24hrs

	Initial concentration (nM)	0hr	1hr	4hr	12hr	24hr
50nm Carboxy PS NPs	0.25	0.002	0.003	0.004	0.005	0.005
100nm Carboxy PS NPs	0.25	0.002	0.001	0.002	0.003	0.003
500nm Carboxy PS NPs	0.01	0.00007	0.0001	0.0002	0.0003	0.0007

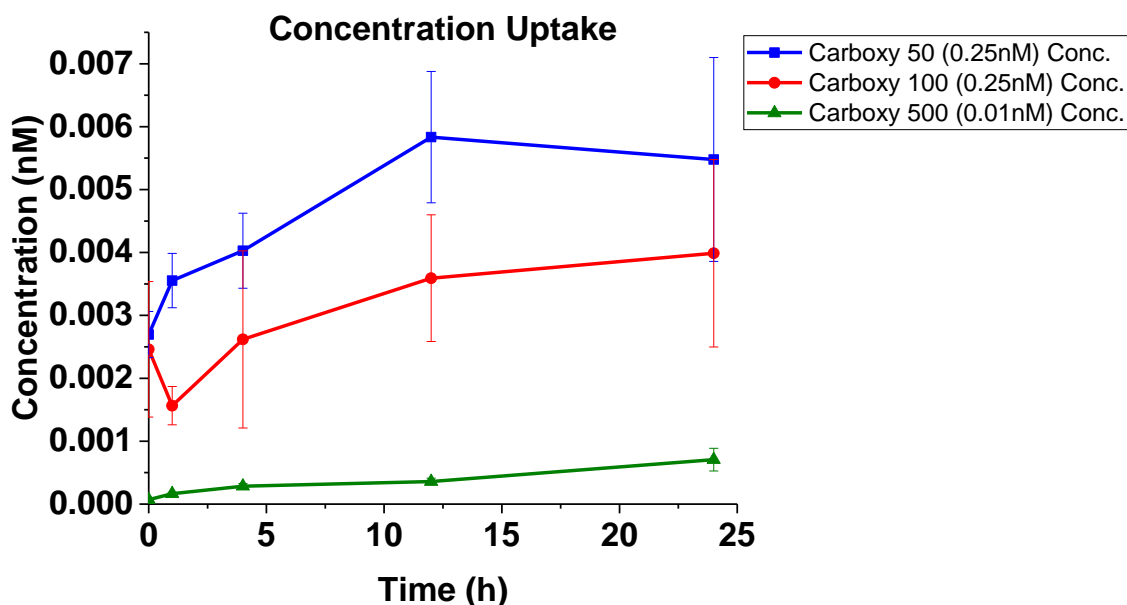


Figure 6-7: This graph shows the concentration of the uptake fraction 50, 100 and 500nm carboxy-functionalized polystyrene nanoparticles. The concentration is the F_{cell} (fraction of dose) multiplied by concentration of the nanoparticle. Standard errors are represented by error bars attached to each point (n=3).

6.1.3 Concentration dependent uptake study

In this study we considered three sets of samples including: 50nm neutral PS NPs of 5 and 10nM in concentration; 50nm amine-functionalized PS NPs of 0.3, 0.5, 0.7, 5 and 10nM in concentration; and 50nm carboxy-functionalized PS NPs of 0.25, 3, 5 and 10nM in concentration.

From the results of the raw fluorescent data of 50nm neutral PS NPs with 5 and 10nM in concentration at time (0, 1, 4, 12 & 24h). We found that the fluorescence of the 10nM is higher than 5nM neutral nanoparticles as shown in *Figure 6-8*. This is because the fluorescent signal comes from both uptake and the brightness of the PS NPs. For the 50nm amine-functionalized PS NPs with 0.3, 0.5, 0.7, 5 and 10nM in concentration at time (0, 1, 4, 12 & 24h). We found that the raw fluorescent data of the 10nM is the highest followed by 5, 0.7, 0.5 and 0.3 amine-functionalized PS NPs as shown in *Figure 6-9*. Regarding the 50nm carboxy-functionalized PS NPs with 0.25, 3, 5 and 10nM in concentration were used. the fluorescence signal of 50nm carboxy-functionalized PS NPs with 0.25, 3, 5 and 10nM in concentration at time (0, 1, 4, 12 & 24h). We found that the fluorescence of the 10nM is the highest followed by 5, 3 and 0.25 carboxy-functionalized PS NPs as shown in *Figure 6-10*. From the observation of the raw fluorescent signal for all the PS NPs with different concentrations, we deduce that as the concentration of PS NPs increase regardless their charge, the raw fluorescent signal increase due to the increase of the labelling on the nanoparticle.⁵⁴

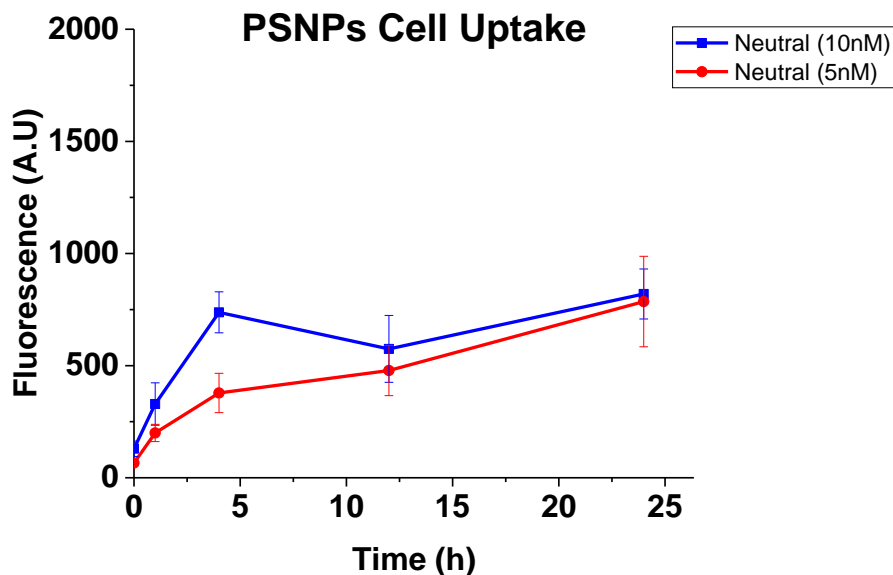


Figure 6-8: This graph shows the uptake profile of 50nm neutral polystyrene nanoparticles with 5 and 10nM concentrations over 24h period. Standard errors are represented by error bars attached to each point (n=3).

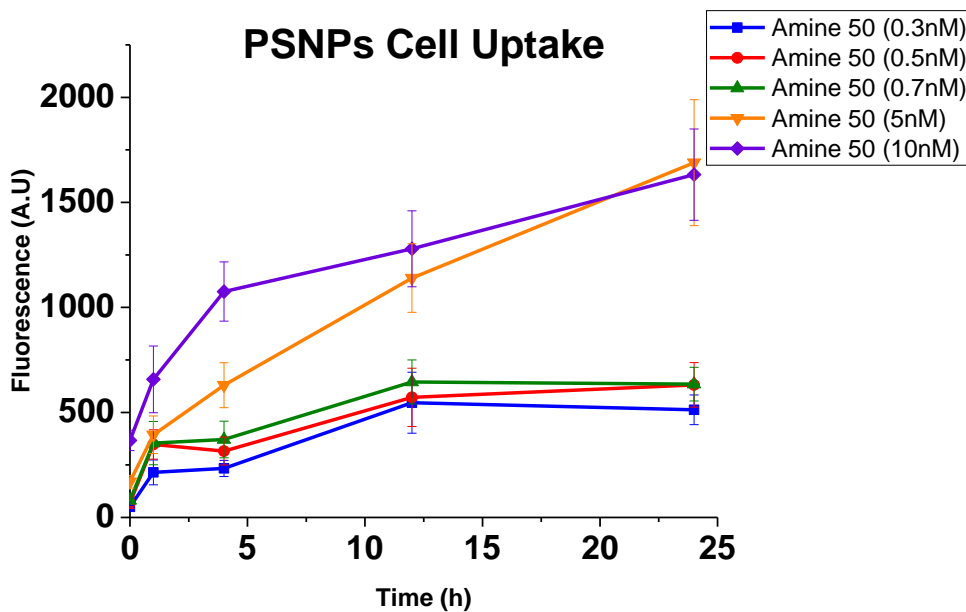


Figure 6-9: This graph shows the uptake profile of 50nm amine-functionalized polystyrene nanoparticles with different concentrations (0.3, 0.5 & 0.7, 5 and 10nM) over 24h period. Standard errors are represented by error bars attached to each point (n=3).

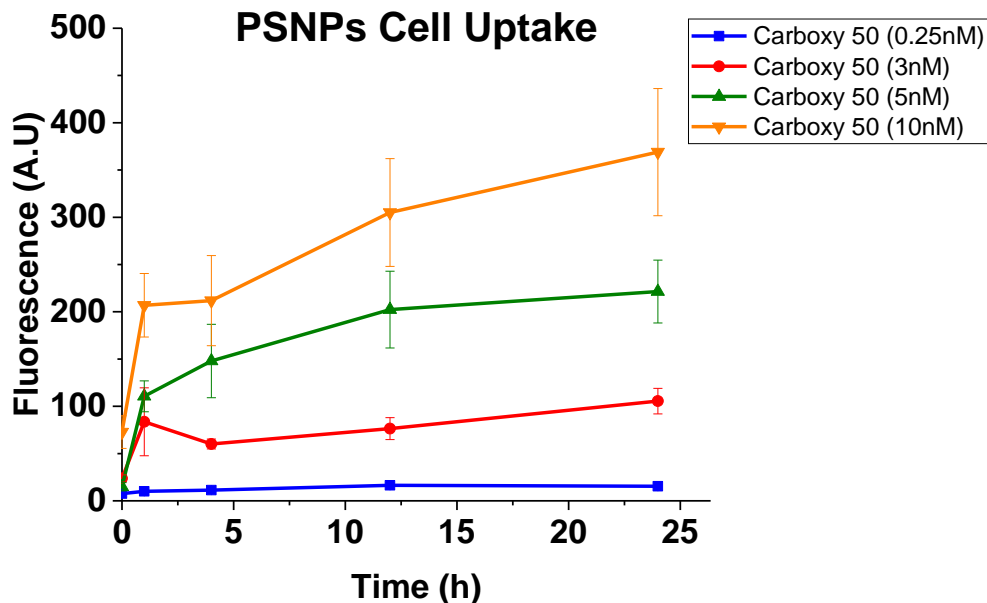


Figure 6-10: This graph shows the uptake profile of 50nm carboxy-functionalized polystyrene nanoparticles with different concentrations (0.25, 3, 5 and 10nM) over 24h period. Standard errors are represented by error bars attached to each point (n=3).

For the 50nm neutral PS NPs of 5 and 10nM in concentration, it was found that the fraction uptake of both 5 and 10nM in the few hours was the same because this reflects the adsorption of the nanoparticles on the surface of the cell. While after 4hr the neutral PS NP 5nM in concentration was higher than the 10nM as shown in *Figure 6-11*. This is because the saturation of the higher concentration occurs earlier than the lower one. This also can be related to the available binding sites for the 5nM is higher than the 10nM. This means that as the concentration of the neutral PS NPs increases, the fraction uptake increase.³

For the 50nm amine PS NPs of 0.3, 0.5, 0.7, 5 and 10nM concentration, it was found that the amine PS NPs with 5nM had the highest fraction uptake followed by the 0.3, 0.5, 0.7 and 10nM amine PS NPs as shown in *Figure 6-12*. It was observed that the 5nM had the highest fraction uptake compared to lower and higher concentrations, this may be due to the optimum concentration

for the cell's uptake. At which the nanoparticles with low concentrations (0.3, 0.7 and 0.7nM) takes longer time for filling the endosome, so they had lower fraction uptake than the 5nM. And the higher concentration (10nM) had lower number of binding sites available for binding, so they had lower fraction uptake. The 5nM made the equilibrium between the available binding sites on the cell membrane and the time needed for filling the endosome.⁵³⁻⁵⁴

Finally, for the 50nm carboxy PS NPs of 0.25, 3, 5 and 10nM concentration, it was found that the fraction uptake of the carboxy PS NPs with 3nM in concentration was the highest followed by 0.25, 5, 10nM carboxy PS NPs as shown in *Figure 6-13*. At which the nanoparticles with low concentrations (0.25nM) takes longer time for filling the endosome, so they had lower fraction uptake than the 3nM. And the higher concentration (5, 10nM) had lower number of binding sites available for binding, so they had lower fraction uptake. The 3nM made the equilibrium between the available binding sites on the cell membrane and the time needed for filling the endosome.⁵³⁻
⁵⁴This means that the fraction uptake of the carboxy-functionalized PS NPs is independent of the concentration.

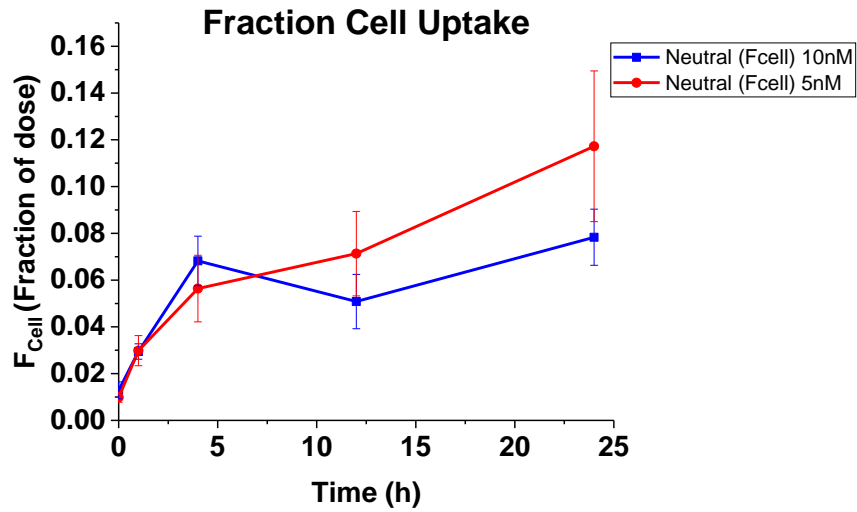


Figure 6-11: Fractional uptake 50nm neutral-functionalized polystyrene nanoparticles of 5 and 10nM concentrations from the ratio between the washed fluorescence at time =x (CK) and the unwashed nanoparticles with cell exposure (CT) at time=0. Standard errors are represented by error bars attached to each point (n=3).

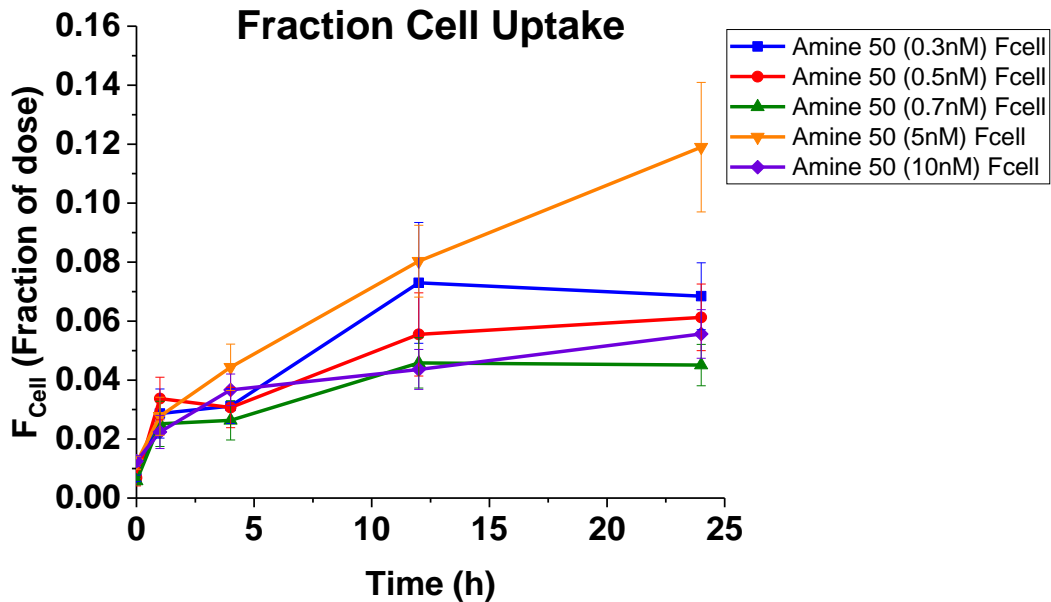


Figure 6-12: Fractional uptake 50nm amine-functionalized polystyrene nanoparticles of 0.3, 0.5, 0.7, 5 and 10nM concentrations from the ratio between the washed fluorescence at time =x (CK) and the unwashed nanoparticles with cell exposure (CT) at time=0. Standard errors are represented by error bars attached to each point (n=3).

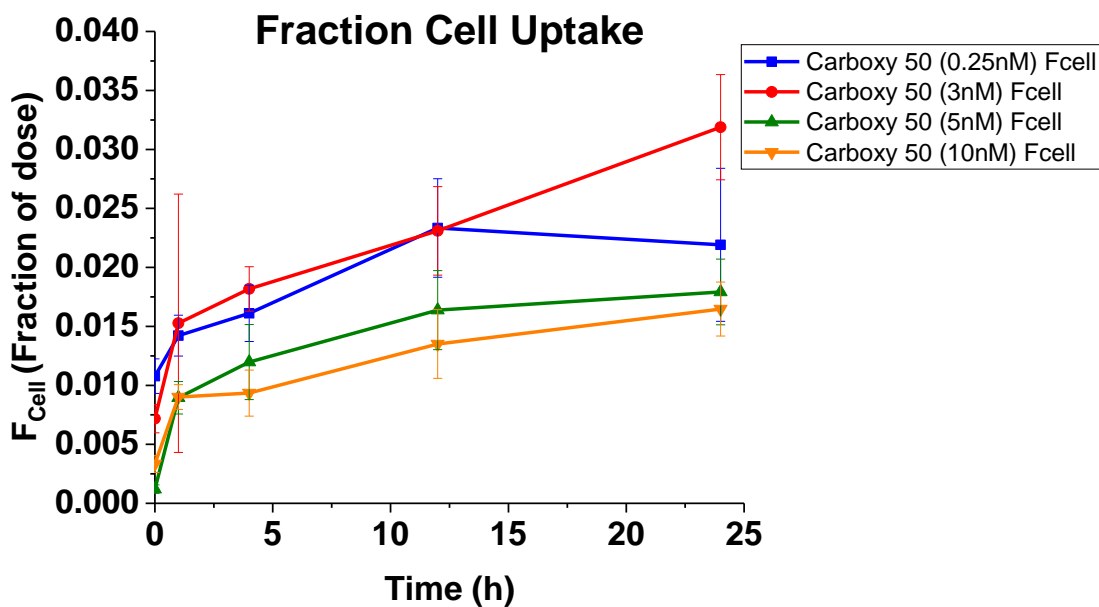


Figure 6-13: Fractional uptake 50nm carboxy-functionalized polystyrene nanoparticles of 0.25, 3, 5 and 10nM concentration from the ratio between the washed fluorescence at time =x (CK) and the unwashed nanoparticles with cell exposure (CT) at time=0. Standard errors are represented by error bars attached to each point (n=3).

Regarding the concentration of PS NPs internalized by cells, it was found that the concentration of uptaken PS NPs by the neutral PS NPs at 24hr was 1.1nM from the 5nM original dose concentration, while it was 0.7nM from the 10nM original dose concentration as shown in *Table 6-3* and *Figure 6-14*. As we observed that when the concentration of the original dose increase, it doesn't increase the internalized fraction concentration. While, the concentration of PS NPs internalized by the 50nm amine PS NPs at 24hr was 1.1nM from the 5nM original dose concentration, while it was 0.5nM from the 10nM original dose, 0.03nM from the 0.7nM original dose, 0.03 from 0.5nM original dose and 0.02 from 0.3nM original dose as shown in *Table 6-4* and *Figure 6-15*. The 5nM amine PS NPs was the highest in both fraction uptake and concentration. While, the fraction uptake of the 10nM amine PS NPs is the lowest but it was higher in the concentration uptake. It doesn't always mean that as the original concentration increase the concentration of PS NPs internalized increases. When it comes to the carboxy-functionalized PS

NPs, it was found that the concentration of PS NPs internalized by the 50nm carboxy PS NPs of 5nM in concentration was the highest followed by 10, 3 and 0.25nM carboxy PS NPs as shown in *Table 6-5* and *Figure 6-16*. There is a threshold and an equilibrium for the adsorption of the nanoparticles occur upon changing the concentration.

Table 6-3: The concentration uptake of 5 and 10nM neutral PS NPs at 0, 1, 4, 12 & 24hrs.

	Initial concentration (nM)	0hr	1hr	4hr	12hr	24hr
Neutral PS NPs	5	0.09	0.29	0.56	0.71	1.17
Neutral PS NPs	10	0.12	0.29	0.68	0.50	0.78

Table 6-4: The concentration uptake of 0.3, 0.5, 0.7, 5 & 10nM amine PS NPs at 0, 1, 4, 12 & 24hrs.

	Initial concentration (nM)	0hr	1hr	4hr	12hr	24hr
Amine PS NPs	0.3	0.002	0.008	0.009	0.02	0.02
Amine PS NPs	0.5	0.003	0.01	0.01	0.02	0.03
Amine PS NPs	0.7	0.004	0.01	0.01	0.03	0.03
Amine PS NPs	5	0.11	0.27	0.44	0.80	1.18
Amine PS NPs	10	0.12	0.22	0.36	0.43	0.55

Table 6-5: The concentration uptake of 0.25, 3, 5 & 10nM amine PS NPs at 0, 1, 4, 12 & 24hrs.

	Initial concentration (nM)	0hr	1hr	4hr	12hr	24hr
Carboxy PS NPs	0.25	0.002	0.003	0.004	0.005	0.005
Carboxy PS NPs	3	0.02	0.04	0.05	0.06	0.09
Carboxy PS NPs	5	0.01	0.08	0.11	0.16	0.17
Carboxy PS NPs	10	0.03	0.09	0.09	0.13	0.16

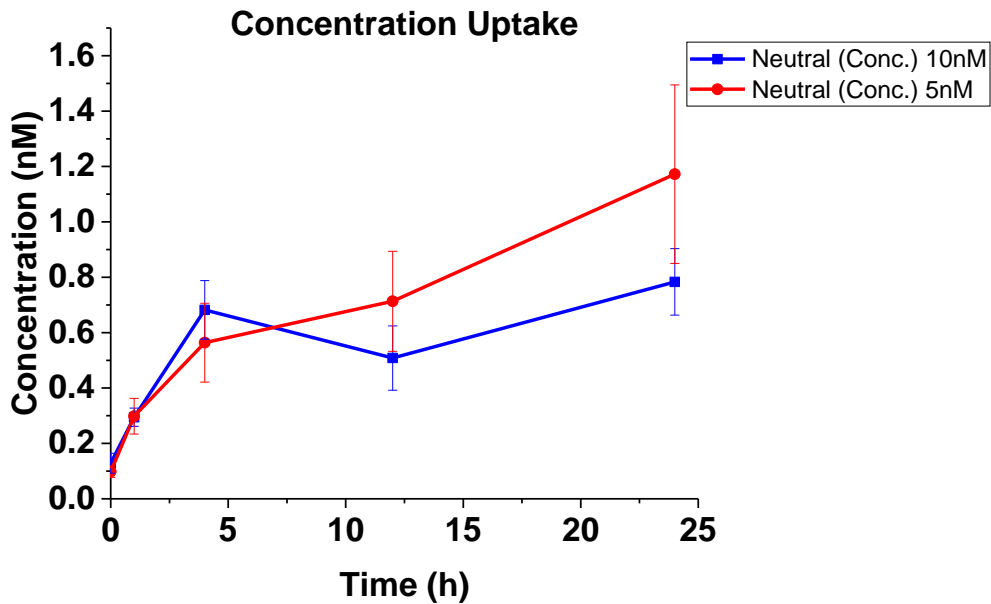


Figure 6-14: Concentration of the uptake fraction of 5 and 10nM neutral polystyrene nanoparticles. The concentration is the F_{cell} (fraction of dose) multiplied by concentration of the nanoparticle. Standard errors are represented by error bars attached to each point (n=3).

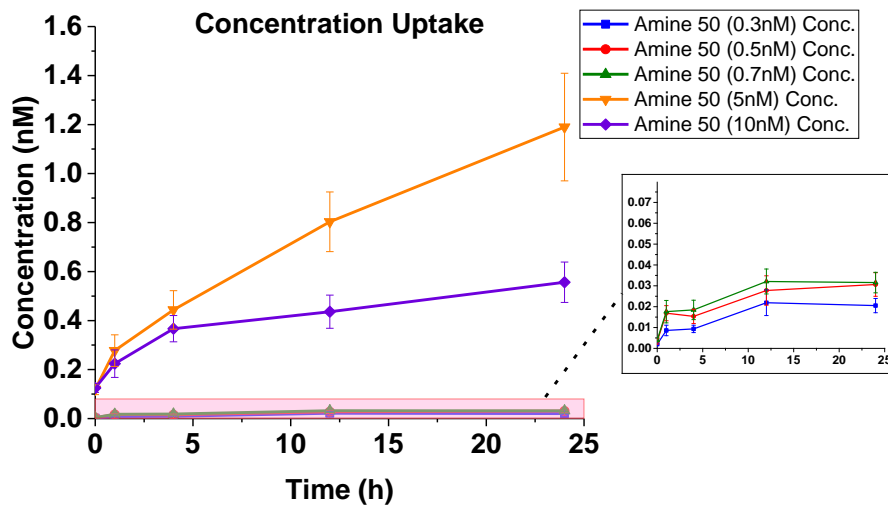


Figure 6-15: Concentration of the uptake fraction of 0.3, 0.5, 0.7, 5 and 10nM amine-functionalized polystyrene nanoparticles. The concentration is the F_{cell} (fraction of dose) multiplied by concentration of the nanoparticle. Standard errors are represented by error bars attached to each point (n=3).

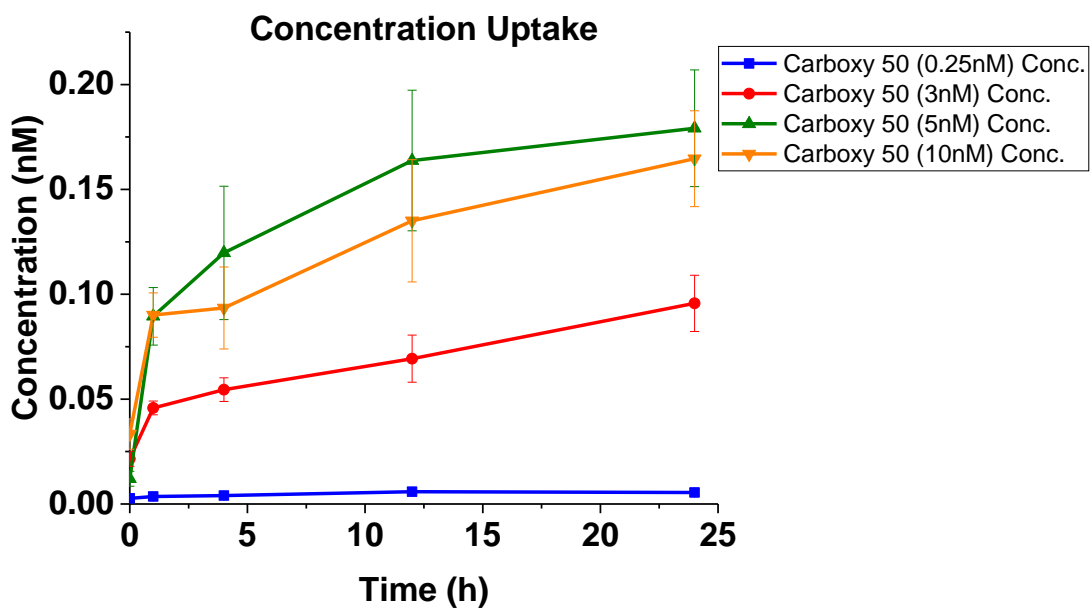


Figure 6-16: Concentration of the uptake fraction of 0.25, 3, 5 and 10nM carboxy-functionalized polystyrene nanoparticles. The concentration is the F_{cell} (fraction of dose) multiplied by concentration of the nanoparticle.

Standard errors are represented by error bars attached to each point (n=3).

6.2 Analysis of the rate of polystyrene nanoparticles uptake

In this section we report our results on the study of the effect of the concentration on the rate of uptake of 50nm neutral, 50nm amine and 50nm carboxy PS NPs. The concentrations of neutral nanoparticles are: 0.25, 0.7, 3, 5 & 10nM, the concentrations of amine nanoparticles are: 0.3, 0.5, 0.7, 5 & 10nM, and the concentrations of carboxy nanoparticles are: 0.25, 3, 5 & 10nM. The log-log plot is done to know the linear relationship between two parameters, in our case the concentration and the uptake. The log of the concentration of internalized PS NPs for each nanoparticle and concentration were obtained and plotted versus log time to produce the trendline for each nanoparticle concentration as shown in *Table 6-6*, *Table 6-7* and *Figure 6-17-A* for neutral PS NPs, *Table 6-8*, *Table 6-9* and *Figure 6-18-A* for amine PS NPs, *Table 6-10*, *Table 6-11* and *6.19-A* for carboxy PS NPs. For time = zero, we calculated log 0.001, because the log of zero is undefined Since, the Log of (x), x must be greater than zero.

Table 6-6: This table shows the concentration of internalized neutral PS NPs with 0.25, 0.7, 3, 5 & 10nM at 0, 1, 4, 12 & 24h time intervals.

Time (hr)	0.25nM	0.7nM	3nM	5nM	10nM
0.001	0.0042442	0.0143159	0.052159	0.1065379	0.147036
1	0.0171081	0.0418136	0.1183225	0.2258476	0.320928
4	0.0214491	0.052683	0.1515027	0.2079264	0.408022
12	0.0198662	0.0552492	0.2018578	0.322759	0.632288
24	0.0184215	0.0667676	0.298195	0.3302928	0.903852

Table 6-7: This table shows the log values for both time and the concentration of internalized neutral PS NPs with 0.25, 0.7, 3, 5 & 10nM.

Time (Log)	0.25nM	0.7nM	3nM	5nM	10nM
-3	-2.372204106	-1.844182587	-1.282670845	-0.972495973	-0.832577052
0	-1.766797274	-1.378681945	-0.926932603	-0.6461845	-0.493592214
0.602059991	-1.668590702	-1.278329848	-0.819579705	-0.682090328	-0.389316544
1.079181246	-1.701885714	-1.257673854	-0.69495447	-0.491121603	-0.199085124
1.380211242	-1.734675264	-1.175434526	-0.52549958	-0.481100925	-0.043902658

Table 6-8: This table shows the concentration of internalized amine PS NPs with 0.3, 0.5, 0.7, 5 & 10nM at 0, 1, 4, 12 & 24h time intervals.

Time (hr)	0.3nM	0.5nM	0.7nM	5nM	10nM
0.001	0.00202	0.00341	0.00405	0.11965	0.12506
1	0.0086	0.01687	0.01761	0.27739	0.22416
4	0.00935	0.01534	0.01845	0.44351	0.36673
12	0.02189	0.02775	0.03208	0.80306	0.43618
24	0.02053	0.03064	0.03156	1.18995	0.55655

Table 6-9: This table shows the log values for both time and the concentration of internalized amine PS NPs with 0.3, 0.5, 0.7, 5 & 10nM

Time (Log)	0.3nM	0.5nM	0.7nM	5nM	10nM
-3	-2.694648631	-2.467245621	-2.392544977	-0.922087297	-0.902881576
0	-2.065501549	-1.772884917	-1.754240644	-0.556909199	-0.649441882
0.602059991	-2.029188389	-1.81417464	-1.73400363	-0.353096584	-0.435653562
1.079181246	-1.659754238	-1.556737013	-1.49376564	-0.095252006	-0.360334252
1.380211242	-1.687611051	-1.513711239	-1.500863005	0.075528713	-0.254495813

Table 6-10: This table shows the concentration of internalized carboxy PS NPs with 0.25, 3, 5 & 10nM at 0, 1, 4, 12 & 24h time intervals.

Time (hr)	0.25nM	3nM	5nM	10nM
0.001	0.001	0.00269	0.02154	0.012
1	1	0.00355	0.07579	0.08949
4	4	0.00403	0.05452	0.11974
12	12	0.00583	0.06929	0.16378
24	24	0.00548	0.09566	0.17915

Table 6-11: This table shows the log values for both time and the concentration of internalized carboxy PS NPs with 0.25, 3, 5 & 10nM

Time (Log)	0.25nM	3nM	5nM	10nM
-3	-2.57025	-1.66675	-1.92082	-1.47651
0	-2.44977	-1.12039	-1.04823	-1.04528
0.60206	-2.39469	-1.26344	-0.92176	-1.02947
1.079181	-2.23433	-1.15933	-0.78574	-0.86947
1.380211	-2.26122	-1.01927	-0.74678	-0.78344

Furthermore, to know the rate of uptake, the slope of the trendlines were plotted versus nanoparticle concentration as shown in *Table 6-12, Table 6-13, Table 6-14, Figure 6-17-B, Figure 6.18-B and Figure 6-19-B*. The slope (dy/dx) reflects the change of the uptake (rate of the nanoparticle uptake nM) over the change of time (hour). The unit of the rate of uptake is nM/hr. For the kinetics profile of the amine and carboxy PS NPs, it was found that they had two different rates of uptake profiles. By comparing both of them, it was observed that the rate of uptake lower than 5nM was different, but higher than 5nM was slightly similar, at which as the concentration of amine PS NPs increase, the rate of uptake decreases, but for the carboxy PS NPs as the concentration of increase, the rate of uptake increases until 5nM. However, for the neutral Ps NPs,

they exhibit a steady state of rate of uptake in between the amine and carboxy PS NPs as shown in *Figure 6-20* for the combine rates of uptake for neutral, amine and carboxy PS NPs.

Table 6-12: The concentration versus the slope of each concentration for the neutral PS NPs with 0.25, 0.7, 3, 5 & 10nM

Concentration (nM)	0.25	0.7	3	5	10
Rate (nM/hr)	0.16046	0.16046	0.16046	0.16046	0.16046

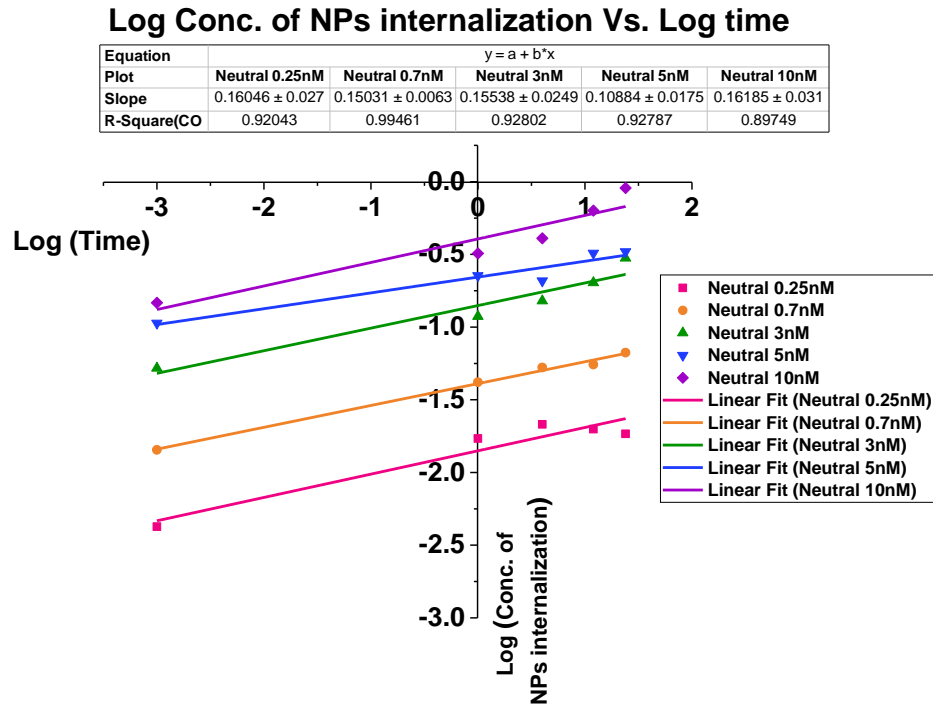
Table 6-13: The concentration versus the slope of each concentration for the amine PS NPs with 0.3, 0.5, 0.7, 5 & 10nM

Concentration (nM)	0.3	0.5	0.7	5	10
Rate (nM/hr)	0.2306	0.2134	0.2059	0.2074	0.1398

Table 6-14: The concentration versus the slope of each concentration for the carboxy PS NPs with 0.25, 3, 5 & 10nM

Concentration (nM)	0.25	3	5	10
Rate (nM/hr)	0.071	0.1334	0.2731	0.1491

A



B

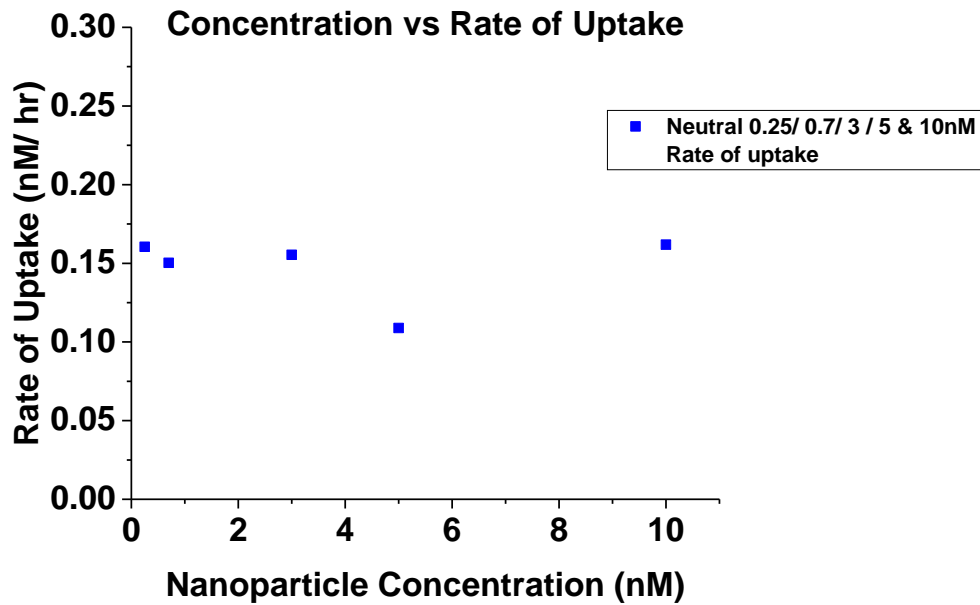
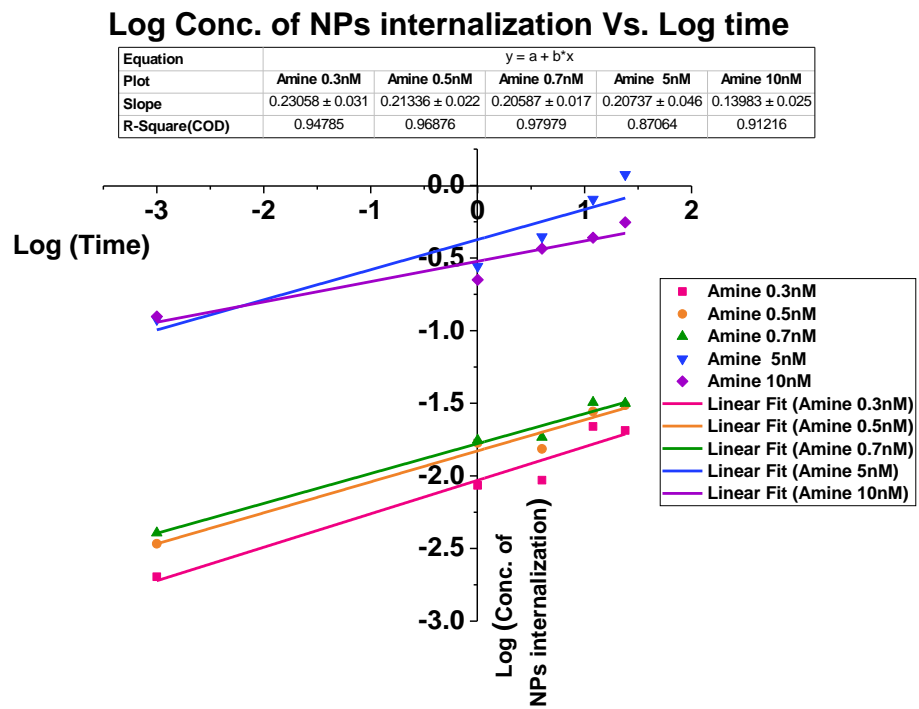


Figure 6-17: This figure shows the rate of neutral- functionalized nanoparticles uptake, A) Log cell uptake versus log time for each concentration 0.25, 0.7, 3, 5 & 10nM. B) the rate of uptake nM/hr of nanoparticles different concentrations.

A



B

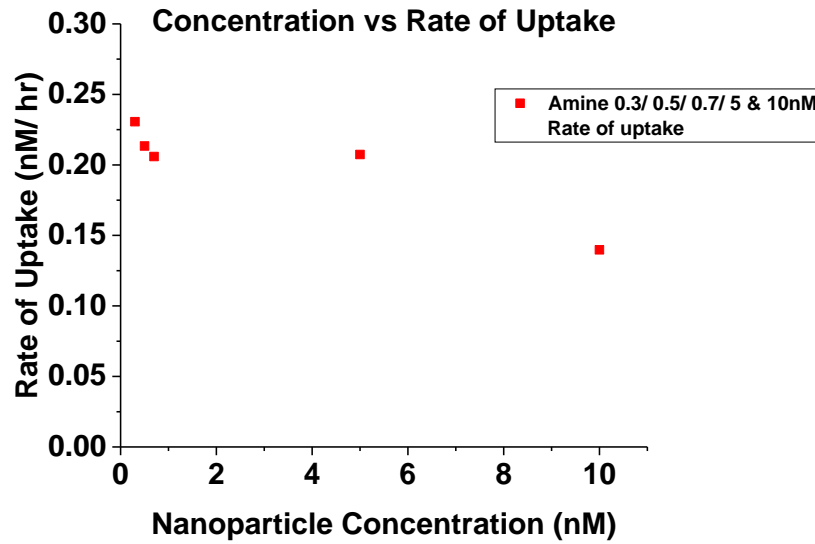
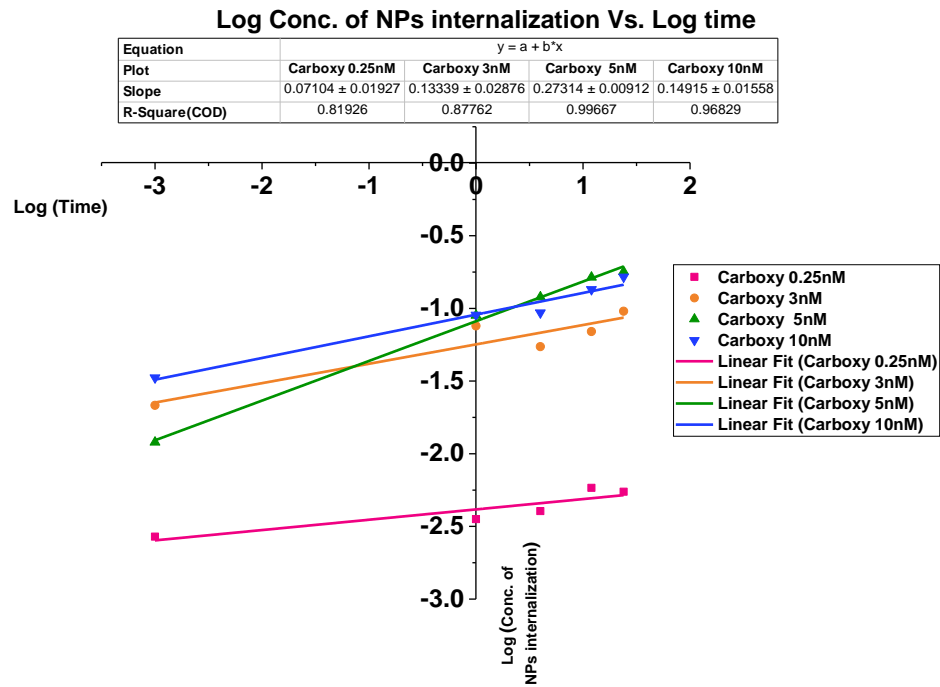


Figure 6-18: This figure shows the rate of amine- functionalized nanoparticles uptake, A) Log cell uptake versus log time for each concentration 0.3, 0.5, 0.7, 5 & 10nM. B) the rate of uptake nM/hr of nanoparticles different concentrations.

A



B

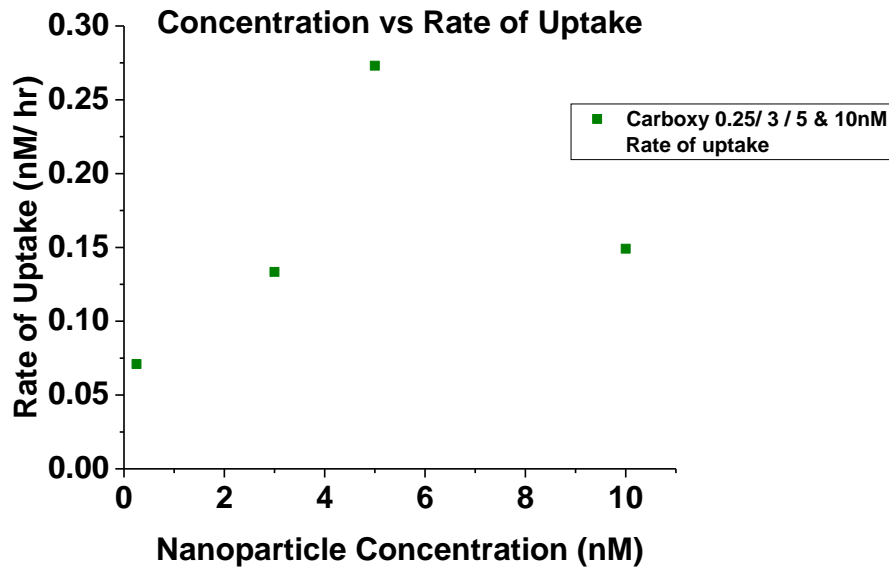


Figure 6-19: This figure shows the rate of carboxy- functionalized nanoparticles uptake, A) Log cell uptake versus log time for each concentration 0.25, 3, 5 & 10nM. B) the rate of uptake nM/hr of nanoparticles different concentrations.

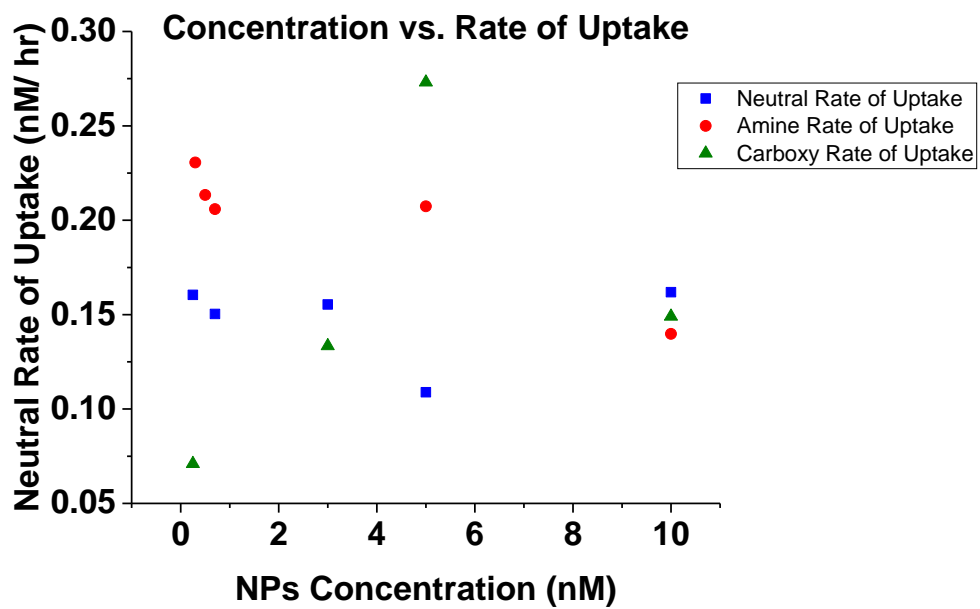


Figure 6-20: Rates of uptake (nM/hr) of neutral, amine and carboxy PS NPs.

CHAPTER 7:

QUALITATIVE MEASUREMENTS BY CONFOCAL IMAGING

The Confocal microscopy is used to visualize the uptake of the fluorescently labelled polystyrene nanoparticles qualitatively by the cells. The nucleus was stained with Hoechst 33342 dye.

7.1.1 Charge dependent uptake study

The confocal images shown in *Figure 7-1* are aligned with the raw fluorescent data for the 5nM neutral, amine and carboxy PS NPs at time 0, 1, 4, 12 & 24hr in *Figure 6-1*. It was found that the fluorescence of the 5nM neutral and carboxy-functionalized PS NPs started to appear at time = 4hr within the AML12 cells with lower uptake for the carboxy ones. However, the 5nM amine-functionalized PS NPs appeared at time = 0 and 1hr. Surprisingly, no cells were found in the case of the 5nM amine PS NPs from time = 4 until 24hr, this can be due to the stress made by the amine-functionalized PS NPs and hence cells do not attach on petri dishes for confocal staining and this agreed with the cytotoxicity results stated previously.

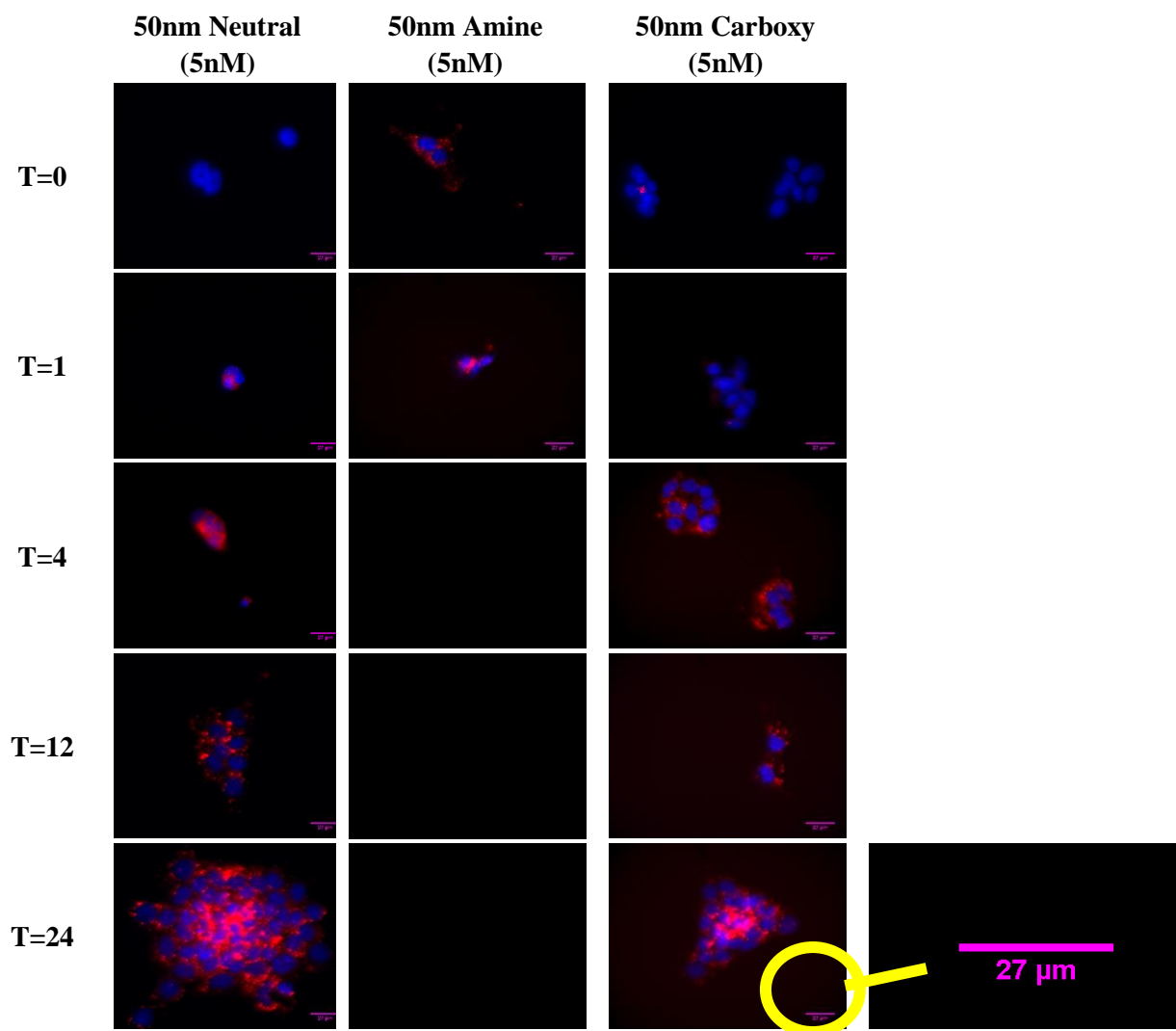


Figure 7-1: Confocal images for the uptake of 50nm neutral, amine and carboxy-functionalized polystyrene nanoparticles 5nM in concentration at 0, 1, 4, 12 & 24h time interval. The blue color indicates the nucleus and the red color indicates the PS NPs.

7.1.2 Size dependent uptake study

Also, the confocal images in *Figure 7-2* matched with the quantitative raw fluorescence data obtained in *Figure 6-5*, the uptake of the 100nm carboxy PS NPs (0.25nM) begin uptake by time = 4h and was slightly stable until time =24hr until, but it was higher than that of the 50nm carboxy PS NPs (0.25nM). Although, the concentration used for the 500nm carboxy PS NPs (0.01nM) was lower than the 50 and 100nm carboxy PS NPs, but their fraction uptake was higher due to the change in the mechanism of uptake.

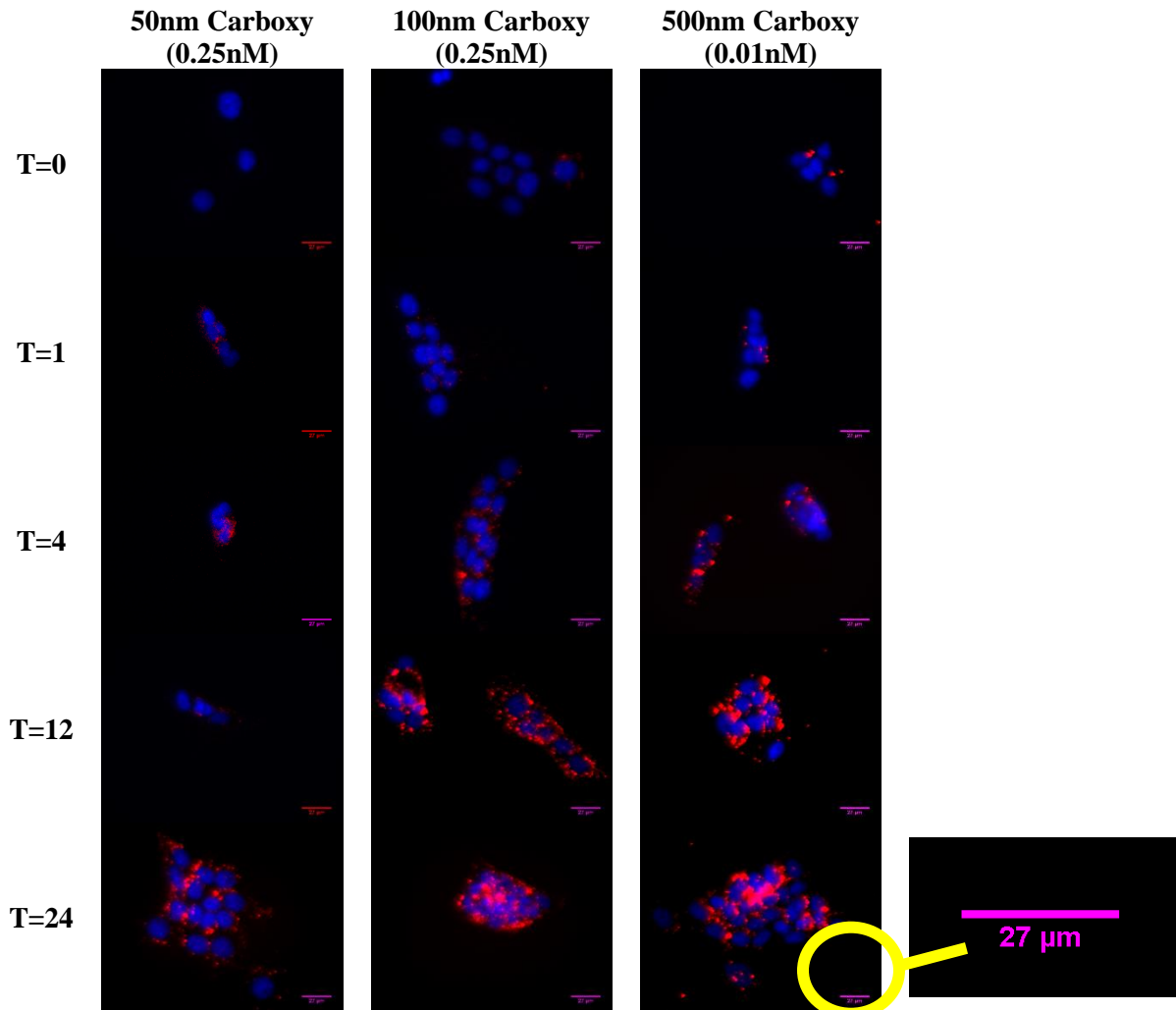


Figure 7-2: Confocal images for the uptake of 50, 100 & 500nm carboxy-functionalized polystyrene nanoparticles at 0, 1, 4, 12 & 24h time interval. The blue color indicates the nucleus and the red color indicates the PS NPs.

7.1.3 Concentration dependent uptake study

The confocal images shown in *Figure 7-4* aligned with the raw fluorescent data of the neutral PS NPs of 5 and 10nM in concentration. It was found that the uptake of the 10nM neutrals PS NPs is higher than that of the 5nM neutrals PS NPs. Both began uptake by time = 1hr and kept increasing until time = 24hr

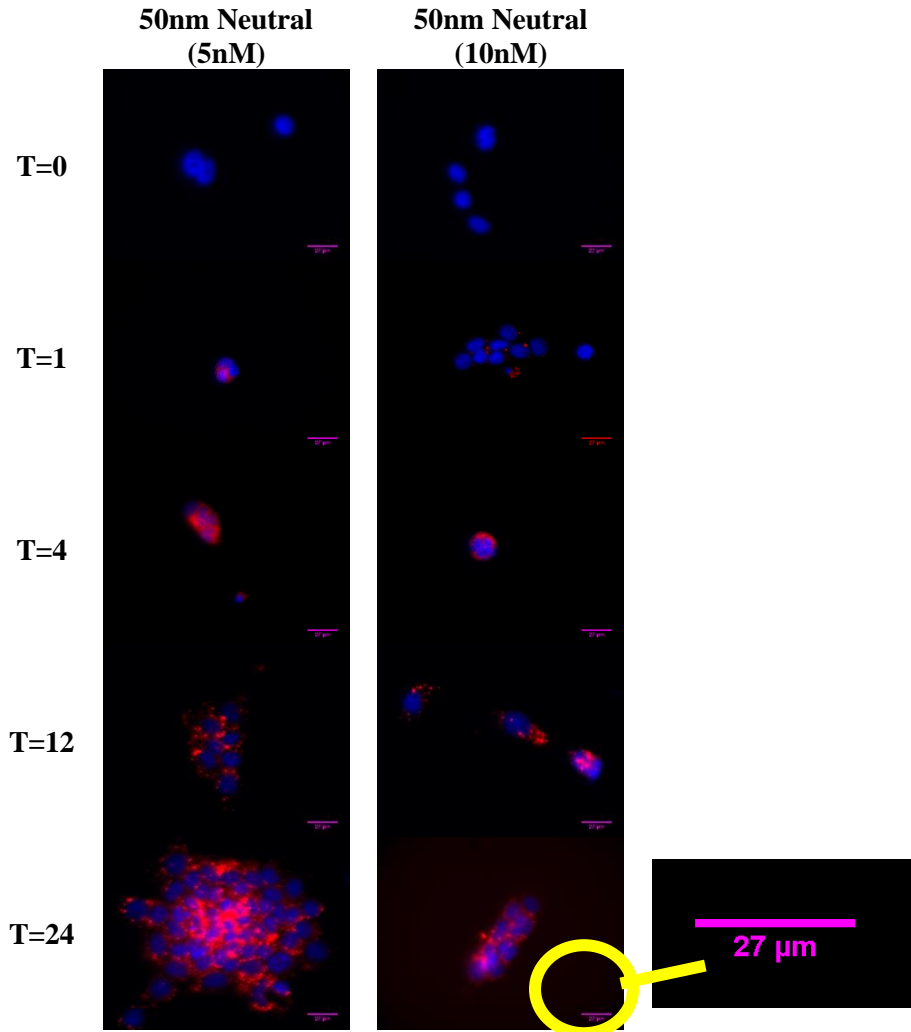


Figure 7-3: Confocal images for the uptake of 5 and 10nM neutral polystyrene nanoparticles at 0, 1, 4, 12 & 24h time interval. The blue color indicates the nucleus and the red color indicates the PS NPs.

The confocal images shown in *Figure 7-5* for the raw fluorescent data of 0.3, 0.5, 0.7, 5 & 10nM amine-functionalized PS NPs in *Figure 6-9*. It was found that both 5 & 10nM amine PS NPs started uptake at $t = 0$, while the 0.3, 0.5 and 0.7 amine PS NPs started at $t = 1$. These images showed the cells from $t = 0 - 24\text{hr}$ for 0.3, 0.5 and 0.7 amine PS NPs.

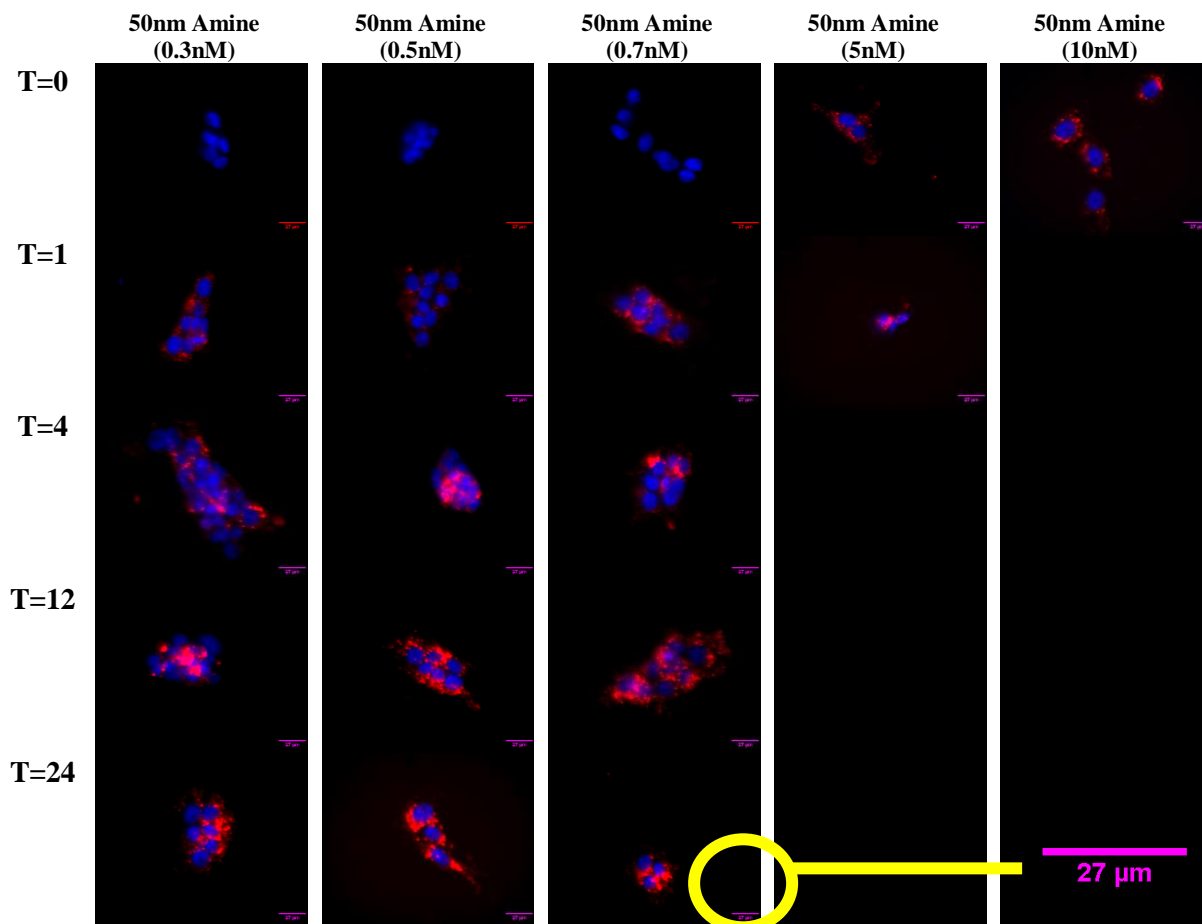


Figure 7-4: Confocal images for the uptake of 0.3, 0.5, 0.7, 5 and 10nM amine-functionalized polystyrene nanoparticles at 0, 1, 4, 12 & 24h time interval. The blue color indicates the nucleus and the red color indicates the PS NPs.

To confirm that the low conc. of amine PS NPs applied to the cells, decrease the stress made by amine PS NPs on the cells, and hence, they can attach onto the petri dishes for the confocal imaging, and at the same time these conc. 0.3, 0.5 and 0.7nM amine have lower toxicity than the 5 and the 10nM. Actually, the stress made by the amine PS NPs is the cytotoxicity and the proton sponge effect as stated in Chapter 5, at which the nanoparticles are liberated from the internalized

endosome leading to cell death.^{13-14, 48} The overall fluorescence increased ascendingly from 0.3, 0.5, 0.7, 5 & 10nM.

The confocal images shown in *Figure 7-6* for the carboxy functionalized PS NPs with different concentrations (0.25nM, 3, 5 and 10nM). These images matched with the raw fluorescence data of the carboxy-functionalized PS NPs shown in *Figure 6-10*.

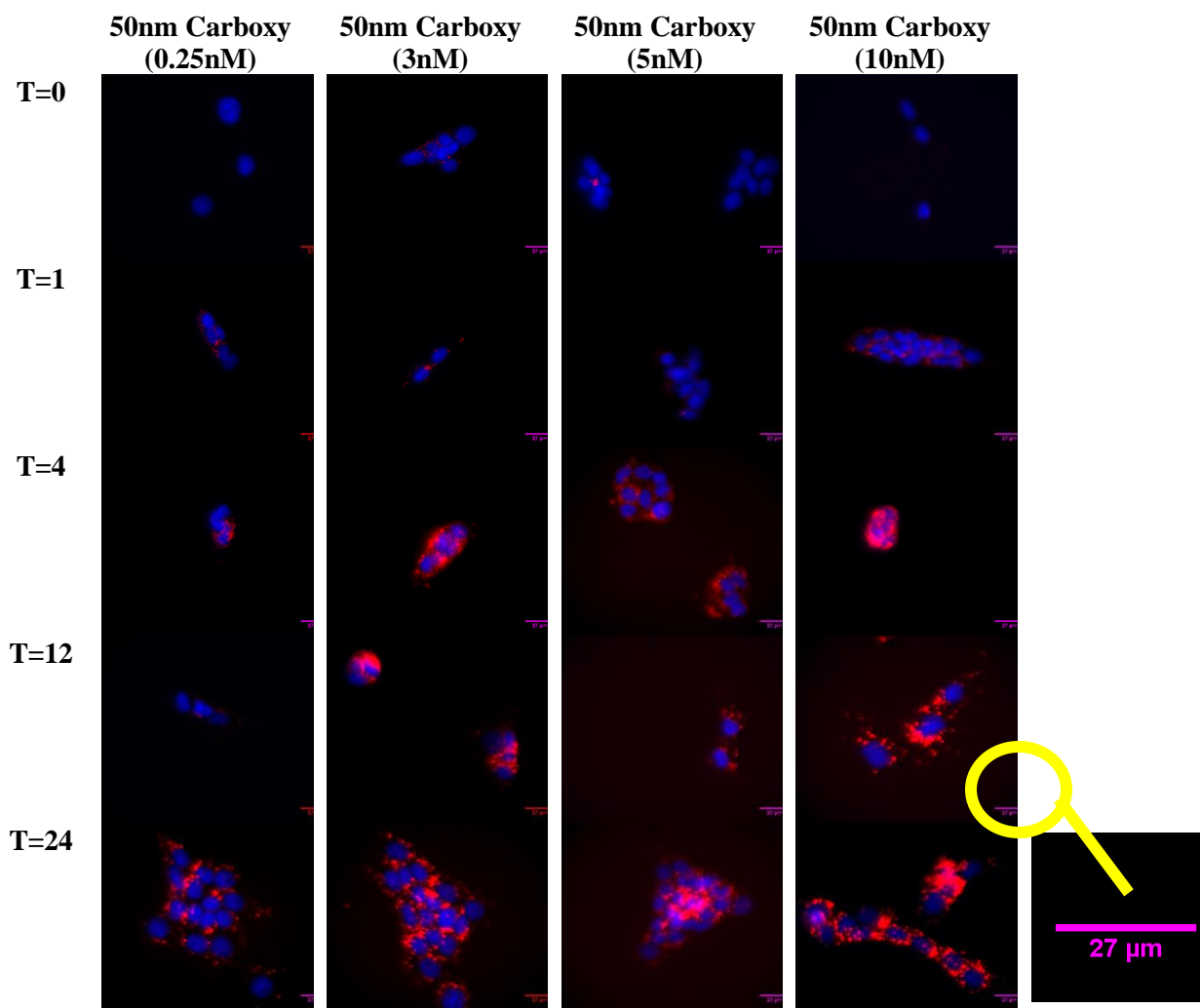


Figure 7-5: Confocal images for the uptake of 0.25, 3, 5 and 10nM carboxy-functionalized polystyrene nanoparticles at 0, 1, 4, 12 & 24h time interval. The blue color indicates the nucleus and the red color indicates the PS NPs.

It was found that the uptake of 3, 5 and 10nM started at time = 1hr, but with very high uptake at time = 4hr. The uptake of the 0.25nM carboxy-functionalized PS NPs was very low, even though

the uptake began at time =1h, but it appeared clearly at time = 24hr. This means that as the concentration increases, the fluorescence signal increase as well.

CHAPTER 8:

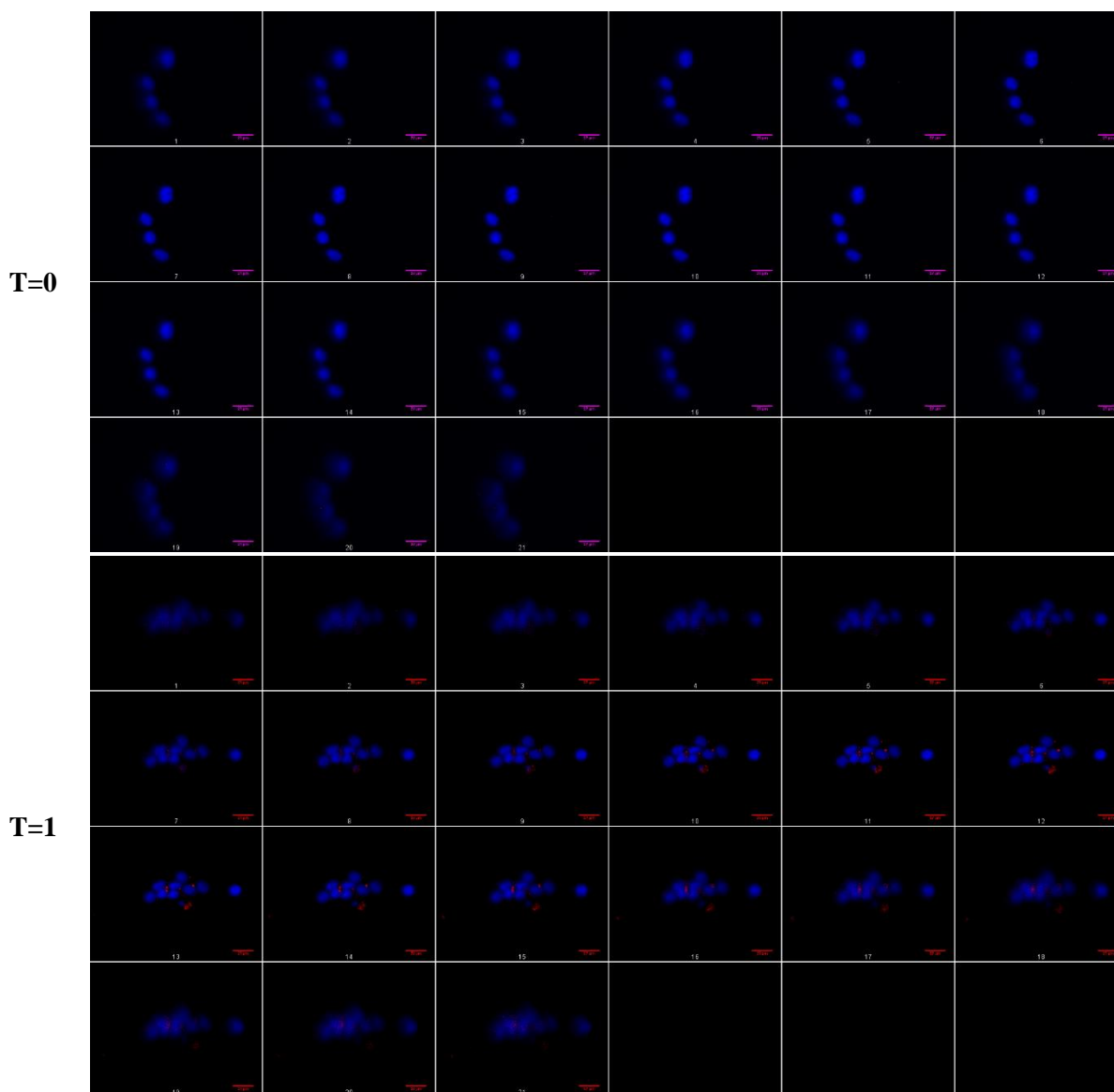
CONCLUSION AND FUTURE WORK

In conclusion, we tested the uptake profile of nanoparticles as a function of nanoparticle's charge, size and concentration. Characterization of the neutral, amine and carboxy-functionalized PS NPs was done by UV-Visible spectrophotometer, dynamic light scattering and the zeta sizer to know the absorption peak, size and charge for the nanoparticles in our study. Three different uptake studies were done; charge, size and concentration dependent. Moreover, degradation of the polystyrene nanoparticles was calculated. Furthermore, the rate of uptake of the amine and the carboxy-functionalized PS NPs was calculated. Also, we obtained the confocal images for the different PS NPs as a qualitative measurement for uptake. *Firstly*, we found that the amine-functionalized PS NPs were toxic to the cells due to a phenomenon called "proton sponge". Regarding the uptake studies, it was found that the amine-functionalized PS NPs had the highest uptake compared to the carboxy-functionalized PS NPs, due to the mechanism of interaction with the cell. *Secondly*, it was observed that even the concentration used for the 500nm carboxy PS NPs (0.01nM) was lower than the 50 and 100nm carboxy PS NPs, but their fraction uptake was higher due to the change in the mechanism of uptake. For different concentrations of neutral PS NPs (5 & 10nM), it was found that as the concentration of the neutral PS NPs increases, the fraction uptake increase. While, for the amine-functionalized PS NPs (0.3, 0.5, 0.7, 5 & 10nM), it was observed that the 5nM had the highest fraction uptake compared to lower and higher concentrations, this may be due to the optimum concentration for the cell's uptake. At which the nanoparticles with low concentrations (0.3, 0.7 and 0.7nM) takes longer time for filling the endosome, so they had lower fraction uptake than the 5nM. And the higher concentration (10nM) had lower number of binding sites available for binding, so they had lower fraction uptake. The 5nM made the

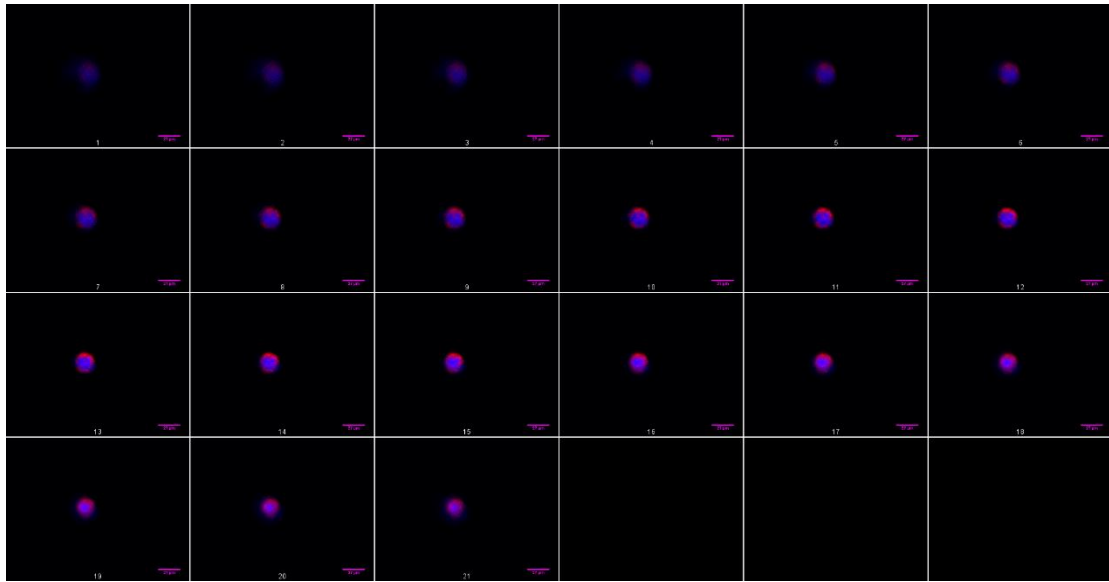
equilibrium between the available binding sites on the cell membrane and the time needed for filling the endosome. But for the 50nm carboxy-functionalized PS NPs (0.25, 3, 5 & 10nM). **Thirdly**, for the kinetics profile of the amine and carboxy PS NPs, it was found that they had two different rates of uptake profiles. It was also observed that the rate of uptake lower than 5nM was different, but higher than 5nM was slightly similar, at which as the concentration of amine PS NPs increase, the rate of uptake decreases, but for the carboxy PS NPs as the concentration of increase, the rate of uptake increases until 5nM. However, for the neutral Ps NPs, they exhibit a steady state of rate of uptake in between the amine and carboxy PS NPs. **Finally**, we noticed that the confocal imaged matched the raw fluorescent data. It was confirmed by the confocal images that as the concentration of amine PS NPs increase, the stress on the cells increase, leading to the cell death. At which in the case of higher concentrations (5 & 10nM) of the amine-functionalized PS NPs the cells were not found, but it was found in lower concentrations (0.3, 0.5 & 0.7nM). These results were aligned with the results obtained from the cytotoxicity test. To wrap up, there are different physicochemical parameters affecting the uptake of the polystyrene nanoparticles. In the future, more concentrations and nanoparticle functionalization will be used, in addition to different cell lines that will be tested and kinetics simulation as well, for building a full picture about the in-vitro uptake profile for polystyrene nanoparticles.

APPENDIX:
CONFOCAL IMAGES

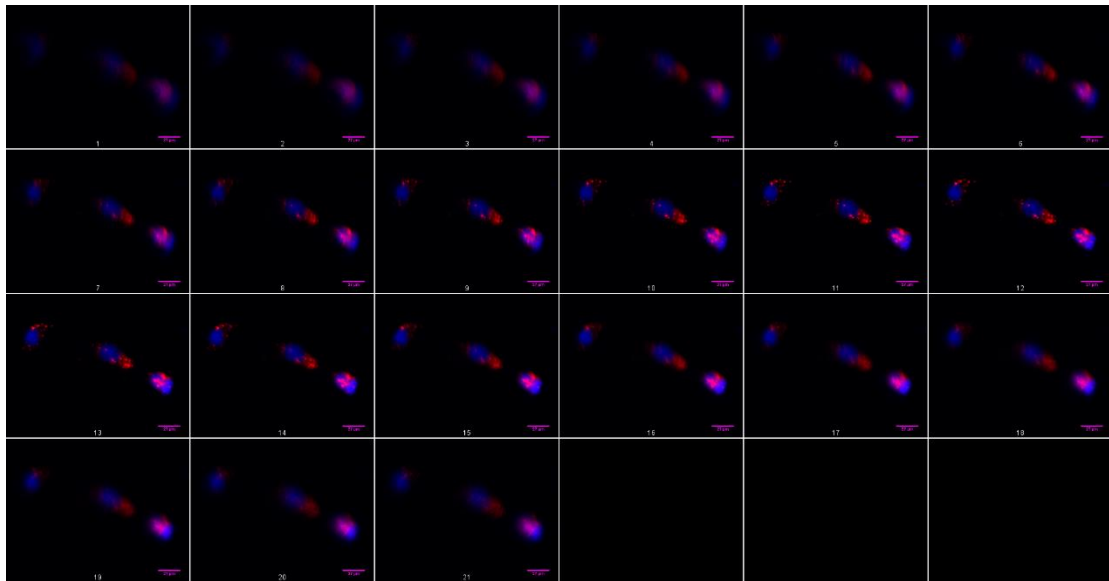
50nM NEUTRAL POLYSTYRENE NANOPARTICLES (10nM)



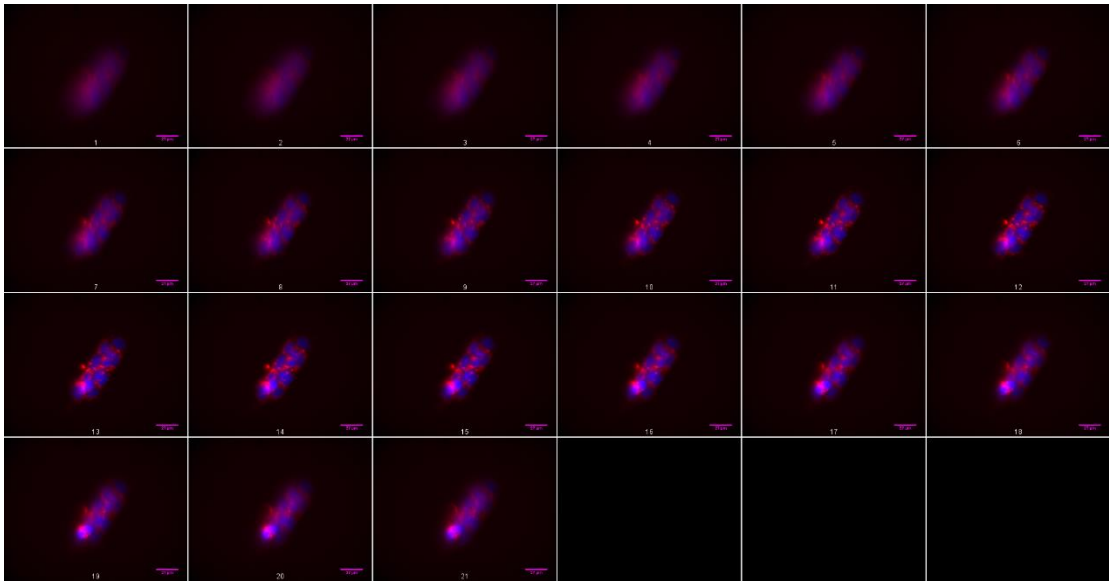
T=4



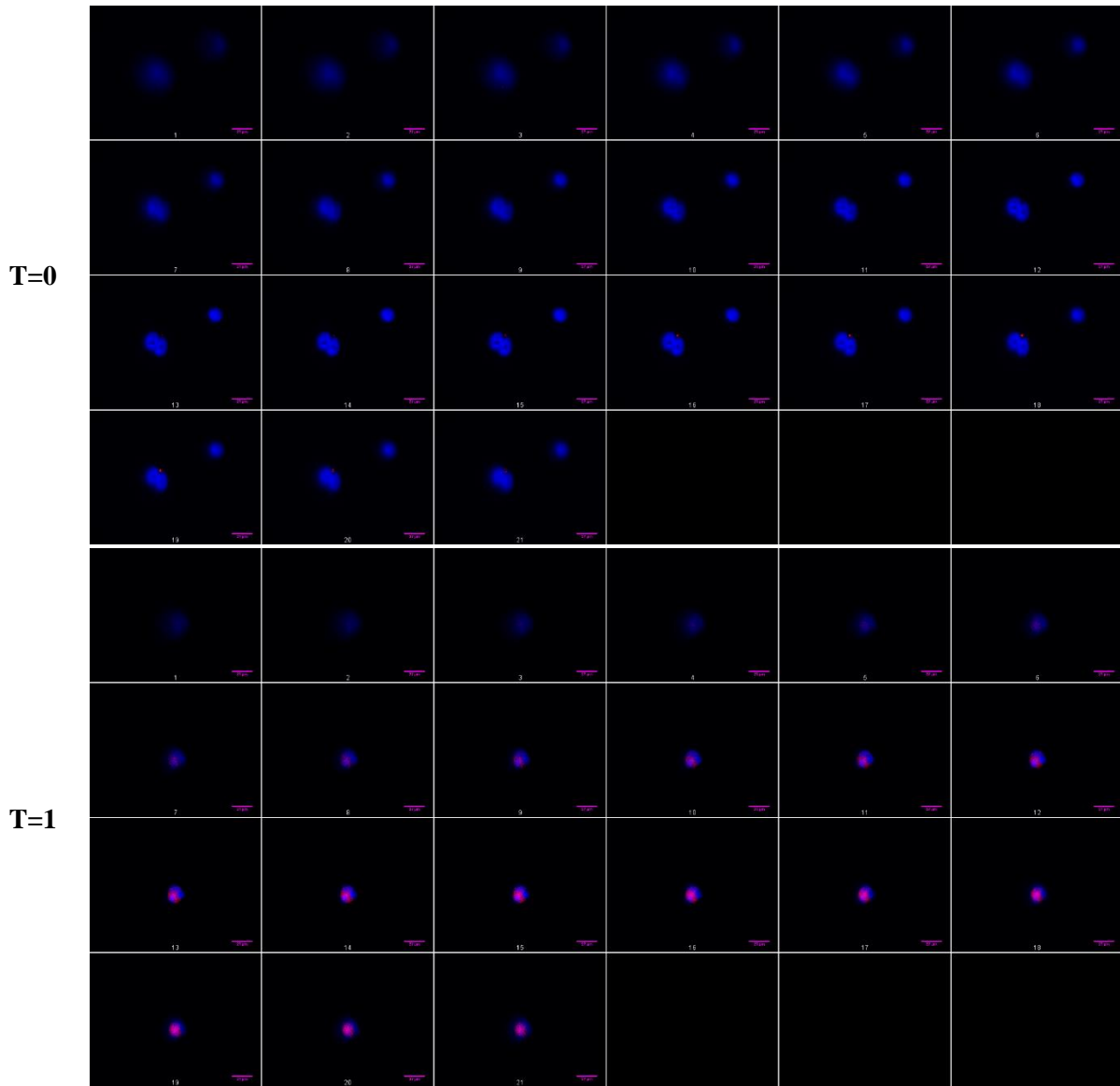
T=12



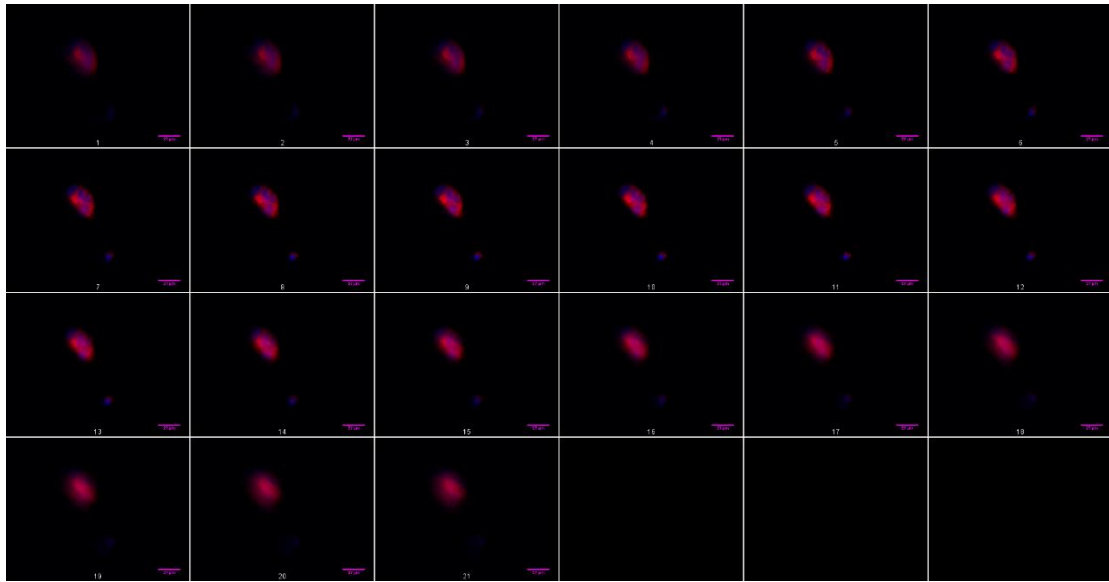
T=24



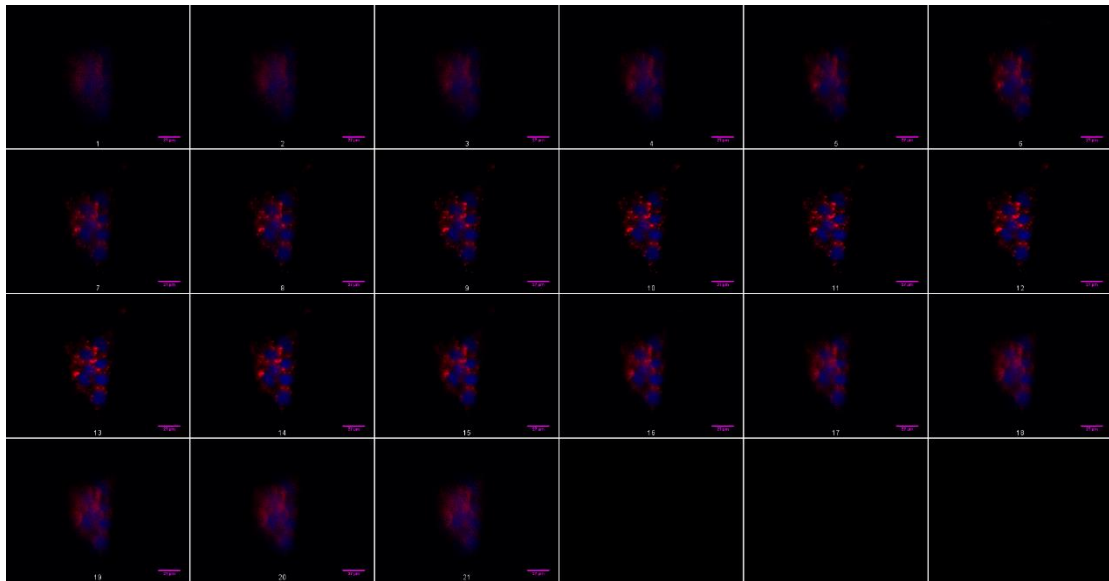
50nM NEUTRAL POLYSTYRENE NANOPARTICLES (5nM)



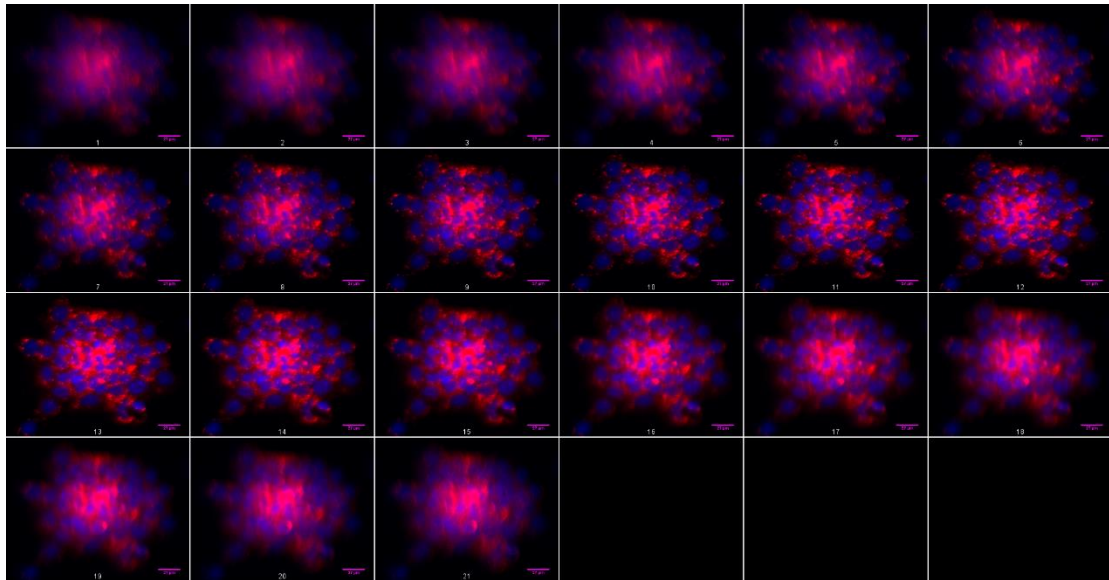
T=4



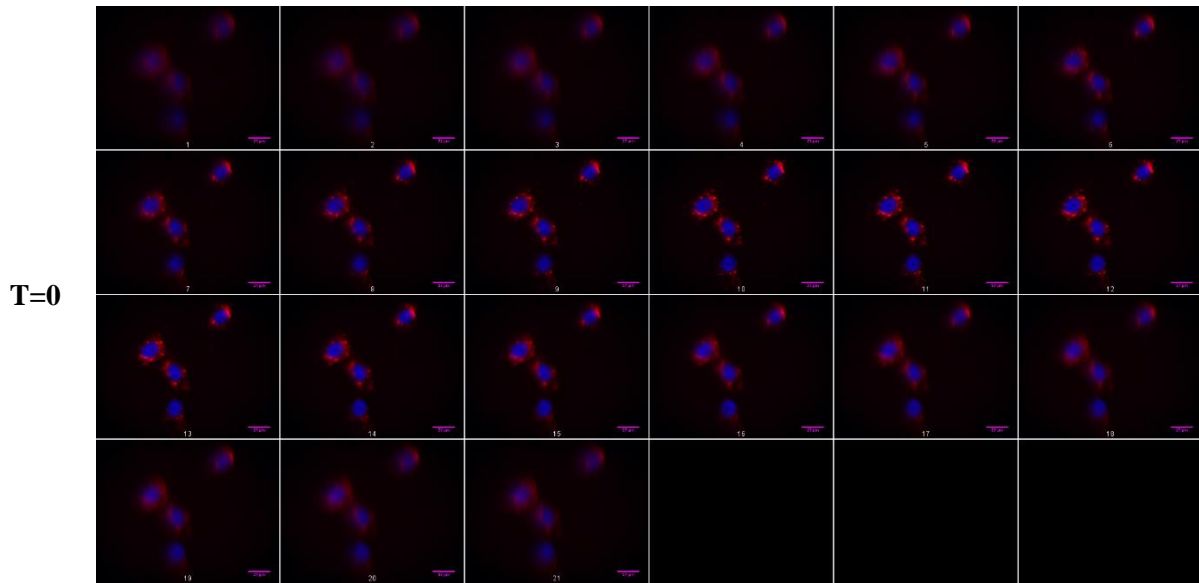
T=12



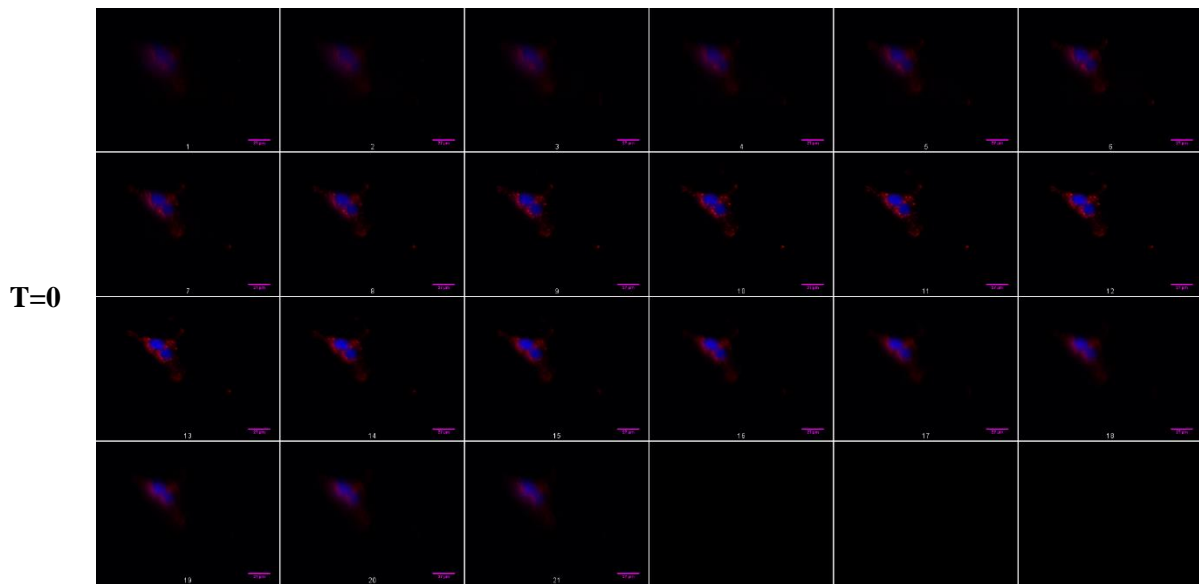
T=24



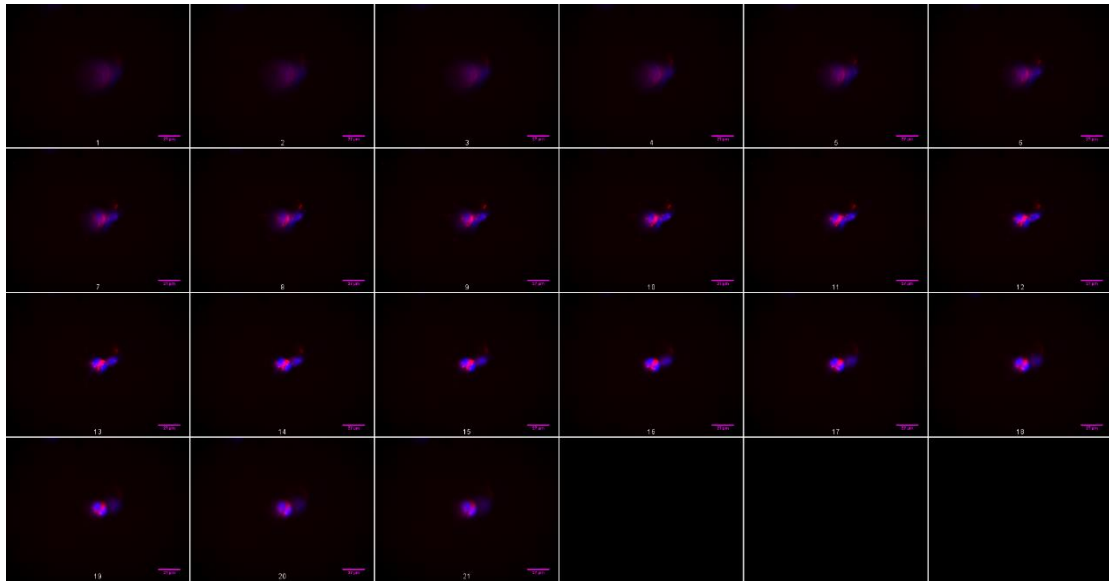
50nM AMINE POLYSTYRENE NANOPARTICLES (10nM)



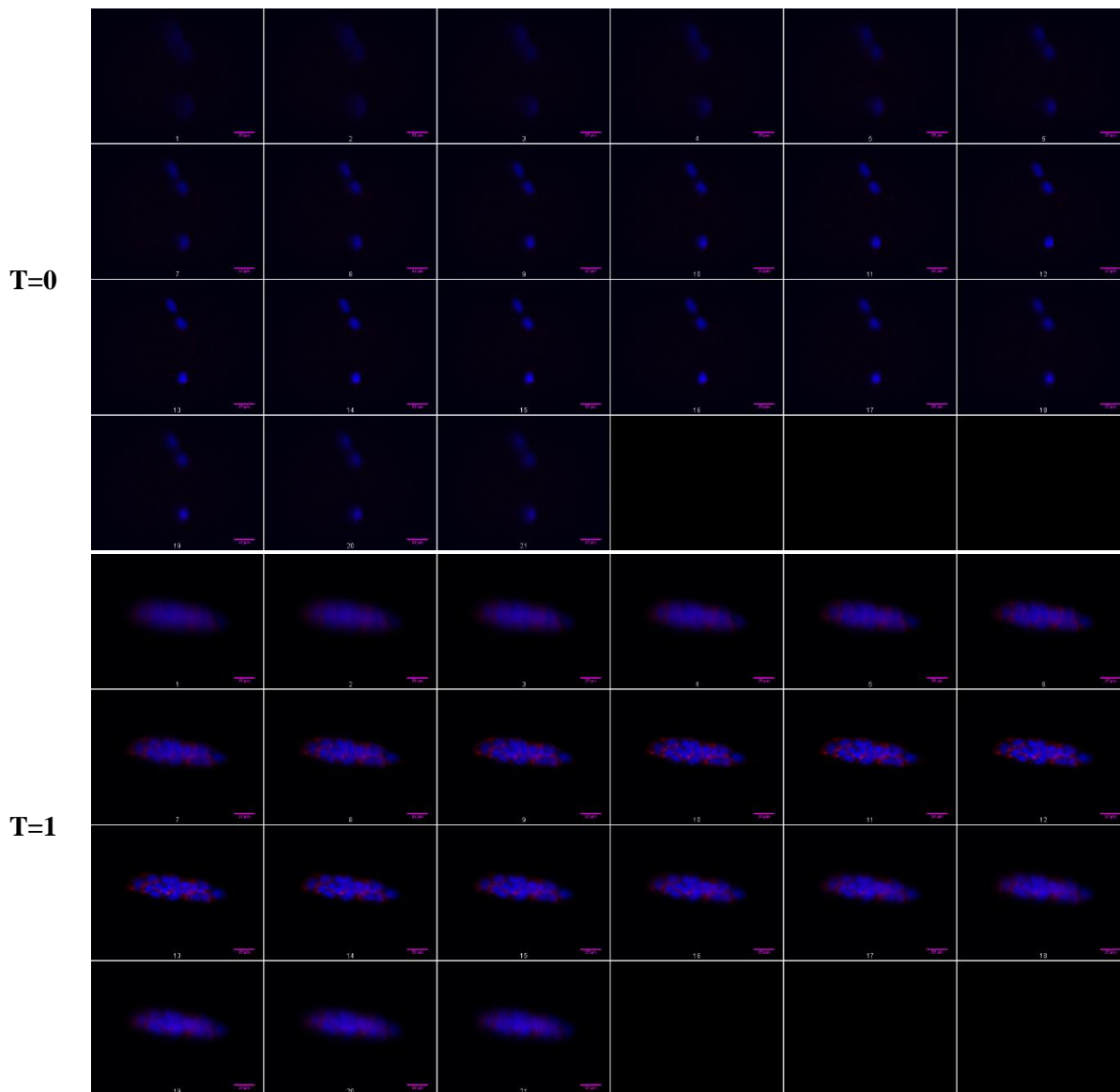
50nM AMINE POLYSTYRENE NANOPARTICLES (5nM)



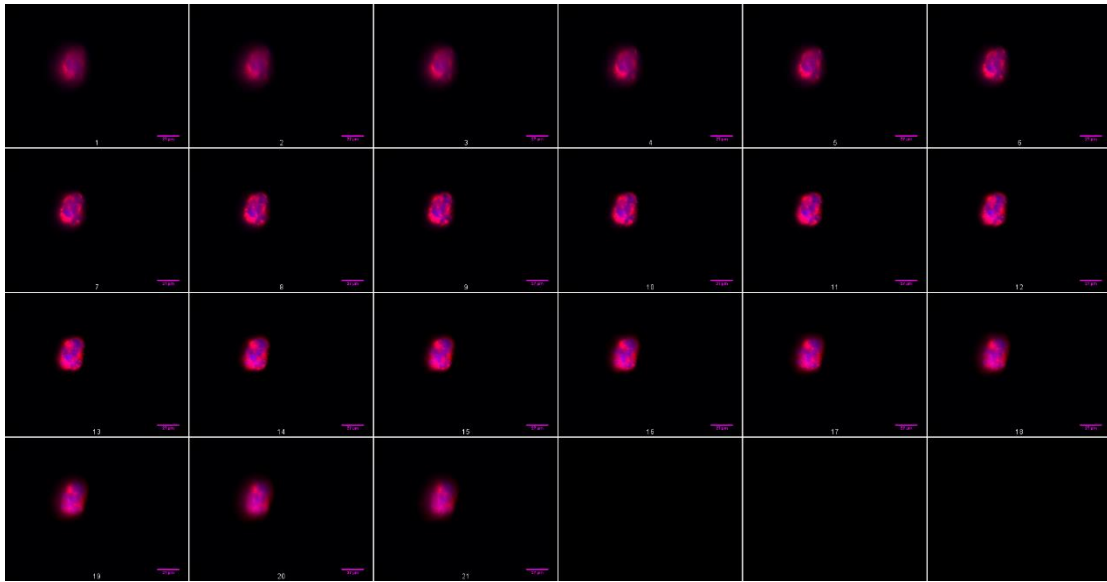
T=1



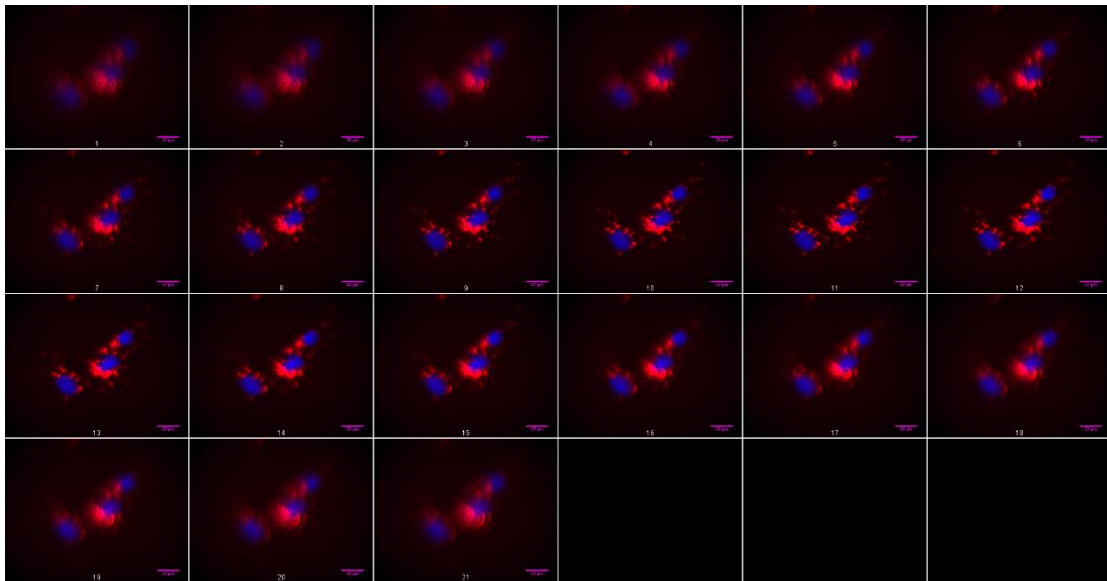
50nM CARBOXY POLYSTYRENE NANOPARTICLES (10nM)



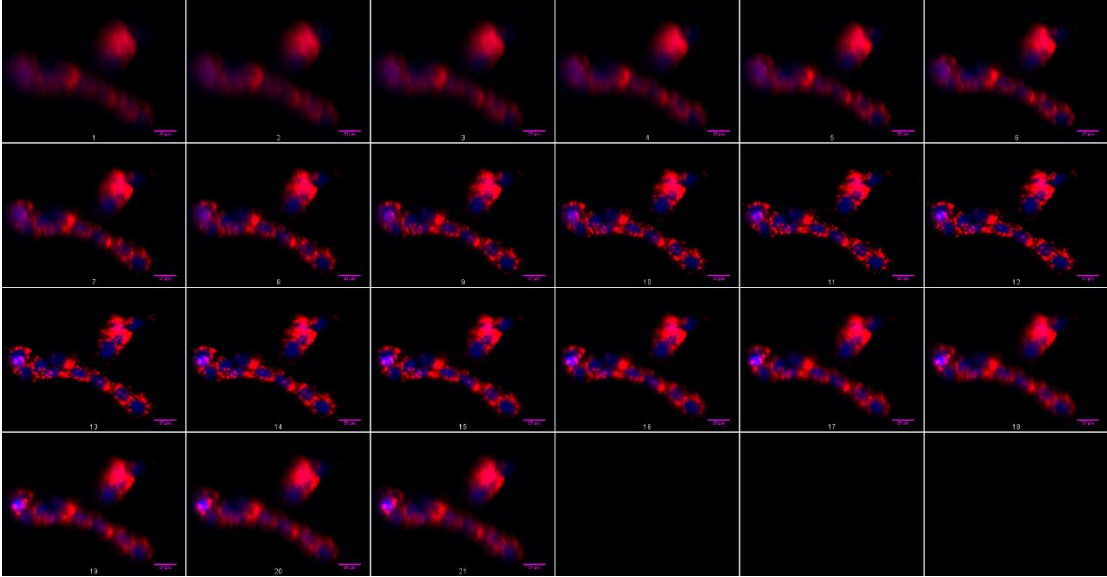
T=4



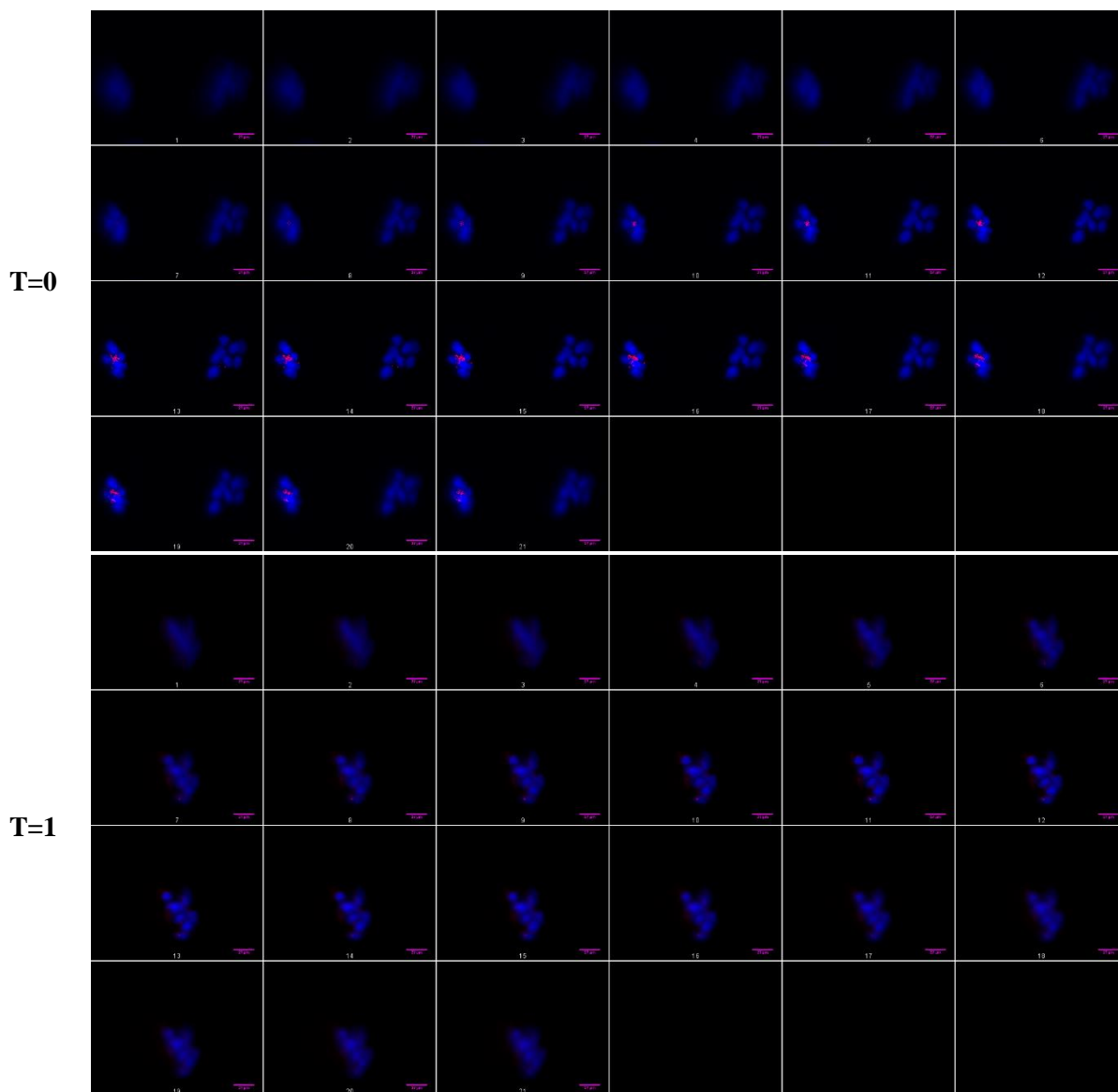
T=12



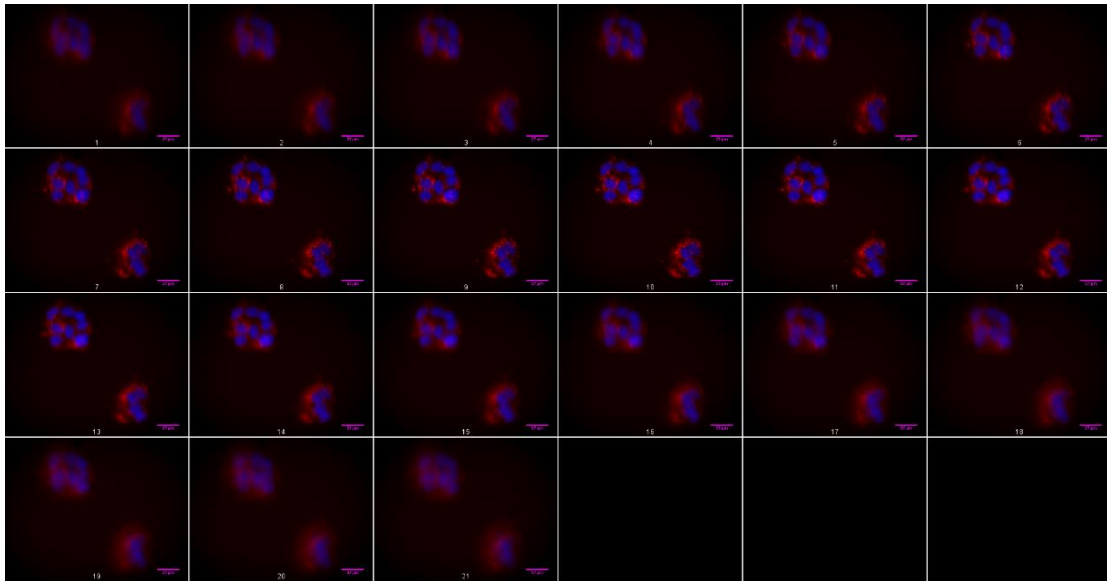
T=24



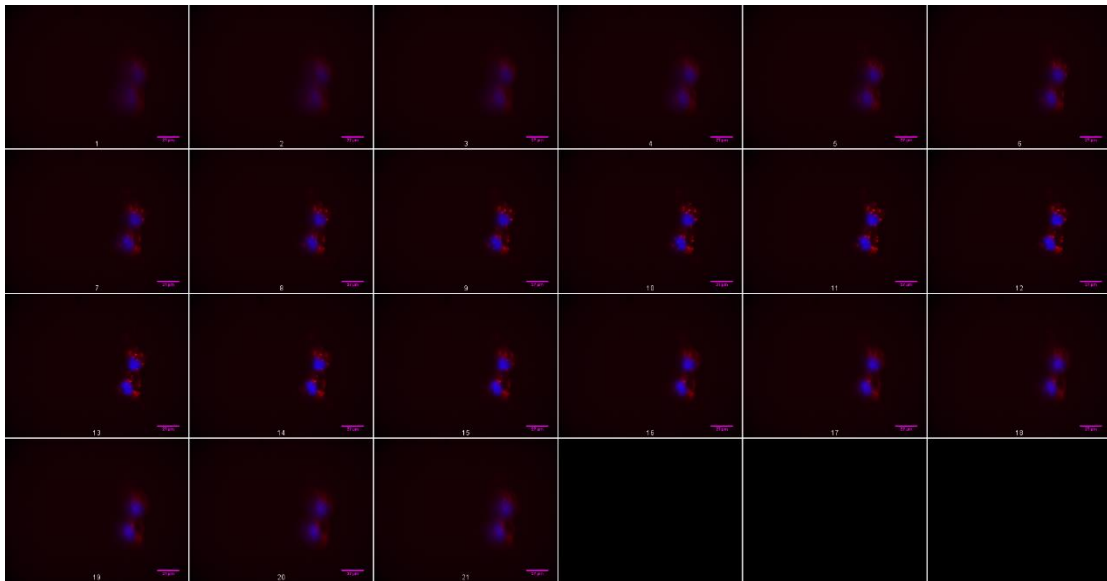
50nM CARBOXY POLYSTYRENE NANOPARTICLES (5nM)



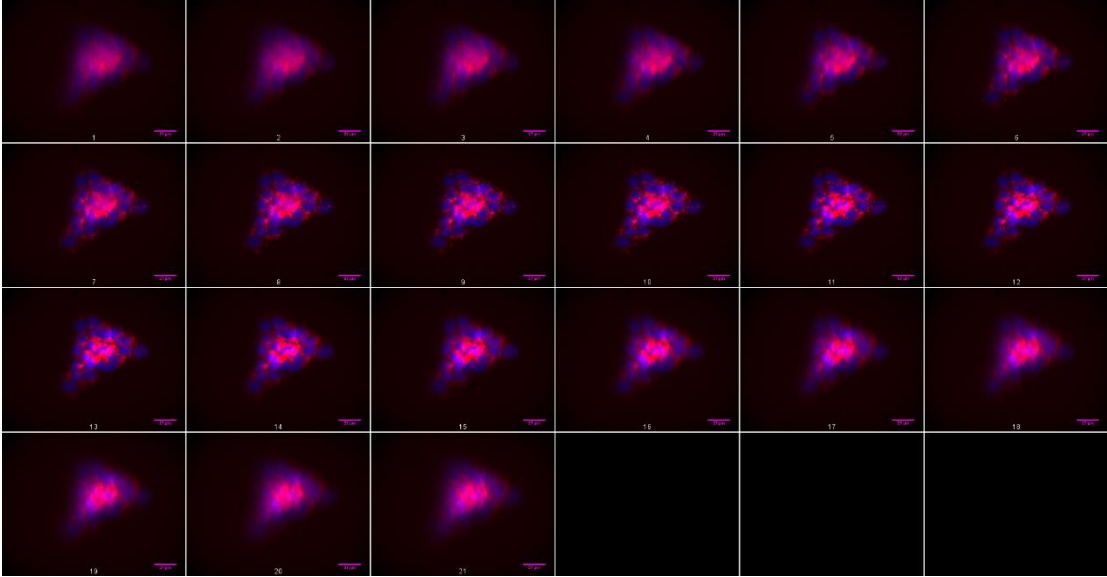
T=4



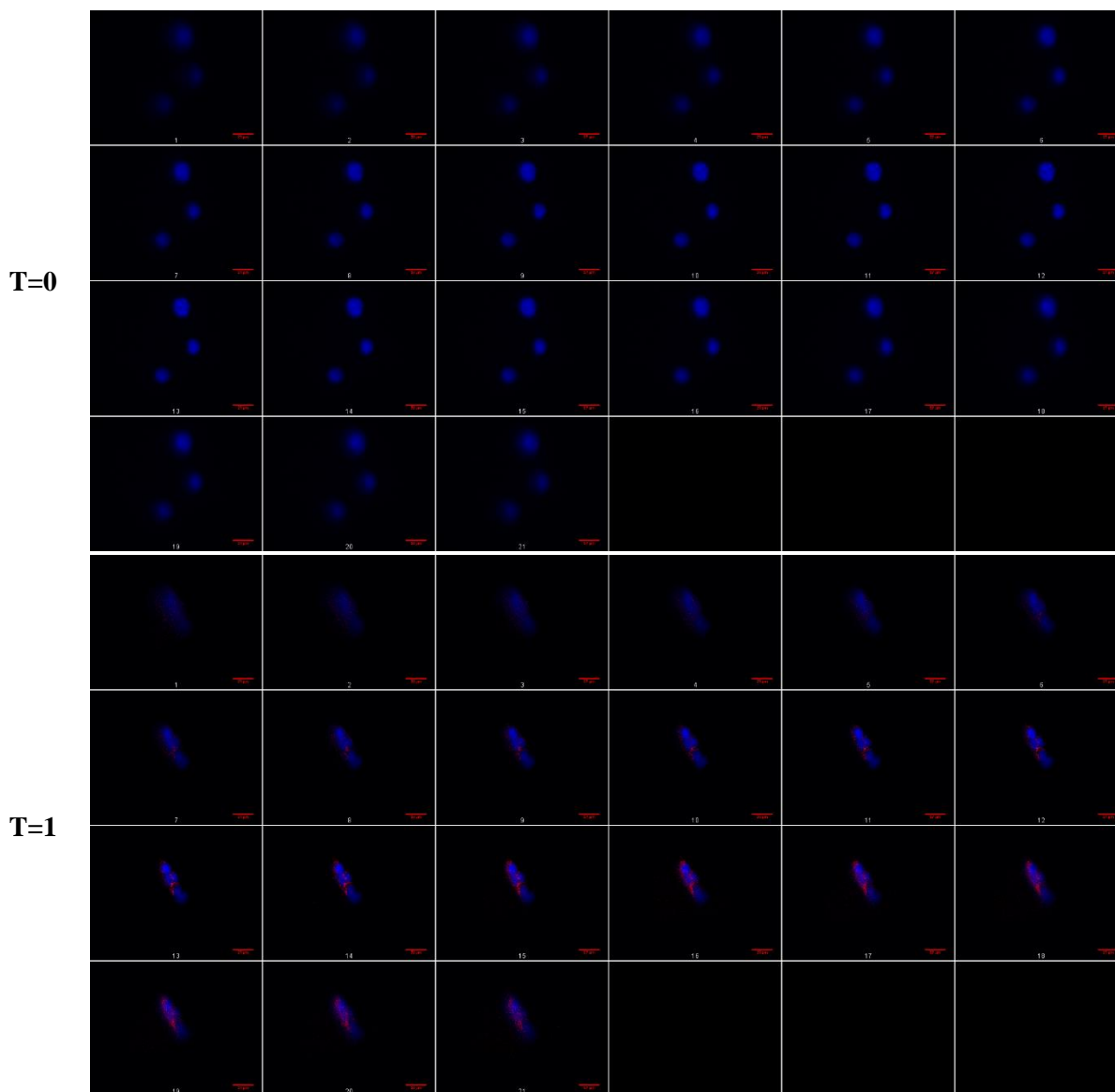
T=12



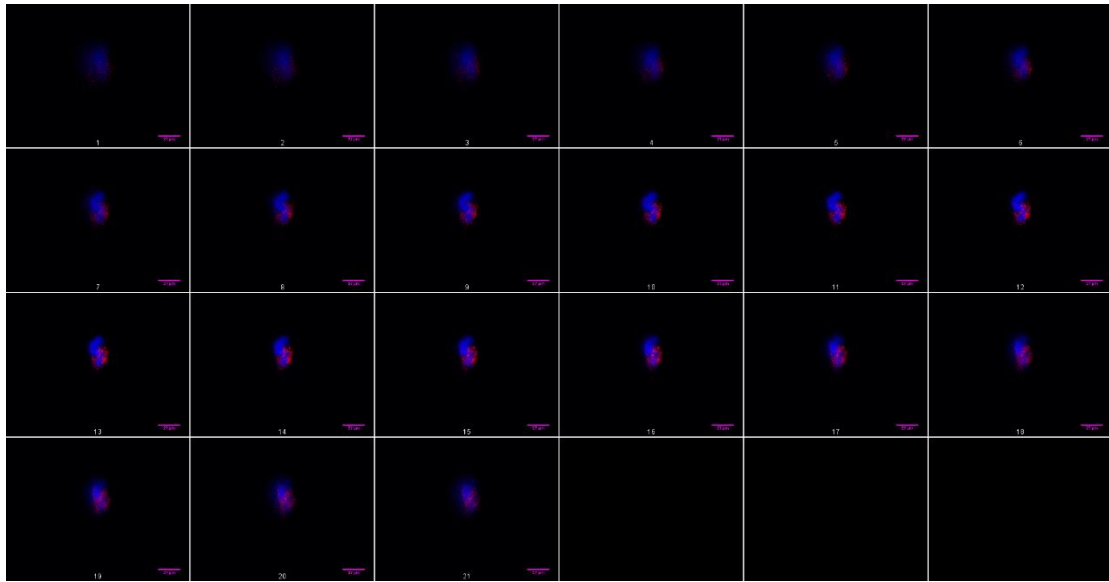
T=24



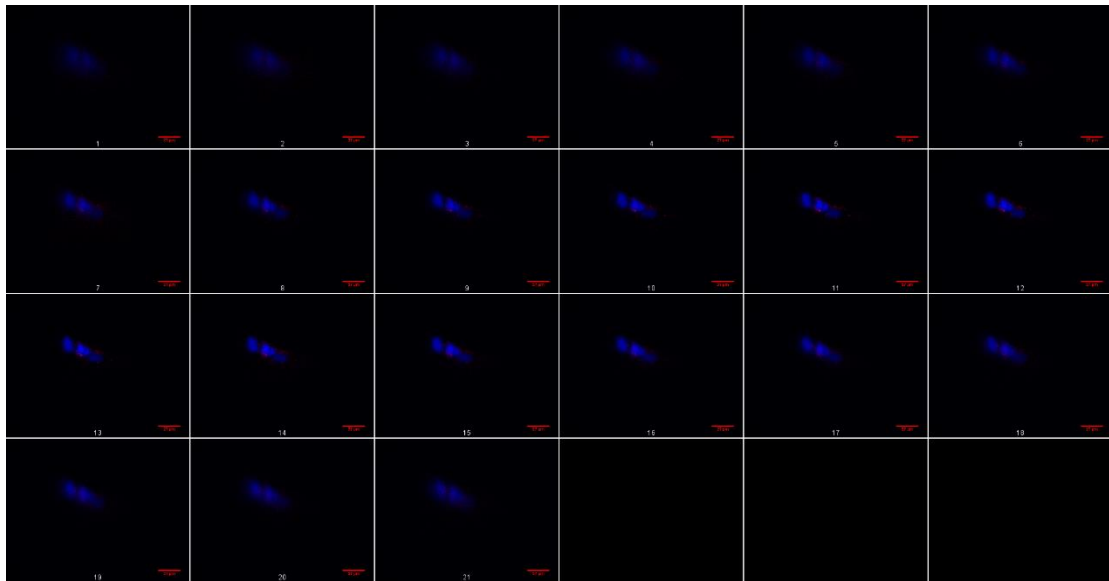
50nm CARBOXY POLYSTYRENE NANOPARTICLES (0.25nM)



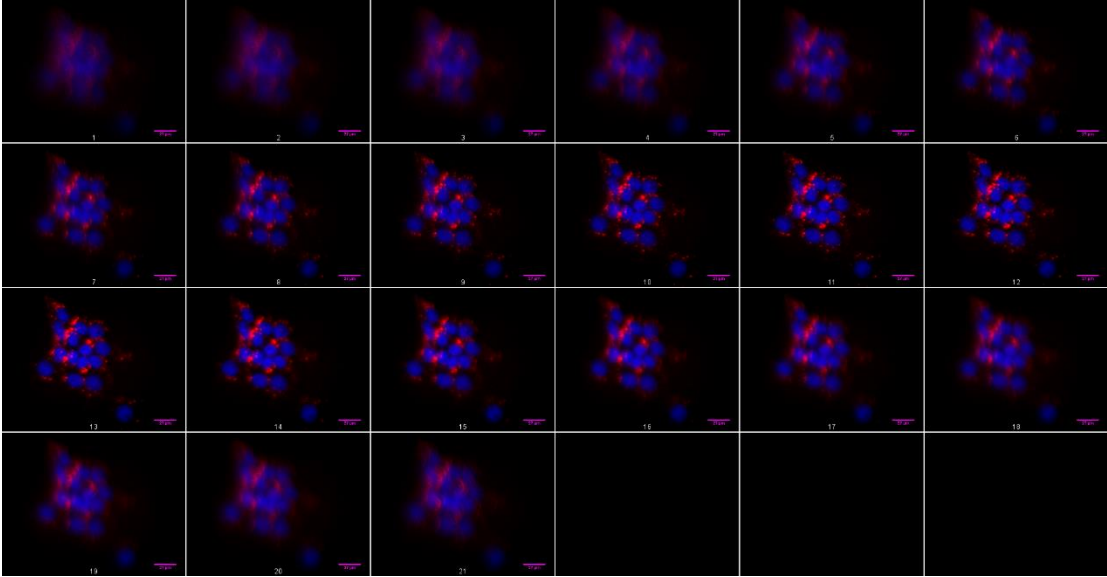
T=4



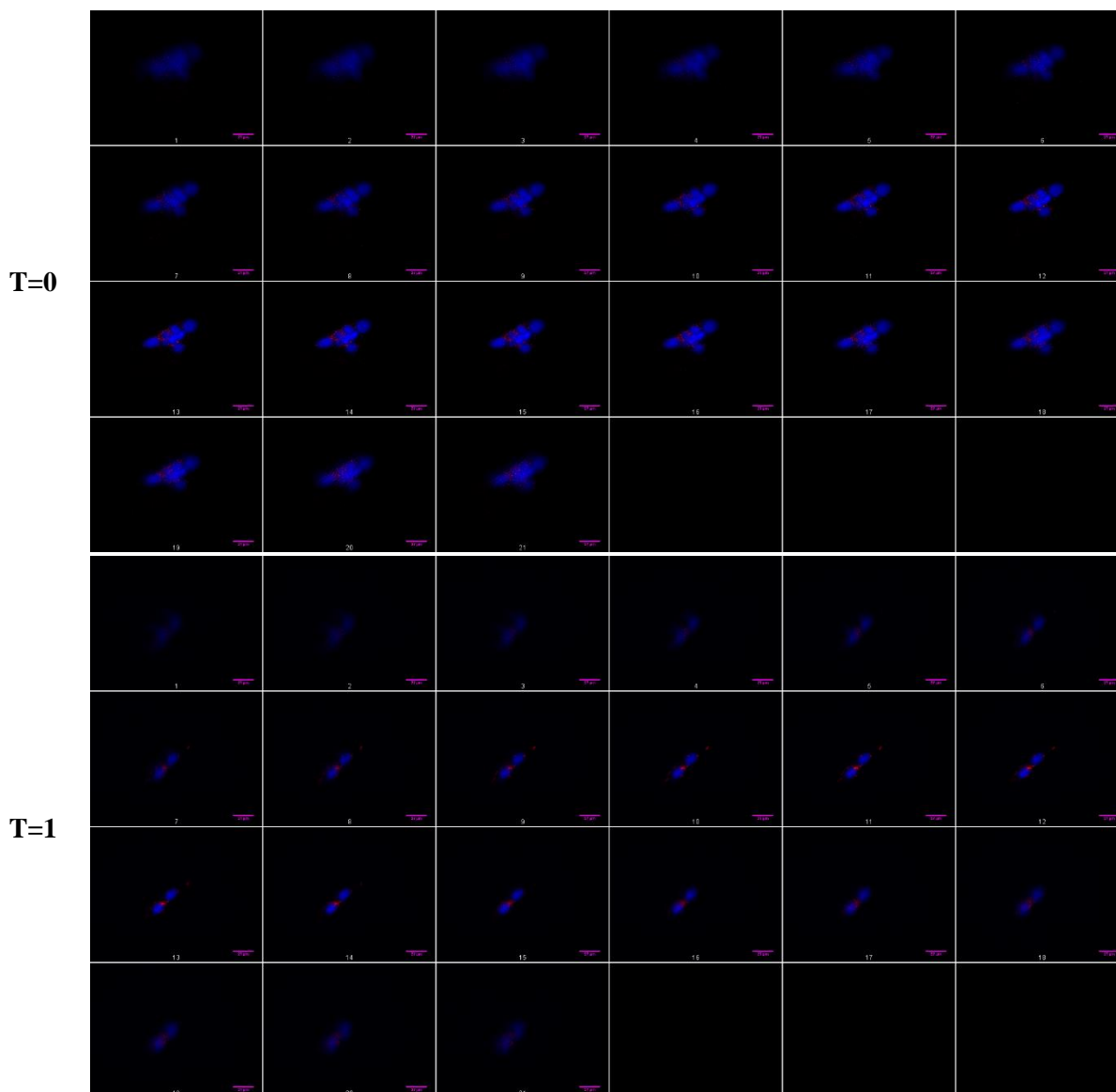
T=12



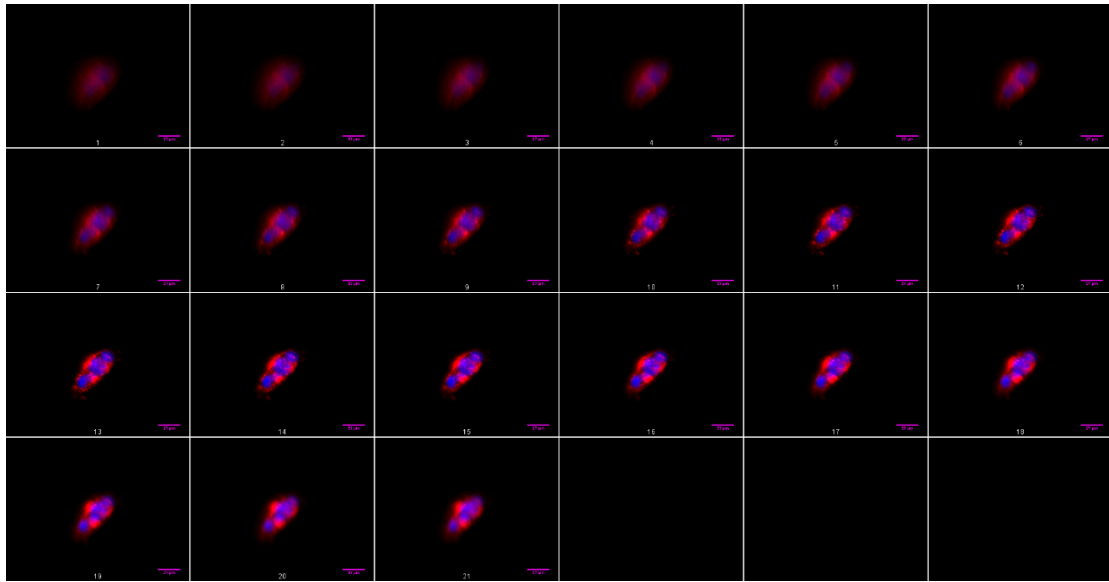
T=24



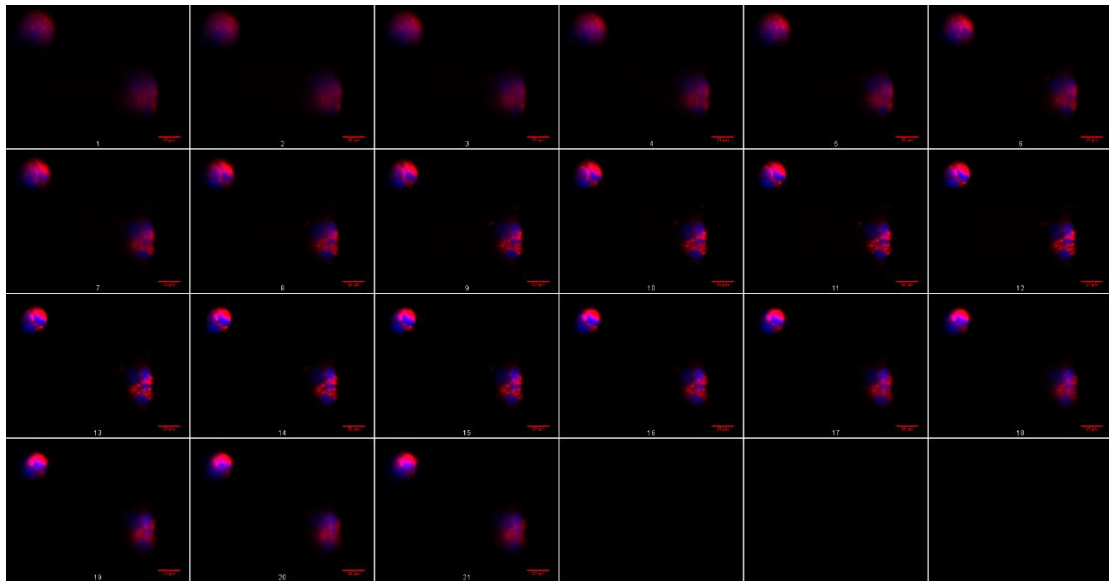
50nm CARBOXY POLYSTYRENE NANOPARTICLES (3nM)



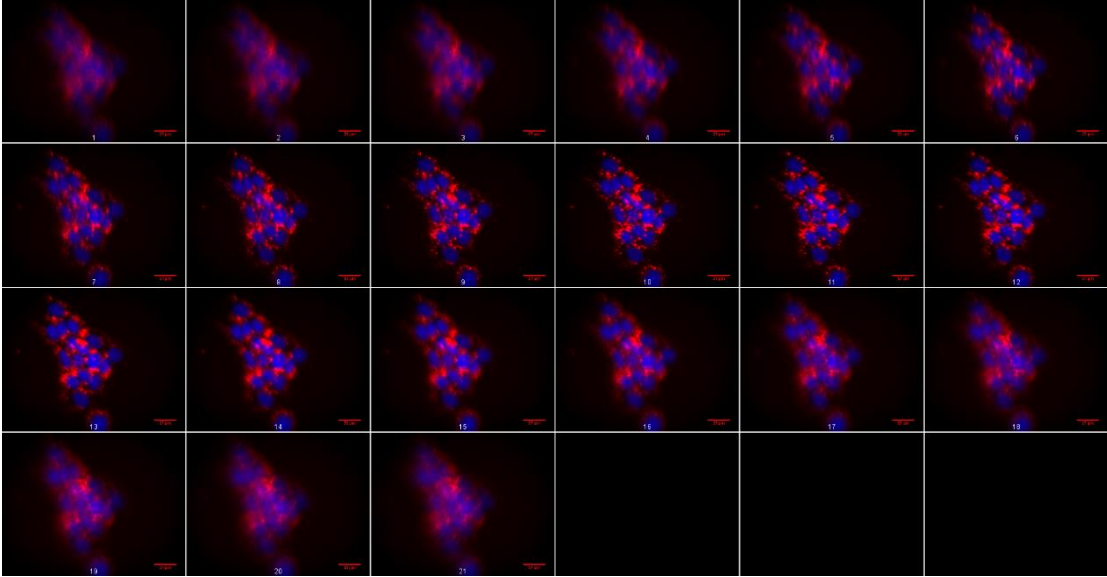
T=4



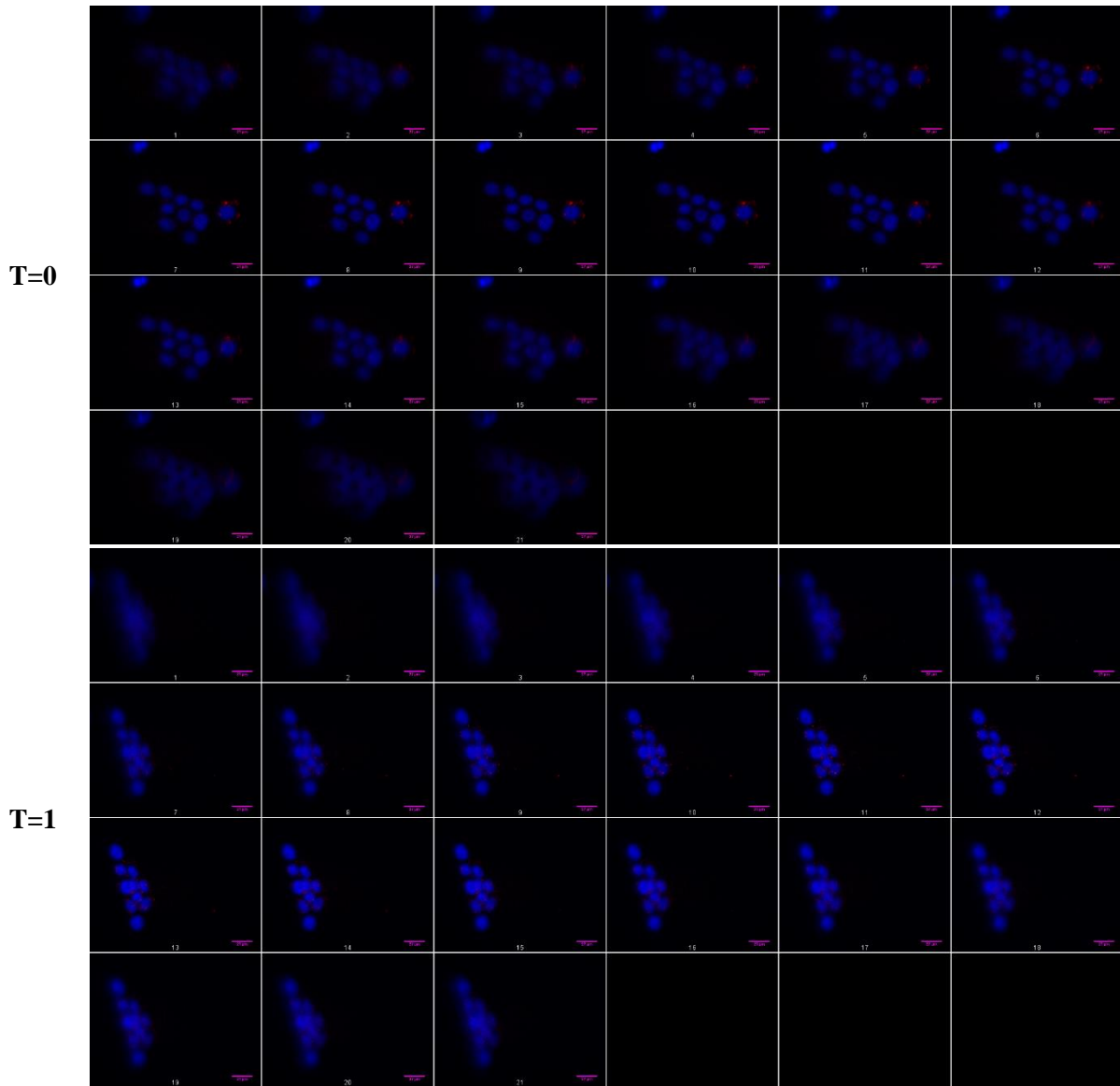
T=12



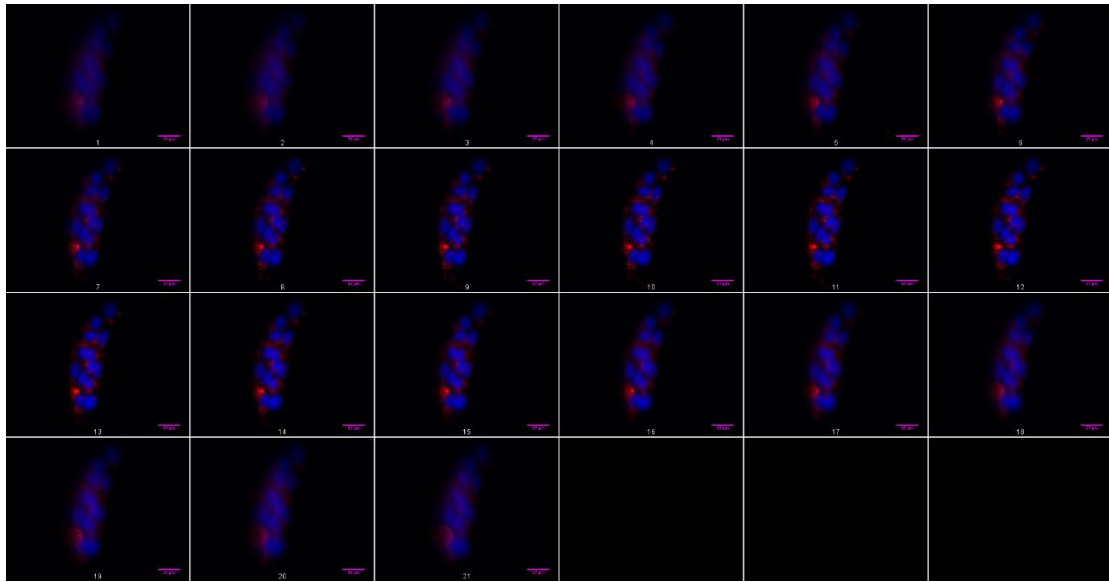
T=24



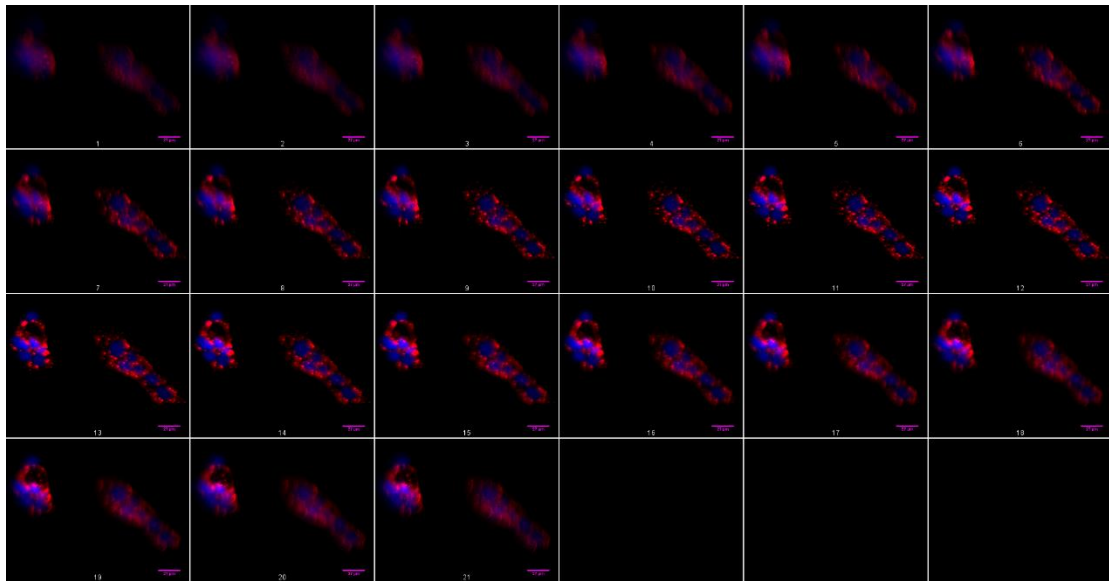
100nm CARBOXY POLYSTYRENE NANOPARTICLES (0.25nM)



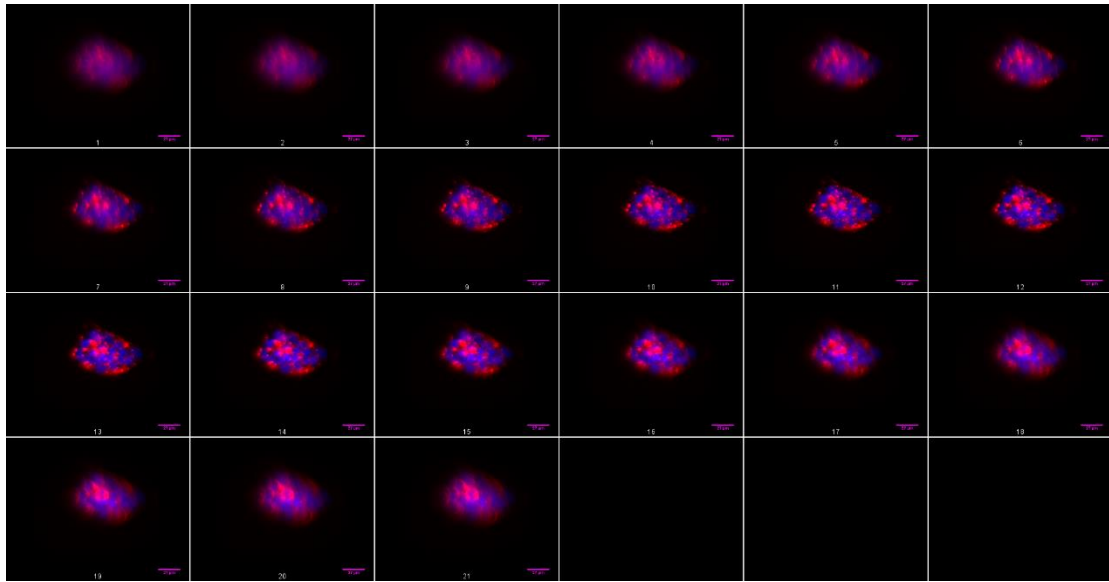
T=4



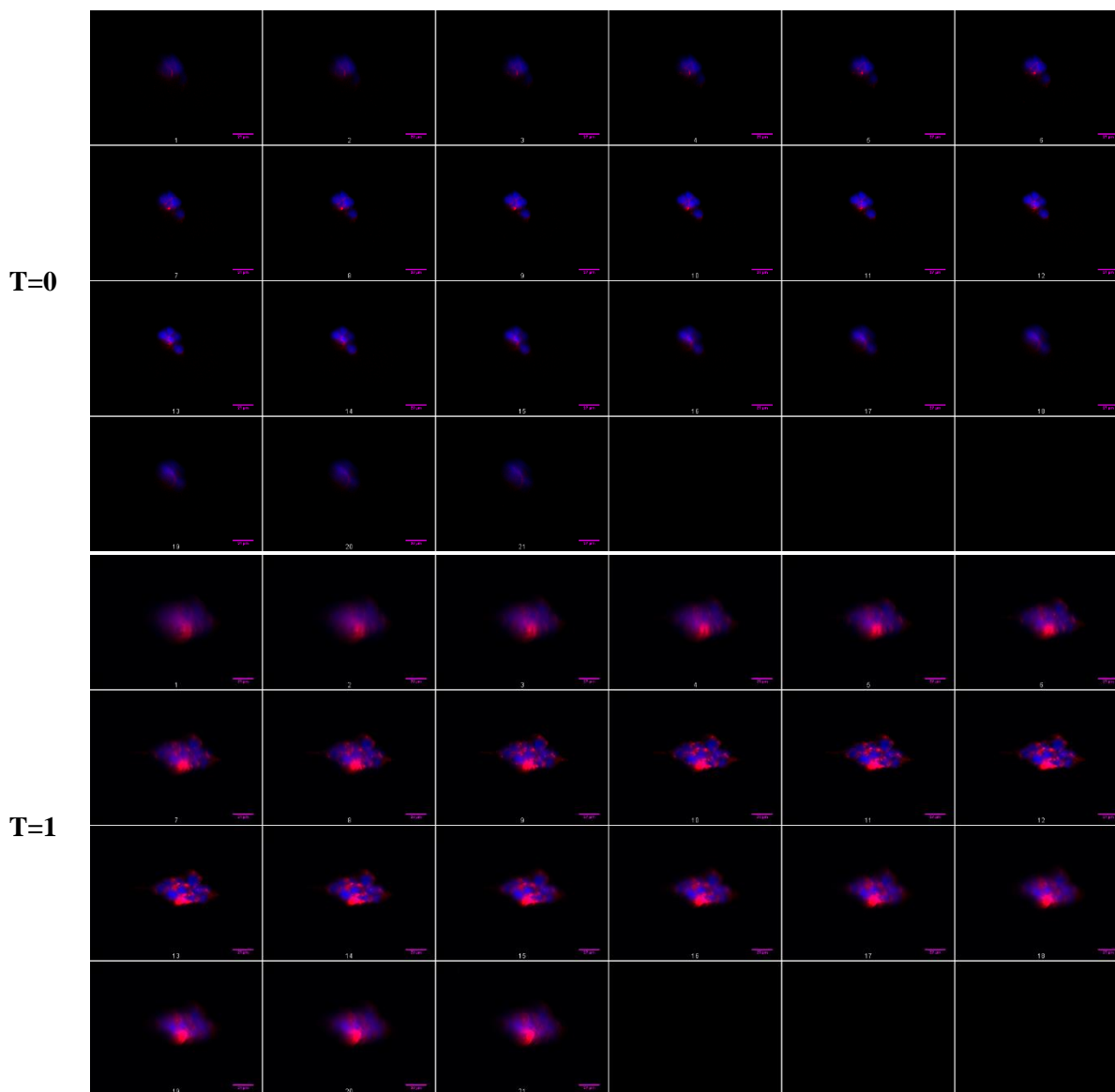
T=12



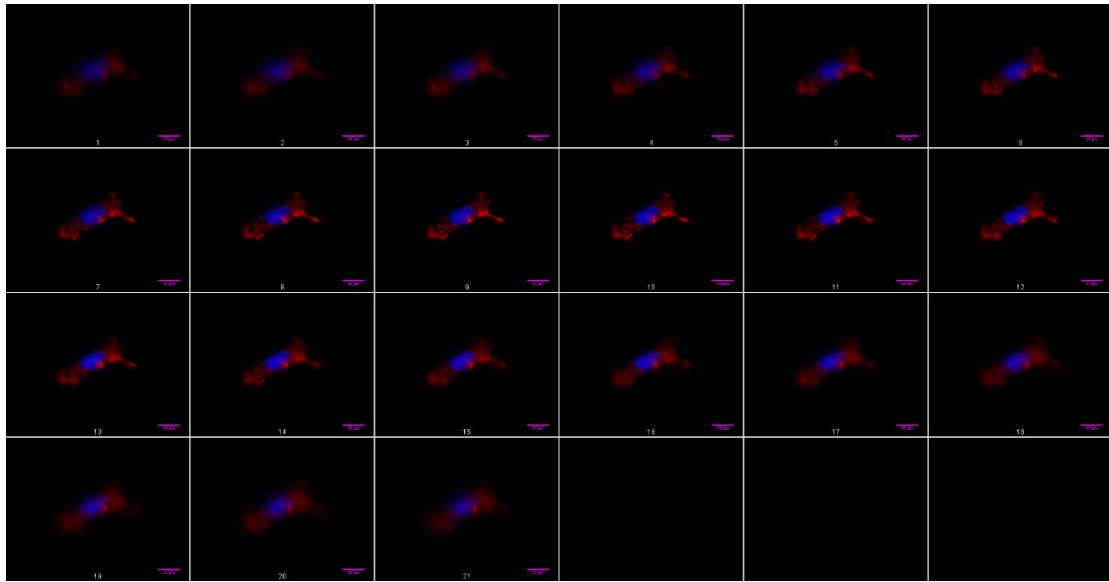
T=24



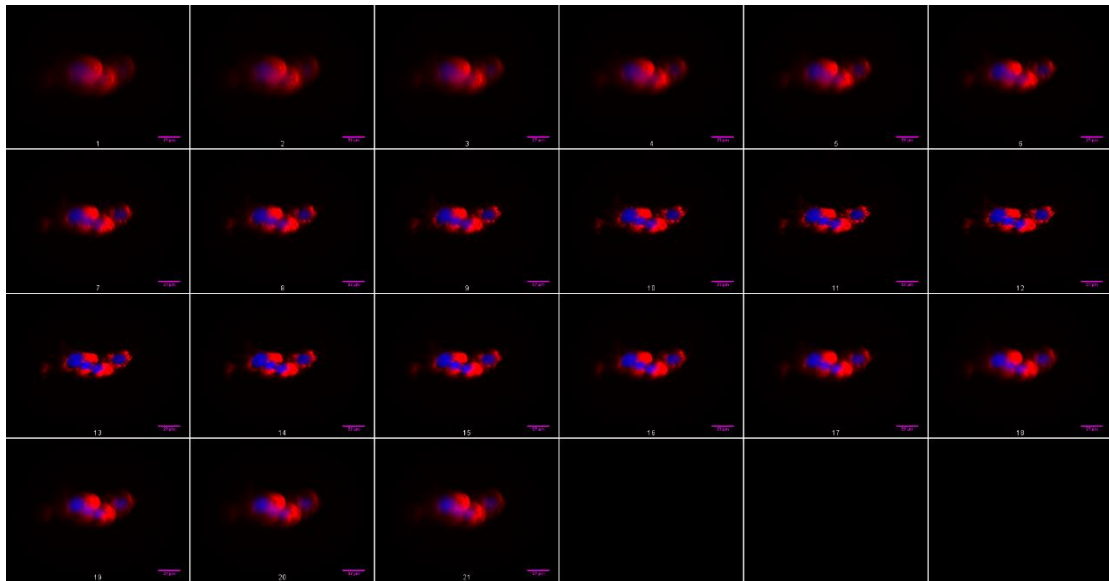
100nm CARBOXY POLYSTYRENE NANOPARTICLES (3nM)



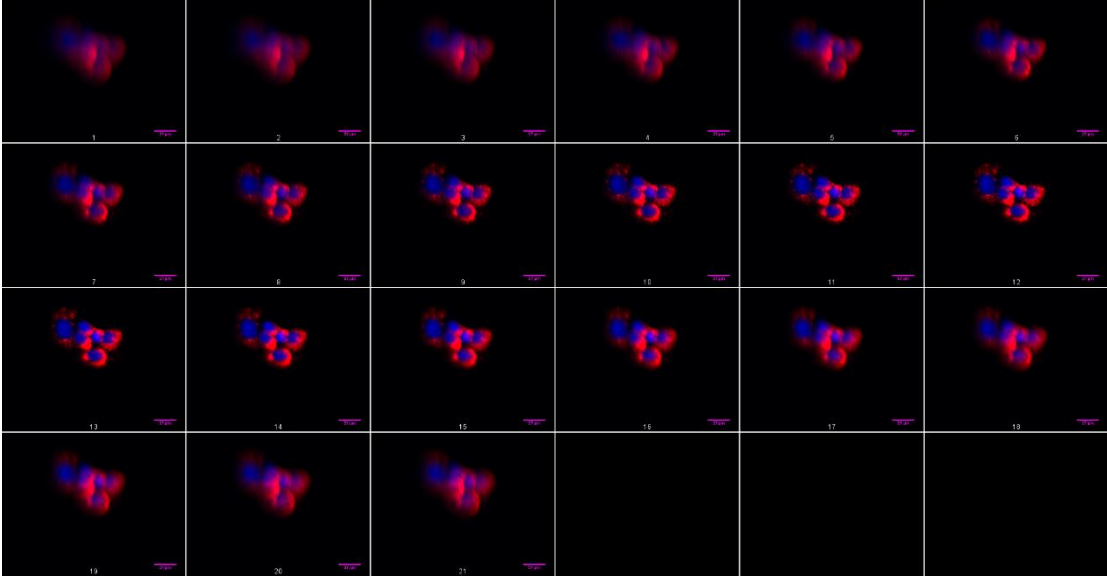
T=4



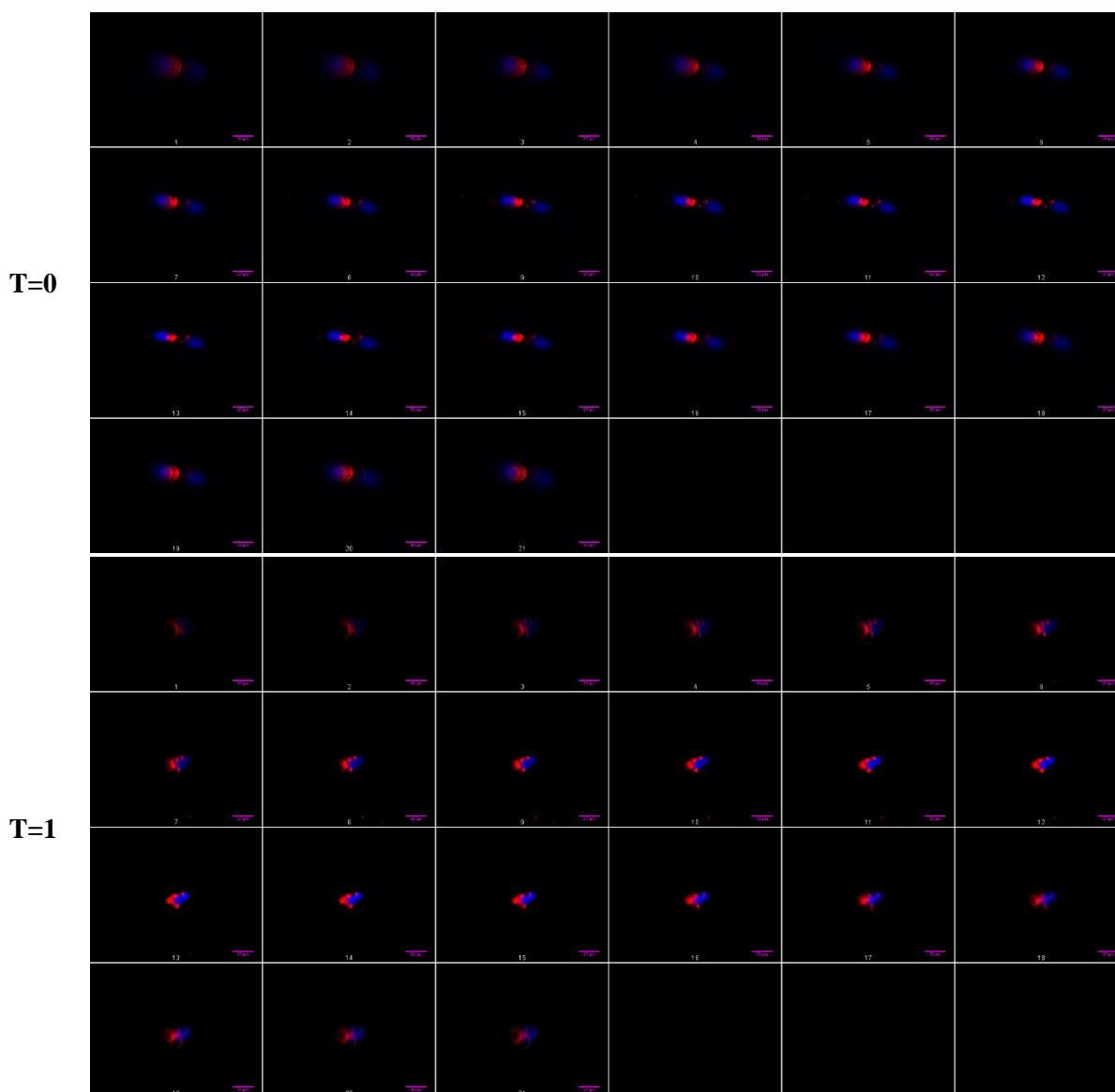
T=12



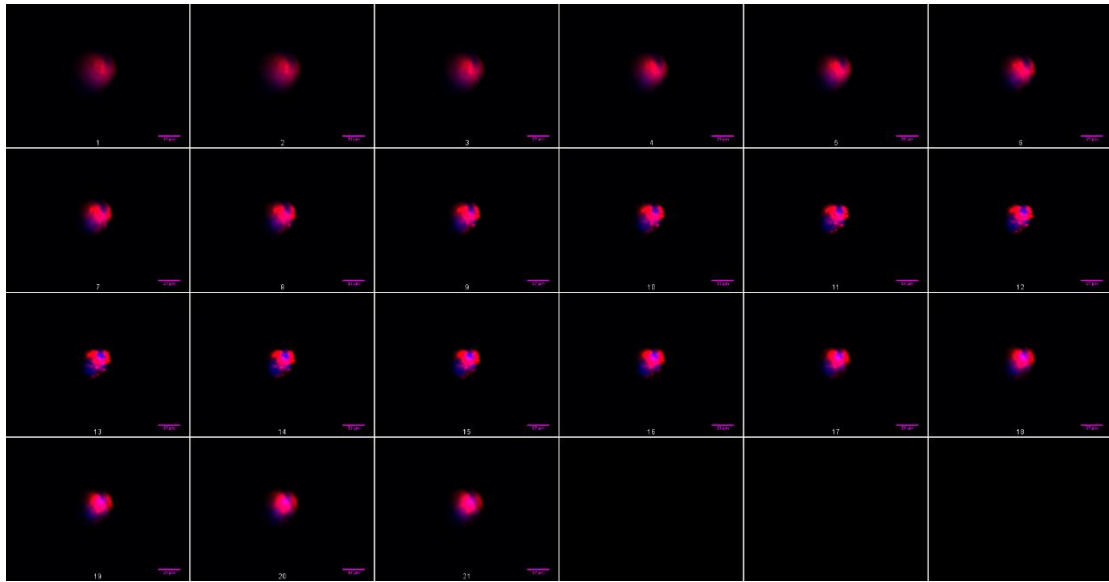
T=24



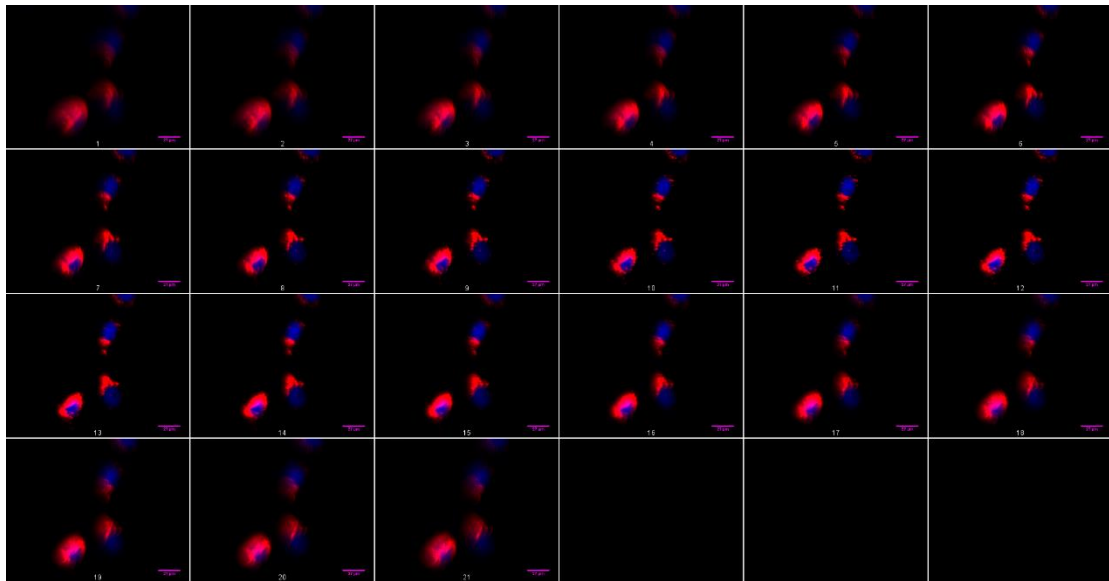
500nm CARBOXY POLYSTYRENE NANOPARTICLES (0.03nM)



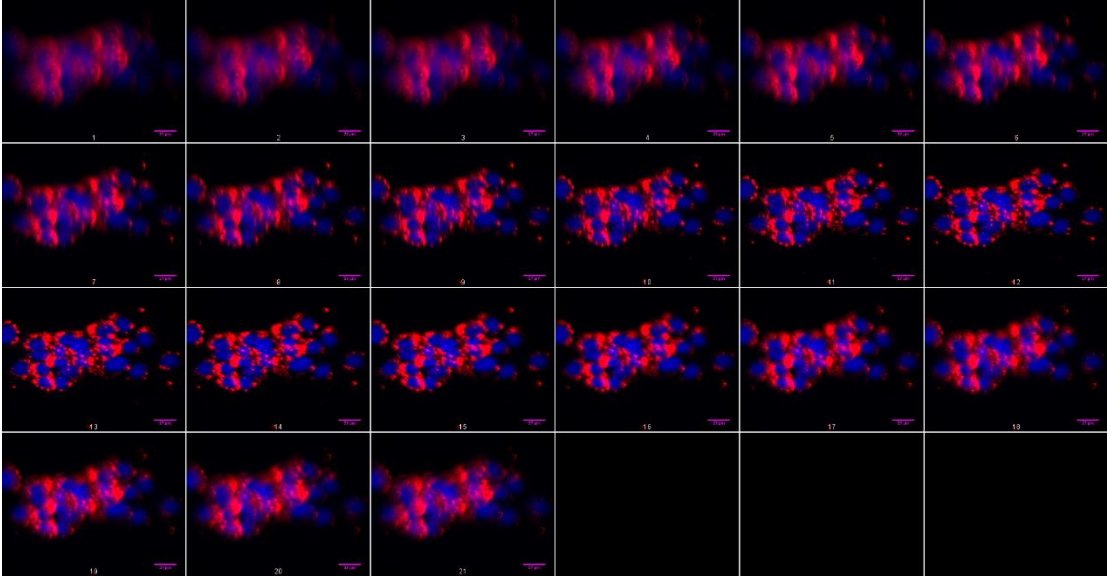
T=4



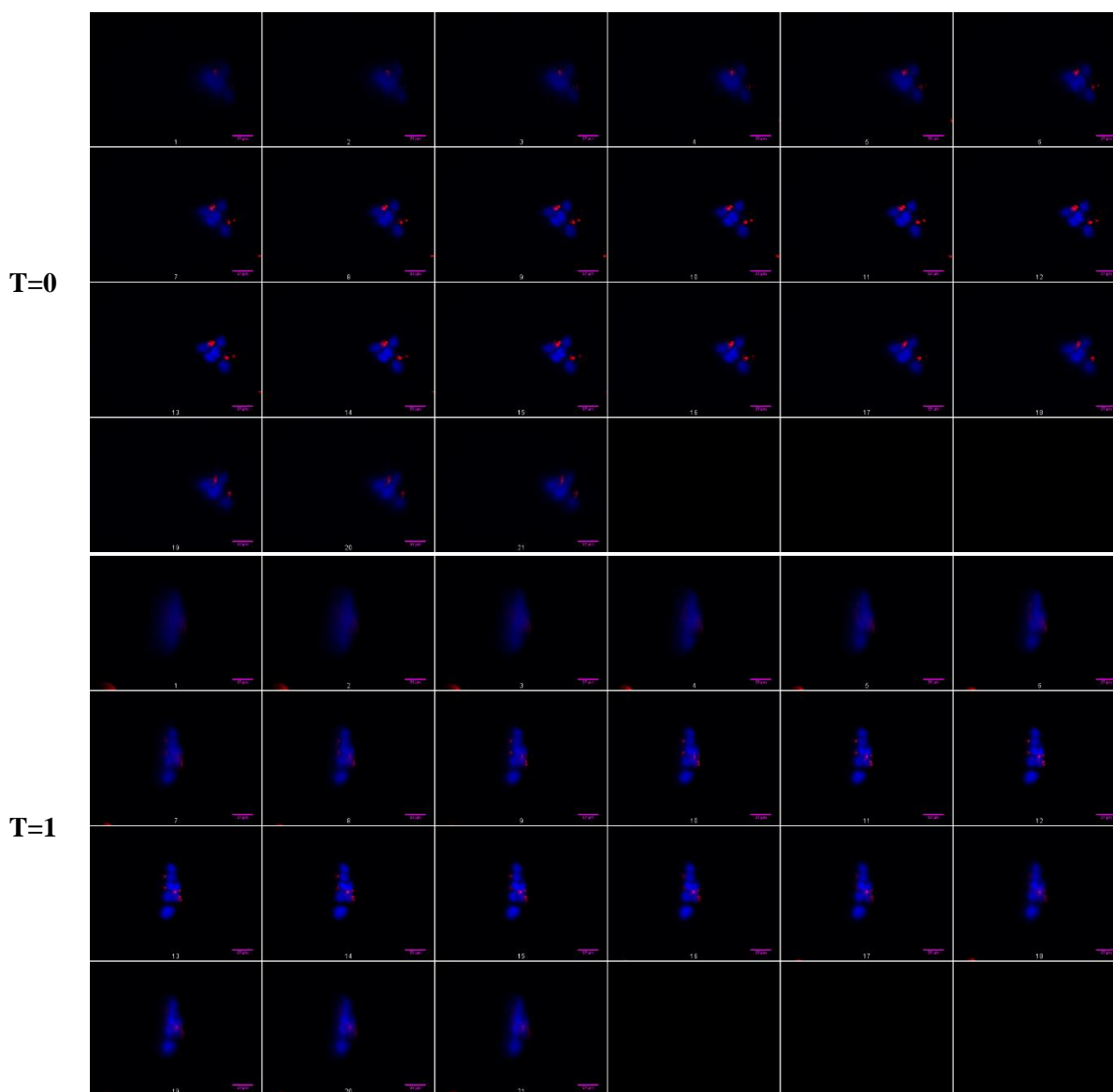
T=12



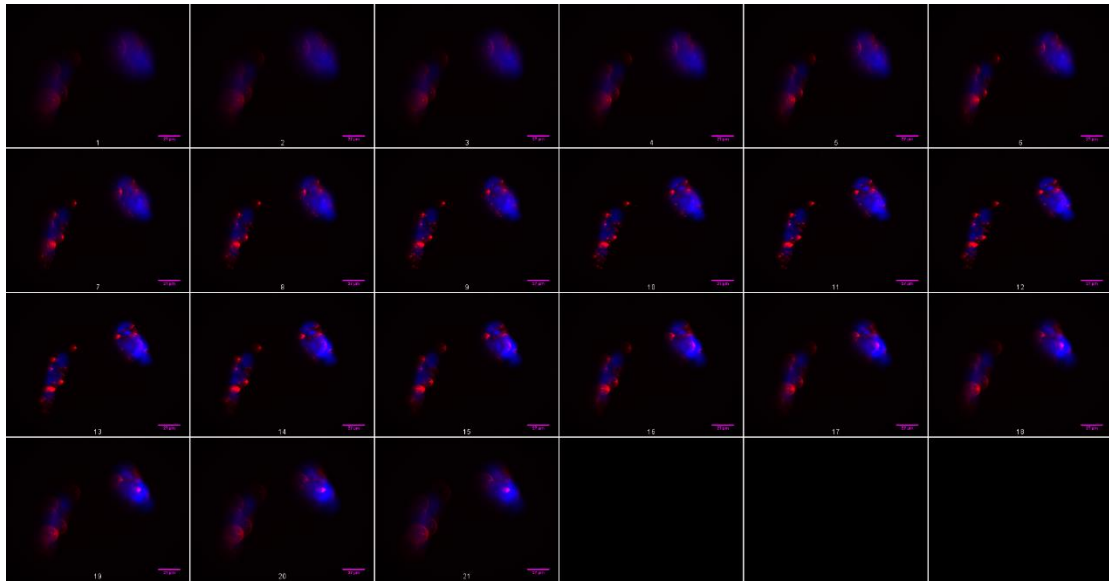
T=24



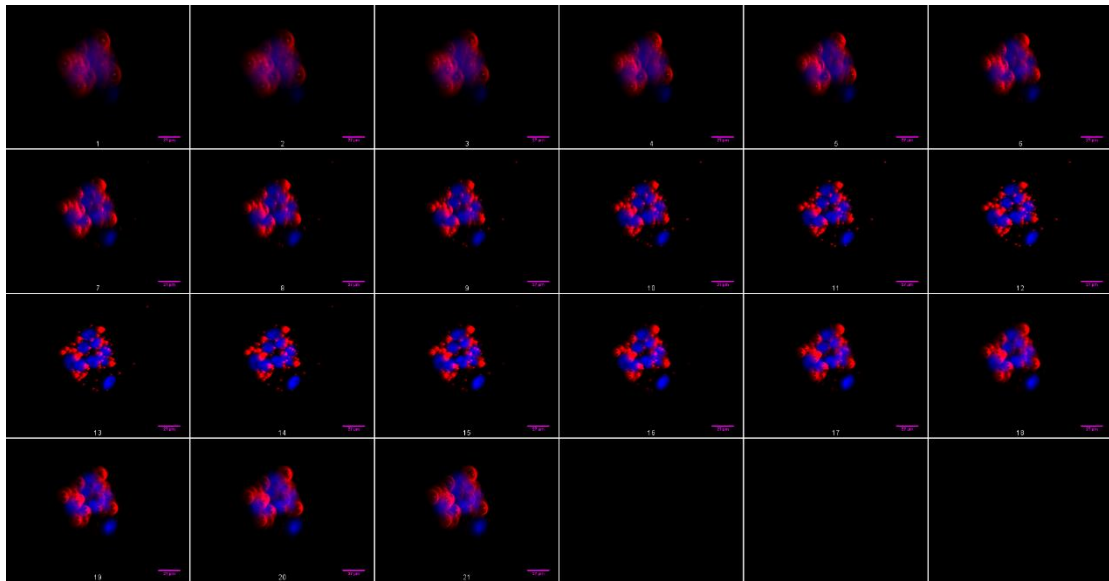
500nm CARBOXY POLYSTYRENE NANOPARTICLES (0.01nM)



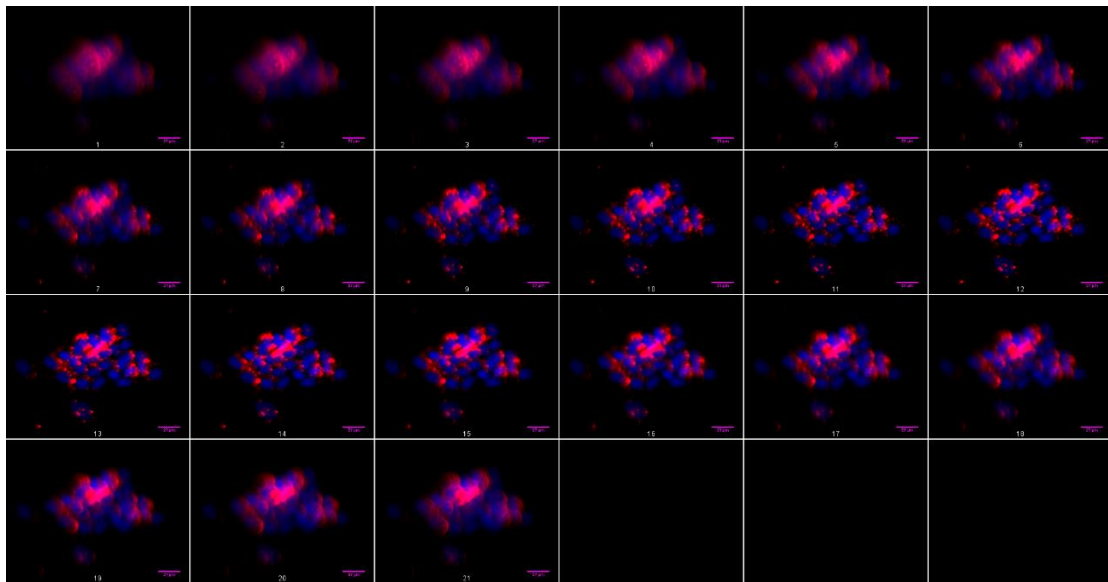
T=4



T=12

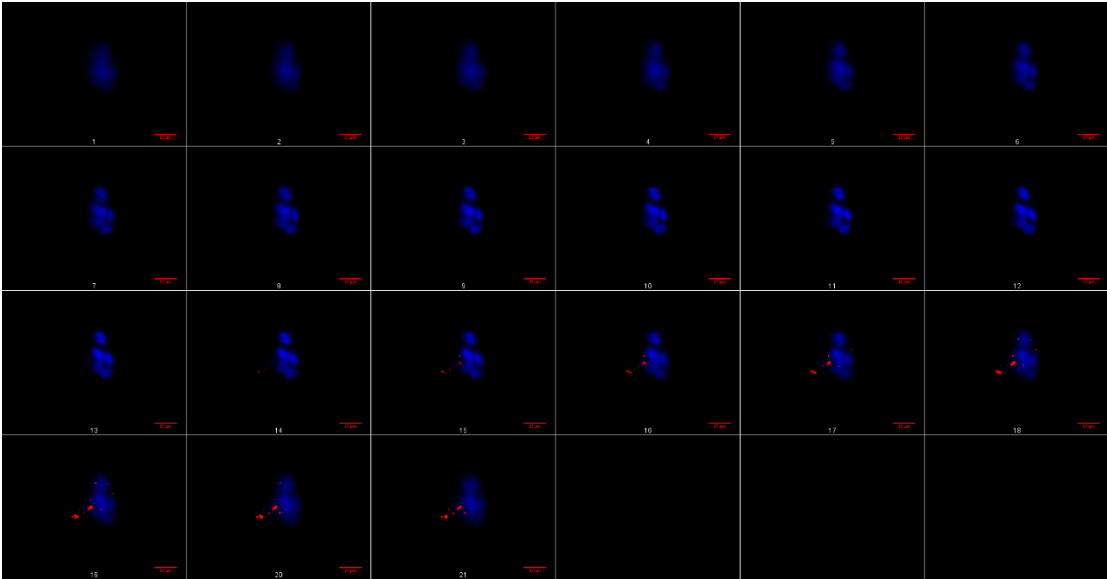


T=24

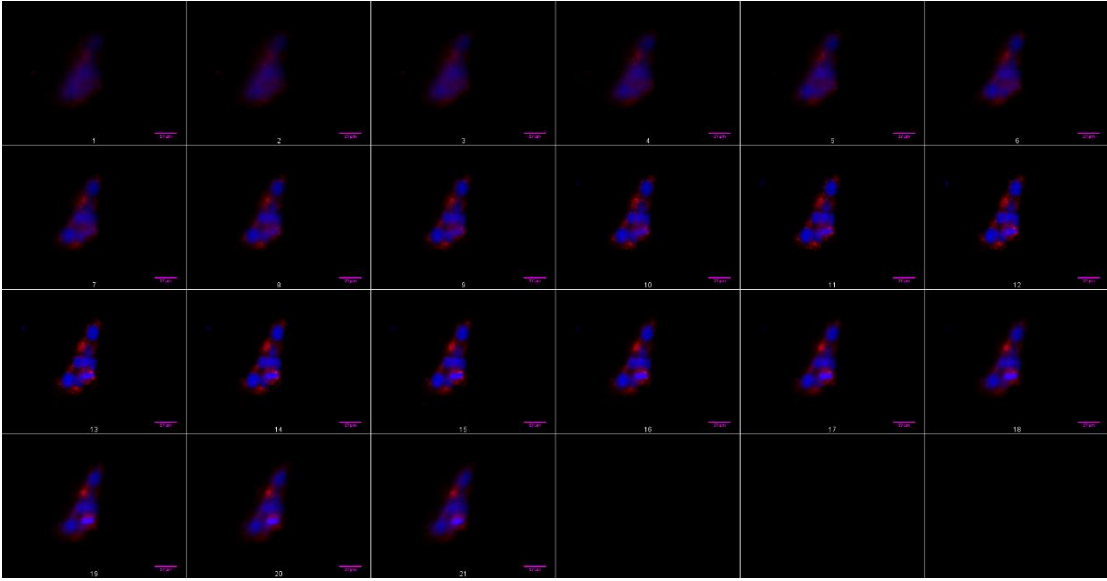


50nM AMINE POLYSTYRENE NANOPARTICLES (0.3nM)

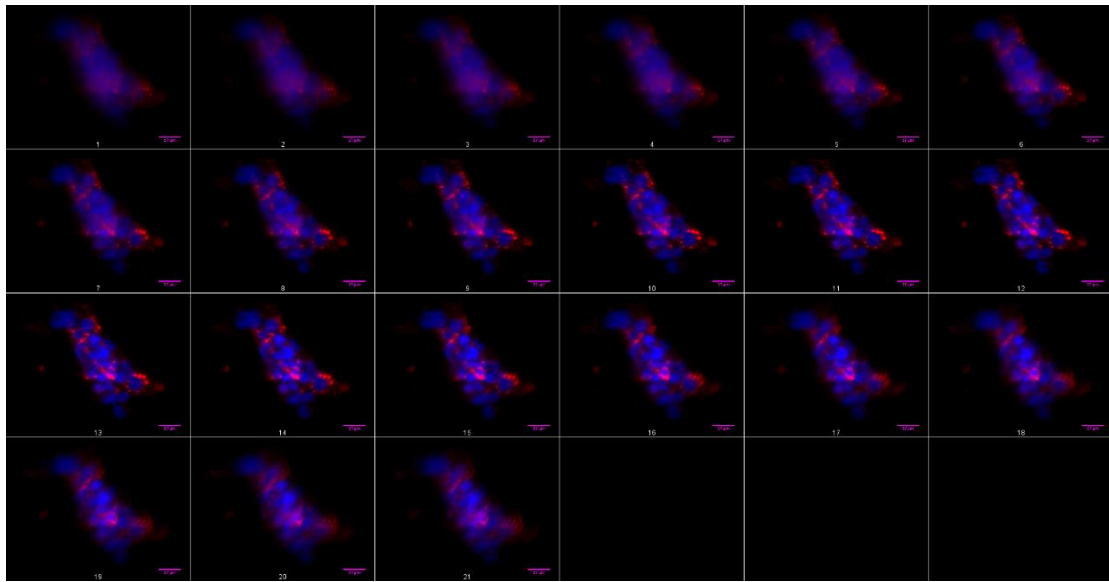
T=0



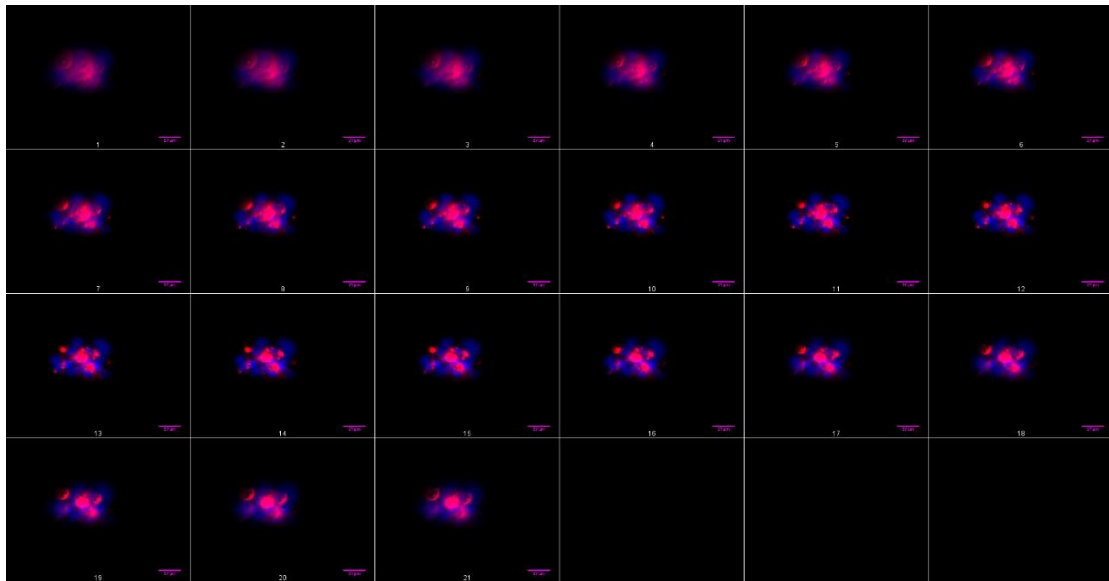
T=1



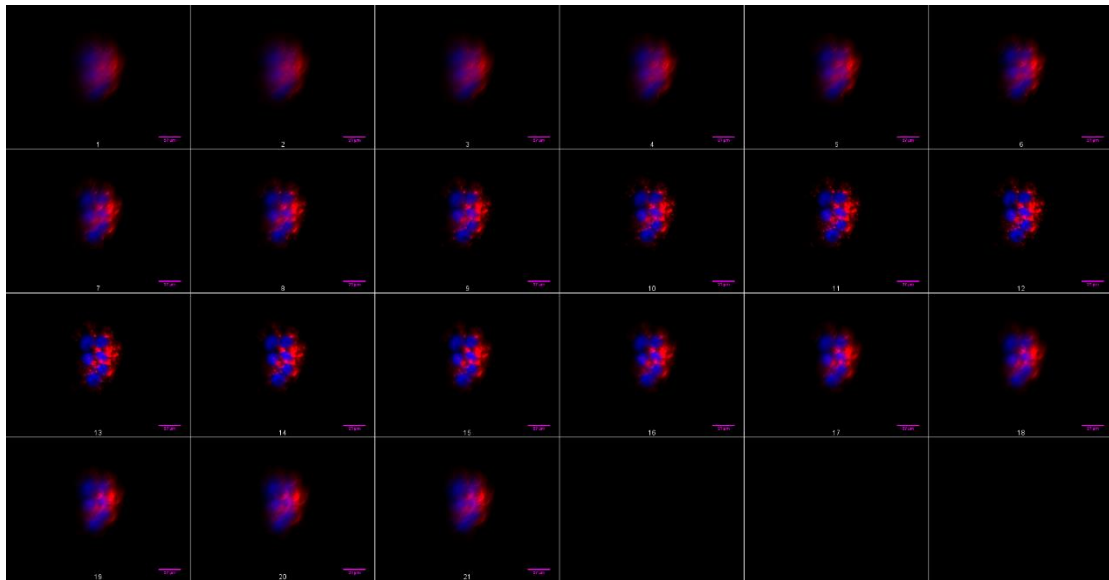
T=4



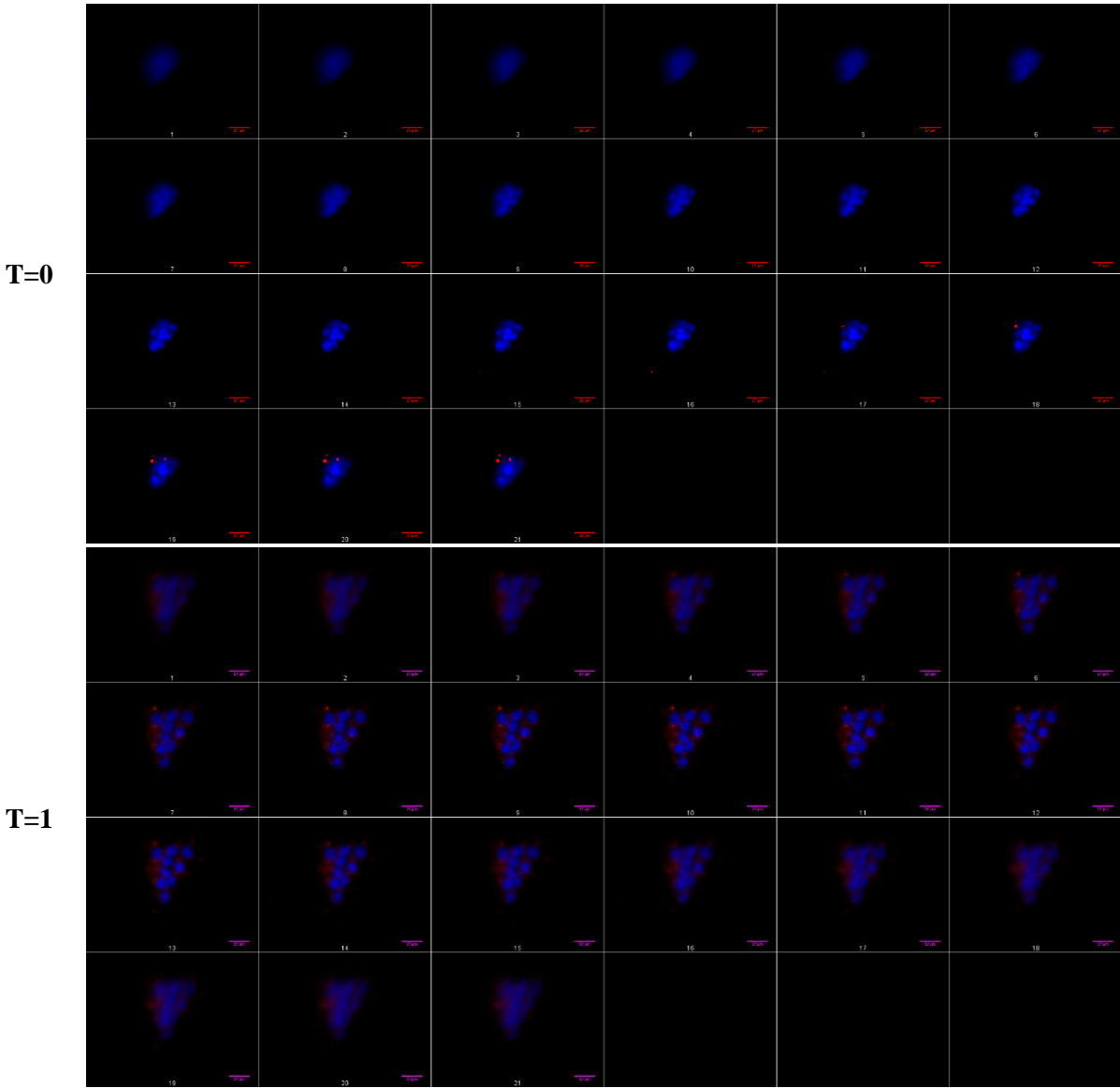
T=12



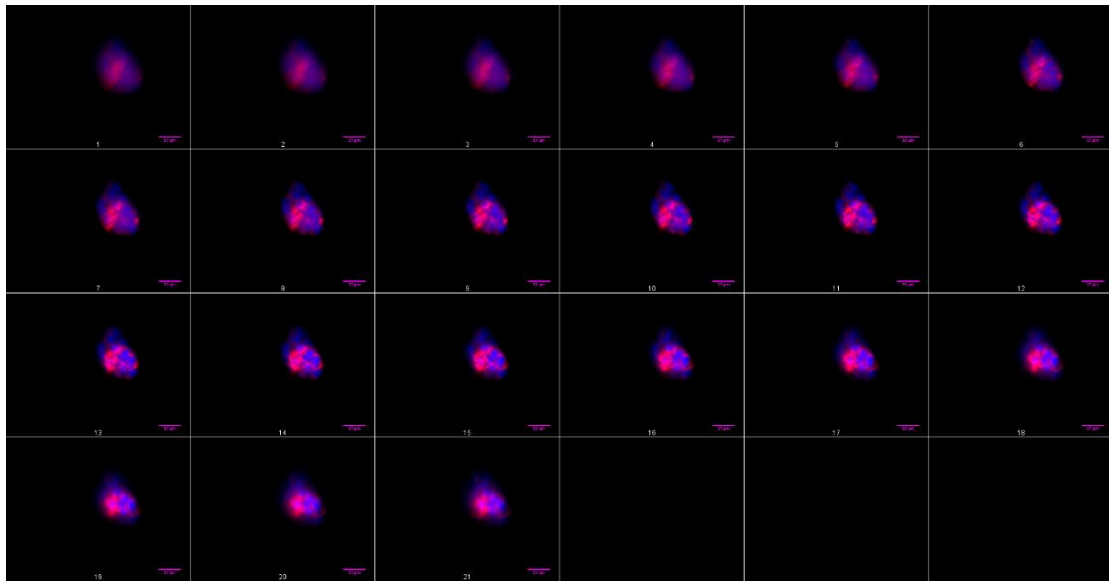
T=24



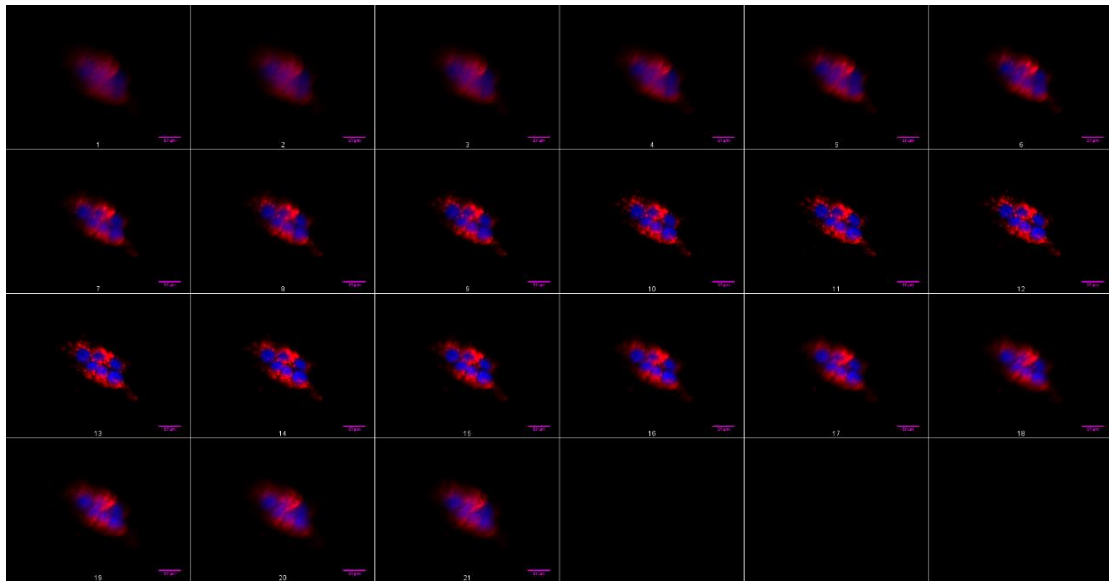
50nM AMINE POLYSTYRENE NANOPARTICLES (0.5nM)



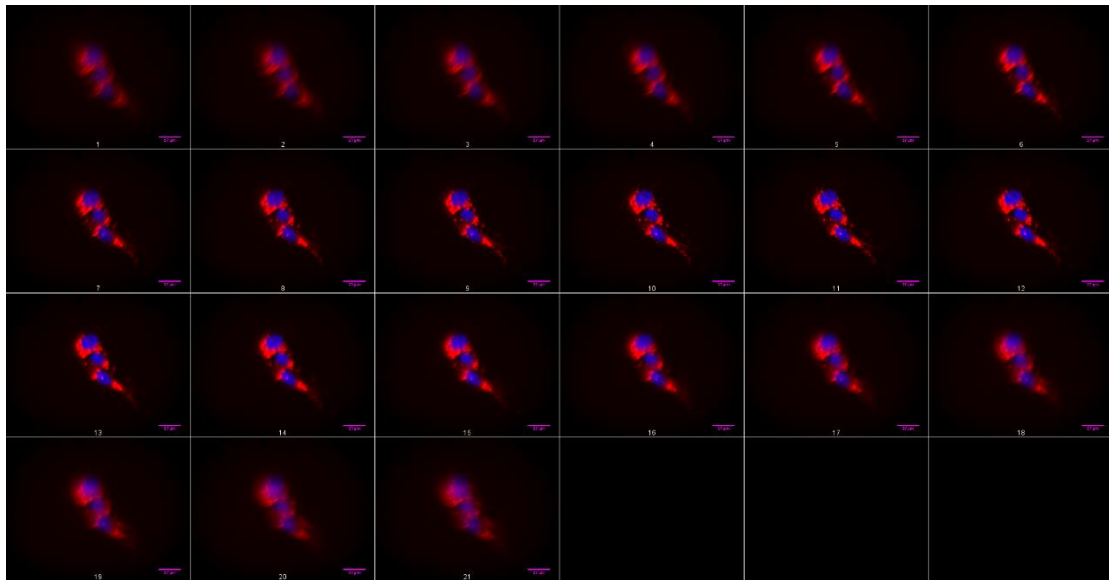
T=4



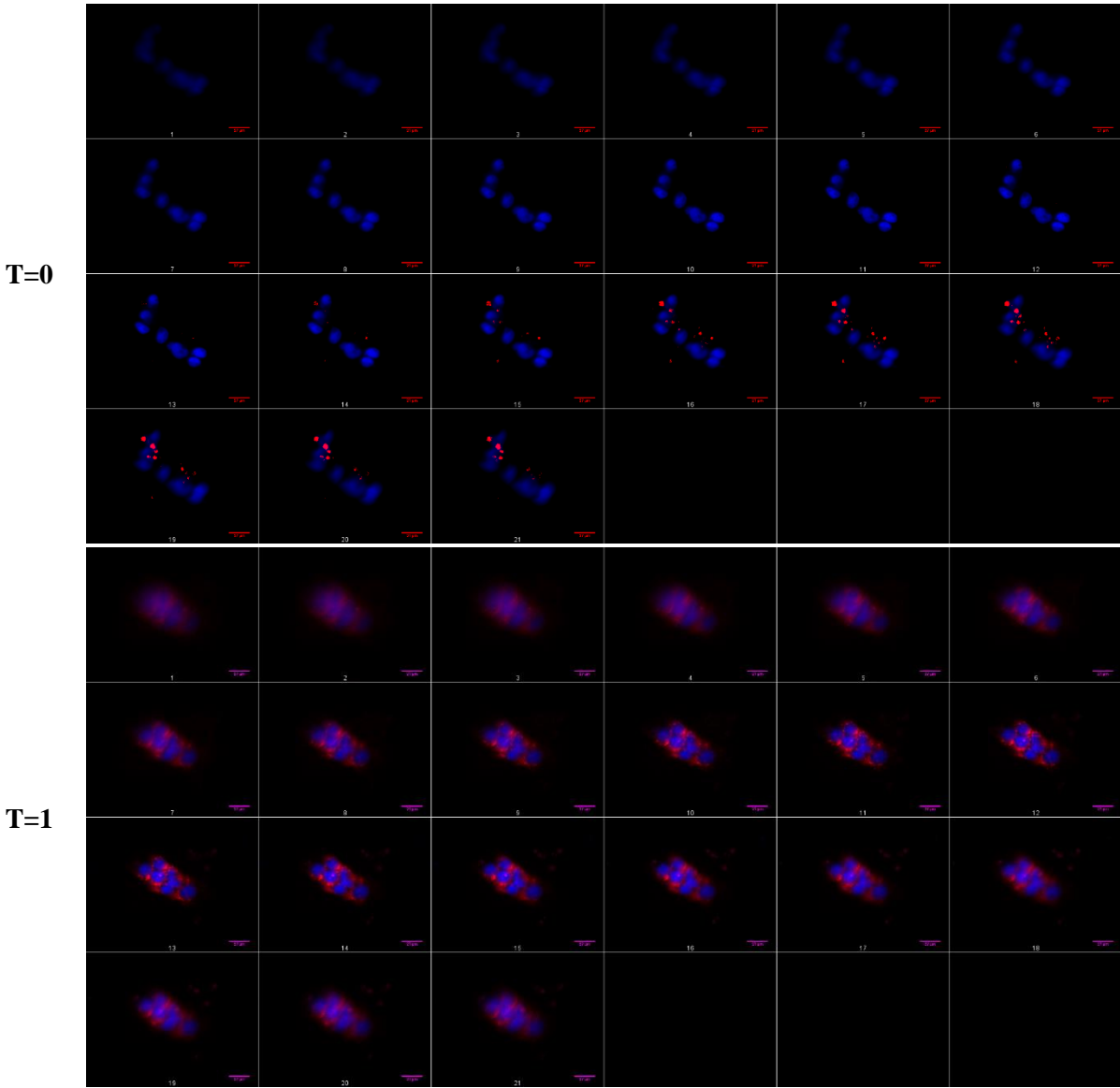
T=12



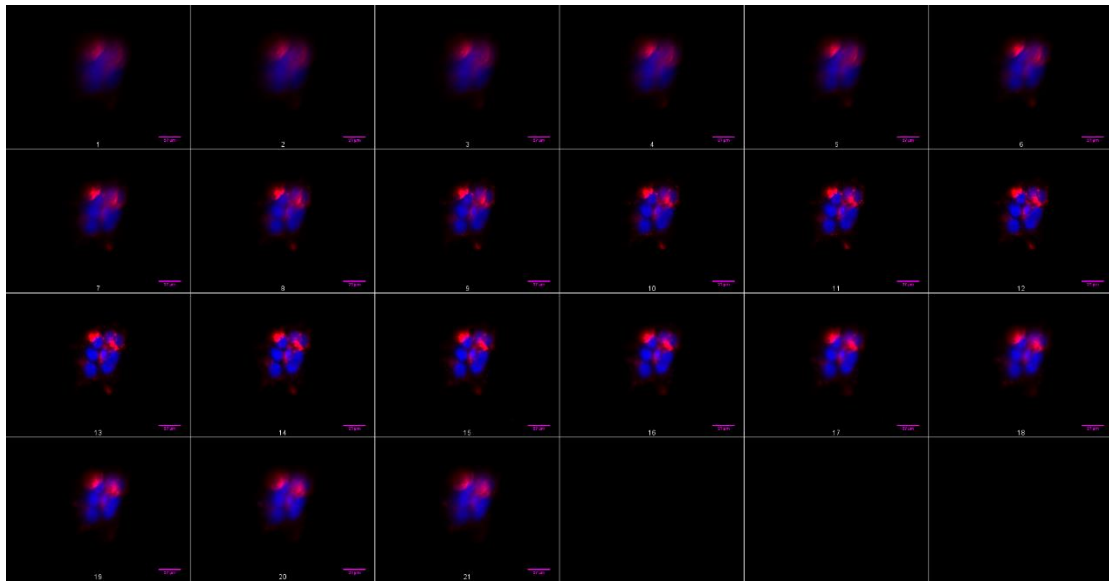
T=24



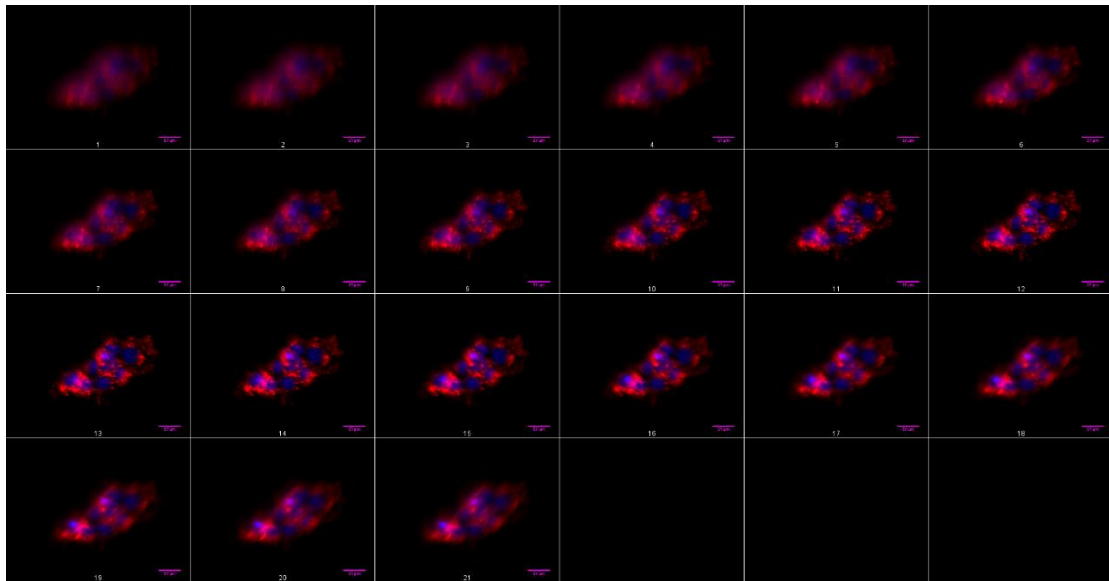
50nM AMINE POLYSTYRENE NANOPARTICLES (0.7nM)



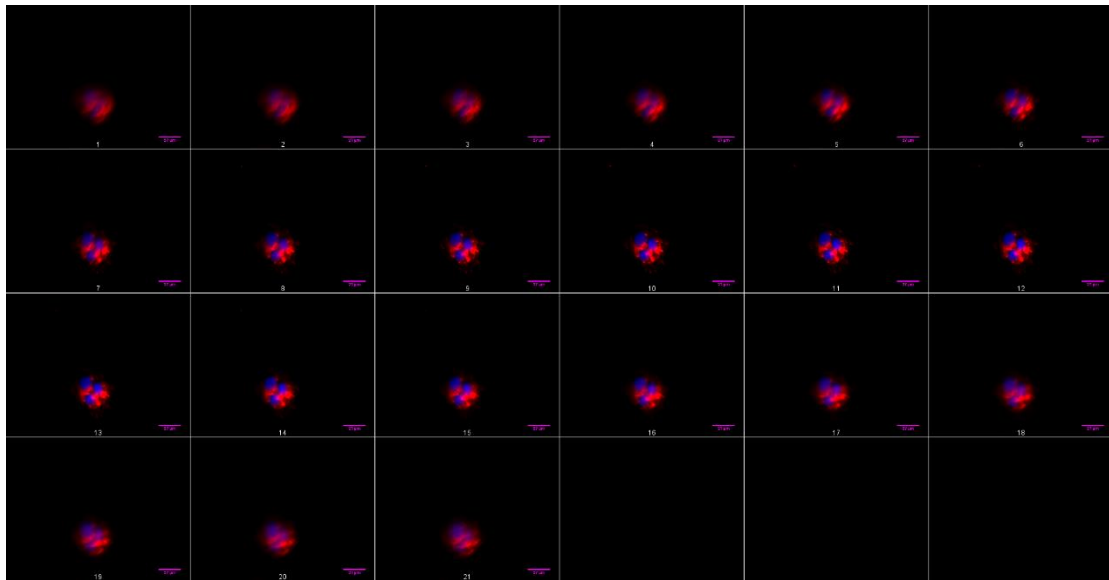
T=4



T=12



T=24



LIST OF REFERENCES

1. Abhilash, M., Potential applications of Nanoparticles *International Journal of Pharma and Bio Sciences* **2010**, *1* (1), 1-12.
2. Salata, O., Applications of nanoparticles in biology and medicine. *Journal of Nanobiotechnology* **2004**, *2*, 1-6.
3. Agata P. Walczak, E. K., Peter J. M. Hendriksen, Richard Helsdingen, Meike van der Zande, Ivonne M. C. M. Rietjens, Hans Bouwmeester, In vitro gastrointestinal digestion increases the translocation of polystyrene nanoparticles in an in vitro intestinal co-culture model. *Nanotoxicology*, **2015**, *9* (7), 886-894.
4. Samir Dekali, C. G., Thierry Kortulewski, Kelly Blazy, Patrice Rat, Ghislaine Lacroix, Assessment of an in vitro model of pulmonary barrier to study the translocation of nanoparticles *Toxicology Reports* **2014**, *1*, 157–171.
5. Wolfgang Zauner , N. A. F., Adrian M.R. Haines, In vitro uptake of polystyrene microspheres: effect of particle size, cell line and cell density. *Journal of Controlled Release* **2001**, *71*, 39–51.
6. Charlotte M. Beddoes . C. Patrick Case , W. H. B., Understanding nanoparticle cellular entry: A physicochemical perspective. *Advances in Colloid and Interface Science* **2015**, *218*, 48-68.
7. Helinor J. Johnston, M. S.-B., David M. Brown , Wolfgang Kreyling , Lang Tran , Vicki Stone, Evaluating the uptake and intracellular fate of polystyrene nanoparticles by primary and hepatocyte cell lines in vitro *Toxicology and Applied Pharmacology* **2010**, *242*, 66–78.
8. Cornelia Loos, T. S., Anna Musyanovych, Volker Mailänder, Katharina Landfester, G. Ulrich Nienhaus and Thomas Simmet, Functionalized polystyrene nanoparticles as a platform for studying bio–nano interactions. *Beilstein J. Nanotechnol* **2014**, *5*, 2403-2412.

9. Wünsch, J. R., *Polystyrene: Synthesis, Production and Applications*. 2000.
10. EPA, AP-42: Compilation of Air Emission Factors. In *Chapter 6: Organic Chemical Process Industry, 6.6.3 polystyrene* [Online] 5 ed.; Agency, E. P., Ed. 1991; p. 15.
11. Daria Maria Monti, D. G., Giuliana Napolitano, Renata Piccoli, Paolo Netti, Sabato Fusco, Angela Arciello, Biocompatibility, uptake and endocytosis pathways of polystyrene nanoparticles in primary human renal epithelial cells. *Journal of Biotechnology* **2015**, *193* 3–10.
12. FDA *Code of Federal Regulation, title 21, INDIRECT FOOD ADDITIVES: POLYMERS*; Department of health and human services: 2017.
13. Amir K. Varkouhi , M. S., Gert Storm , Hidde J. Haisma, Endosomal escape pathways for delivery of biologicals. *Journal of Controlled Release* **2011**, *151*, 220–228.
14. Pakatip Ruenraroengsak, T. D. T., Differential bioreactivity of neutral, cationic and anionic polystyrene nanoparticles with cells from the human alveolar compartment: robust response of alveolar type 1 epithelial cells. *Particle and Fibre Toxicology* **2015**, *12* (19), 1-20.
15. Rebuma Firdessa, T. A. O., Heidrun Moll, Identification of multiple cellular uptake pathways of polystyrene nanoparticles and factors affecting the uptake: Relevance for drug delivery systems. *European Journal of Cell Biology* **2014**, *93* 323–337.
16. Anna Salvati, I. N., Andrea Haase, Christoffer Åberg, Sergio Moya, An Jacobs, Fatima Alnasser, Tony Bewersdorff, Sarah Deville, Andreas Luch, Kenneth A. Dawsonf, Quantitative measurement of nanoparticle uptake by flow cytometry illustrated by an interlaboratory comparison of the uptake of labelled polystyrene nanoparticles. *NanoImpact* **2018**, *9*, 42–50.
17. Jordan A. Pitt, J. S. K., Nishad Jayasundara, Andrey Massarsky, Rafael Trevisan, Nick Geitner, Mark Wiesner, Edward D. Levin, Richard T. Di Giulio, Uptake, tissue distribution, and toxicity

- of polystyrene nanoparticles in developing zebrafish (*Danio rerio*). *Aquatic Toxicology* **2018**, *194* 185–194.
18. Yeon Kyung Lee, e.-J. C., Thomas J. webster, Sang-Hyun Kim, Dongwoo Khang, effect of the protein corona on nanoparticles for modulating cytotoxicity and immunotoxicity. *International Journal of Nanomedicine* **2015**, *10* 97–113.
 19. Claudia Corbo, R. M., Alessandro Parodi, Naama E. Toledano Furman, Francesco Salvatore, Ennio Tasciotti, The impact of nanoparticle protein corona on cytotoxicity, immunotoxicity and target drug delivery. *Nanomedicine (Lond.)* **2016**, *11* (1), 81–100.
 20. Azzah M. Bannunah, D. V., Jennie Lord, Snjezana Stolnik, Mechanisms of Nanoparticle Internalization and Transport Across an Intestinal Epithelial Cell Model: Effect of Size and Surface Charge. *Mol. Pharmaceutics* **2014**, *11*, 4363-4373.
 21. Feng Zhao, Y. Z., Ying Liu, Xueling Chang , Chunying Chen , Yuliang Zhao, Cellular Uptake, Intracellular Trafficking, and Cytotoxicity of Nanomaterials. *small* **2011**, *10*, 1322-1337.
 22. Sean D. Conner, S. L. S., Regulated portals of entry into the cell. *NATURE* **2003**, *422*, 37-44.
 23. Ayush Verma, F. S., Effect of Surface Properties on Nanoparticle–Cell Interactions. *small* **2010**, *6* (1), 12-21.
 24. Xiue Jiang, A. M., Carlheinz Röcker, Katharina Landfester, Volker Mailänder, G. Ulrich Nienhaus, Specific effects of surface carboxyl groups on anionic polystyrene particles in their interactions with mesenchymal stem cells. *Nanoscale* **2011**, *3*, 2028–2035.
 25. Joanna REJMAN, V. O., Inge S. ZUHORN, Dick HOEKSTRA, Size-dependent internalization of particles via the pathways of clathrin and caveolae-mediated endocytosis. *Biochem. J.* **2004**, *377*, 159–169.

26. Ravi Shukla, V. B., Minakshi Chaudhary, Atanu Basu, Ramesh R. Bhonde, Murali Sastry, Biocompatibility of Gold Nanoparticles and Their Endocytotic Fate Inside the Cellular Compartment: A Microscopic Overview. *Langmuir* **2005**, *21*, 10644-10654.
27. Tiantian Wang, J. B., Xiue Jiang, G. Ulrich Nienhaus, Cellular Uptake of Nanoparticles by Membrane Penetration: A Study Combining Confocal Microscopy with FTIR Spectroelectrochemistry. *ACS NANO* **2012**, *6* (2), 1251–1259.
28. Qingshan Mu, N. S. H., Łukasz Krzemiński, Andy P Brown, Lars JC Jeuken, Michael N Routledge, Mechanism of cellular uptake of genotoxic silica nanoparticles. *Mu et al. Particle and Fibre Toxicology* **2012**, *9* (29), 1-11.
29. Samantha K. Kloet, Agata P. Walczak, Jochem Louisse, Hans H.J. van den Berg, Hans Bouwmeester, Peter Tromp, Remco G. Fokkink, Ivonne M.C.M. Rietjens, Translocation of positively and negatively charged polystyrene nanoparticles in an in vitro placental model. *Toxicology in Vitro* **2015**, *29*, 1701-1710.
30. Xiue Jiang, J. D., Katharina Landfester, Margit Hafner, Volker Mailänder, Anna Musyanovych, Carlheinz Röcker, G. Ulrich Nienhaus, Specific Effects of Surface Amines on Polystyrene Nanoparticles in their Interactions with Mesenchymal Stem Cells. *Biomacromolecules* **2010**, *11*, 748–753.
31. Maneerat Ekkapongpisit, A. G., Carlo Follo, Giuseppe Caputo, Ciro Isidoro, Biocompatibility, endocytosis, and intracellular trafficking of mesoporous silica and polystyrene nanoparticles in ovarian cancer cells: effects of size and surface charge groups. *International Journal of Nanomedicine* **2012**, *7*, 4147–4158.
32. Oleg Lunov, T. S., G. Ulrich Nienhaus, Cornelia Loos, Johanna Beil, Michael Delacher, Kyrylo Tron, Anna Musyanovych, Volker Mailander, Katharina Landfester, Thomas Simmet,

Differential Uptake of Functionalized Polystyrene Nanoparticles by Human Macrophages and a Monocytic Cell Line. *ACS NANO* **2011**, 5 (3), 1657–1669.

33. Sung-Hyun Hwang, F. T., Jiyoung Jeong, Youngju Han, Sunay V. Chankeshwara, Mark Bradley, Wan-Seob Cho, Dual contribution of surface charge and proteinbinding affinity to the cytotoxicity of polystyrene nanoparticles in nonphagocytic A549 cells and phagocytic THP-1 cells. *JOURNAL OF TOXICOLOGY AND ENVIRONMENTAL HEALTH, PART A* **2016**, 79 (20), 925–937.
34. Amber L. Doiron, B. C., Kristina D. Rinker, Endothelial Nanoparticle Binding Kinetics are Matrix and Size Dependent. *Biotechnology and Bioengineering* **2011**, 108 (12), 2988-2998.
35. Juan A Varela, M. G. B., Christoffer Åberg, Jeremy C Simpson, Kenneth A Dawson, Quantifying size-dependent interactions between fluorescently labeled polystyrene nanoparticles and mammalian cells *Journal of Nanobiotechnology* **2012**, 10 (39), 1-6.
36. Sourav Bhattacharjee, D. E., Kleanthis Fytianos, Jasper van der Gucht, Gerrit M Alink, Ivonne MCM Rietjens, Antonius TM Marcelis, Han Zuilhof, Cytotoxicity and cellular uptake of tri-block copolymer nanoparticles with different size and surface characteristics. *Particle and Fibre Toxicology* **2012**, 9 (11), 1-19.
37. Dominik Hu" hn, K. K., Christian Geidel, Stefan Brandholt, Ine De Cock, Stefaan J. H. Soenen, Pilar Rivera_Gil, Jose-Maria Montenegro, Kevin Braeckmans, Klaus Mu" llen, G. Ulrich Nienhaus, Markus Klapper, Wolfgang J. Parak, Polymer-Coated Nanoparticles Interacting with Proteins and Cells: Focusing on the Sign ofthe Net Charge. *ACS NANO* **2013**, 7 (4), 3253–3263.

38. Maurizio Forte, G. I., Margherita Tussellino, Rosa Carotenuto, Marina Prisco, Maria De Falco, Vincenza Laforgia, Salvatore Valiante, Polystyrene nanoparticles internalization in human gastric adenocarcinoma cells. *Toxicology in Vitro* **2016**, *31* 126–136.
39. Valentina Belli, D. G., Marco Biondi, Francesca della Sala, Paolo A. Netti, Dynamics of nanoparticle diffusion and uptake in three-dimensional cell cultures. *Colloids and Surfaces B: Biointerfaces* **2017**, *149* 7–15.
40. A.M. Nuruzatulifah, A. A. N., N. M. Nasha Ain, Synthesis and characterization of polystyrene nanoparticles with covalently attached fluorescent dye. *Materials Today: Proceedings* **2016**, *3S*, S112 – S119.
41. Birgit Johanna Teubl, C. M., Andreas Eitzlmayr, Andreas Zimmer, Eleonore Fröhlich, Eva Roblegg, In-Vitro Permeability of Neutral Polystyrene Particles via Buccal Mucosa. *small* **2013**, *9* (3), 457-466.
42. Vincent Paget, S. D., Thierry Kortulewski, Romain Grall, Christelle Gamez, Kelly Blazy, Olivier Aguerre-Chariol, Sylvie Chevillard, Anne Braun, Patrice Rat, Ghislaine Lacroix, Specific Uptake and Genotoxicity Induced by Polystyrene Nanobeads with Distinct Surface Chemistry on Human Lung Epithelial Cells and Macrophages. *PLOS ONE* **2015**, *10* (4), 1-20.
43. Promega, CellTiter 96® One Solution Aqueous Cell Proliferation Assay. Corporation, P., Ed. 2012.
44. Sophie Laurent, C. B., Coralie Thirifays, Urs O. Häfeli, Morteza Mahmoudi, Crucial Ignored Parameters on Nanotoxicology: The Importance of Toxicity Assay Modifications and “Cell Vision”. *PLoS ONE* **2012**, *7*, 1-12.

45. Syed K Sohaebuddin, P. T. T., David Baker, John W. Eaton, Liping Tang, Nanomaterial cytotoxicity is composition, size, and cell type dependent *Particle and Fibre Toxicology* **2010**, 7 (22), 1-17.
46. Won Jin Kim, A. C. B., Teruaki Hayakawa, Cheng Xia, Masa-aki Kakimoto, Haridas E. Pudavar, Kwang-Sup Lee, Paras N. Prasad, Hyperbranched polysiloxysilane nanoparticles: Surface charge control of nonviral gene delivery vectors and nanoprobe. *International Journal of Pharmaceutics* **2009**, 376, 141–152.
47. Parisa Foroozandeh, A. A. A., Merging Worlds of Nanomaterials and Biological Environment: Factors Governing Protein Corona Formation on Nanoparticles and Its Biological Consequences. *Nanoscale Research Letters* **2015**, 10 (221), 1-12.
48. Chao Lin, J. F. J. E., Effect of chemical functionalities in poly(amido amine)s for non-viral gene transfection. *Journal of Controlled Release* **2008**, 132 267–272.
49. Sourav Bhattacharjee, L. H. d. H., Nynke M Evers, Xue Jiang, Antonius TM Marcelis, Han Zuilhof, Ivonne MCM Rietjens, Gerrit M Alink, Role of surface charge and oxidative stress in cytotoxicity of organic monolayer-coated silicon nanoparticles towards macrophage NR8383 cells. *Particle and Fibre Toxicology* **2010**, 7 (25), 1-12.
50. Tian Xia, M. K., Jonathan Brant, Matt Hotze, Joan Sempf, Terry Oberley, Constantinos Sioutas, Joanne I. Yeh, Mark R. Wiesner, Andre E. Nel, Comparison of the Abilities of Ambient and Manufactured Nanoparticles To Induce Cellular Toxicity According to an Oxidative Stress Paradigm. *Nano Lett.* **2006**, 6 (8), 1794-1807.
51. JENA, N., DNA damage by reactive species: Mechanisms, mutation and repair. *J. Biosci.* **2012**, 37, 503–517.

52. Terry L Riss, R. A. M., Andrew L Niles, Sarah Duellman, H el ene A Benink, Tracy J. Worzella, Lisa Minor, Cell Viability Assays. *Assay Guidance Manual* **2013**.
53. C. Wilhelm, F. G., J. Roger, J. N. Pons, J.-C. Bacri, Interaction of Anionic Superparamagnetic Nanoparticles with Cells: Kinetic Analyses of Membrane Adsorption and Subsequent Internalization. *Langmuir* **2002**, *18*, 8148-8155.
54. Anna Lesniak, A. S., Maria J. Santos-Martinez, Marek W. Radomski, Kenneth A. Dawson, Christoffer  berg, Nanoparticle Adhesion to the Cell Membrane and Its Effect on Nanoparticle Uptake Efficiency. *J. Am. Chem. Soc.* **2013**, *135*, 1438–1444.
55. Jung Jin Park, S. H. D. P. L., Scott K. Stanley, Brandon M. Vogel, Sangcheol Kim, Jack F. Douglas, Dharmaraj Raghavan, Alamgir Karim, Langmuir Adsorption Study of the Interaction of CdSe/ZnS Quantum Dots with Model Substrates: Influence of Substrate Surface Chemistry and pH. *Langmuir* **2009**, *25*, 443-450.
56. Murzin, D. Y., ON THE VALIDITY OF LANGMUIR ADSORPTION ON SUPPORTED NANOPARTICLES. *React.Kinet.Catal.Lett.* **2007**, *91* (1), 37–43.
57. Pascale Chenevier, B. V., Didier Roux, Nelly Henry-Toulme', Interaction of Cationic Colloids at the Surface of J774 Cells: A Kinetic Analysis. *Biophysical Journal* **2000** *79*, 1298–1309.
58. Kyung-Dall Lee, S. N., Demetrios Papahadjopoulos, Quantitative Analysis of Liposome-Cell Interactions in Vitro: Rate Constants of Binding and Endocytosis with Suspension and Adherent J774 Cells and Human Monocytes. *Biochemistry* **1993**, *32*, 889-899.
59. Farquhar, M. G., RECOVERY OF SURFACE MEMBRANE IN ANTERIOR PITUITARY CELLS. *The Journal Of Cell Biology* **1978**, *77* (3), 35-42.

60. Nicolae Ghinea, N. S., Anionized and Cationized Hemeundecapeptides as Probes for Cell Surface Charge and Permeability Studies: Differentiated Labeling of Endothelial Plasmalemmal Vesicles. *The Journal of Cell Biology* **1985**, *100* (2), 606-612.
61. Kumarasamy Murali, K. K., Yang Li, Kornél Demeter, Zsuzsanna Környei, Emilia Madarász, Uptake and bio-reactivity of polystyrene nanoparticles is affected by surface modifications, ageing and LPS adsorption: in vitro studies on neural tissue cells. *Nanoscale* **2015**, *7*, 4199–4210.